



UNIVERSITA' DEGLI STUDI DI PARMA

DOTTORATO DI RICERCA IN “MEDICINA MOLECOLARE”

CICLO XXX

**Biomarkers investigation in
Chronic Obstructive Pulmonary Disease
and Type 2 Diabetes using
Multiple Reaction Monitoring - Mass Spectrometry**

Coordinatore

Chiar.mo Prof. Luciano Polonelli

Tutore

Chiar.mo Prof. Alberto Spisni

Dottoranda: Giulia Rizzatello

Anni 2014/2017

Table of contents

Table of contents	2
Abstract	4
Riassunto	6
Section 1: Introduction	8
1.1 Biomarkers in medicine	9
1.1.1 Definition, role and criteria	9
1.2 Chronic Obstructive Pulmonary disease	12
1.2.1 Definition	12
1.2.2 Risk Factors	13
1.2.3 Pneumo-histopathology of COPD	16
1.2.4 Histone acetylation and deacetylation: importance in COPD	21
1.2.5 Chronic bronchitis and Emphysema in COPD	23
1.2.6 Pathophysiology of COPD	25
1.2.7 Acute Exacerbation aetiology	27
1.2.8 Stages of COPD	30
1.2.9 COPD biomarkers: state of art	32
1.3 Type 2 Diabetes Mellitus	36
1.3.1 Definition	37
1.3.2 Risk factors and Diagnosis	37
1.3.3 Insulin mechanism of action and GLUT4 transporter	39
1.3.4 Pathology and pathophysiology of T2D	44
1.3.5 Type 2 Diabetes biomarkers: state of art	47
1.3.6 Animal Models of Obesity	49
Aim the thesis	51
Section 2: Materials and Methods	52
2.1 Chronic Obstructive Pulmonary Disease	53
2.1.1 Patients demographic data	53
2.1.2 Plasma samples preparation	54
2.1.3 Chromatographic Separation	55
2.1.4 Parameters selected for HPLC in COPD project	62
2.1.5 Mass Spectrometry (MS) Analysis	63
2.1.6 Multiple Reaction Monitoring – MS (MRM - MS)	69
2.1.7 Parameters selected for MRM-MS in COPD project	75

2.1.8	Statistical Analysis	76
2.2	Type 2 Diabetes Mellitus	77
2.2.1	Patients demographic data	77
2.2.2	Fat samples preparation	78
2.2.3	Chromatographic and MRM-MS analysis	79
2.2.4	Statistical Analysis	80
2.2.5	GLUT4 carbonylation in mice	81
2.2.5.1	Animals and treatments	81
2.2.5.2	Fat sample preparation	83
2.2.5.3	Chromatographic and MRM-MS analysis	85
2.2.5.4	Statistical Analysis	87
Section 3:	Results	88
3.1	Chronic Obstructive Pulmonary Disease	89
3.1.1	Correlation between H3.3 peptide and FEV ₁ /FVC	89
3.1.2	H3.3 increases in patients with most severe GOLD	90
3.1.3	Evaluation of H3.3 as diagnostic biomarker	94
3.1.4	H3.3 peptide increases in proximity of AECOPD events	95
3.1.5	H3.3 and its role in the pathology	96
3.2	Type 2 Diabetes Mellitus	99
3.2.1	Level of GLUT4-HNE after Over-nutrition Diet	99
3.2.2	Level of GLUT4-HNE in non-diabetic and diabetic subjects	100
3.2.3	Murine GLUT4-HNE level	103
Section 4:	Conclusions	105
4.1	Chronic Obstructive Pulmonary Disease	106
4.1.1	Correlation between FEV ₁ /FVC and H3.3 in plasma	107
4.1.2	Histone 3.3 trend between the GOLD stages	108
4.1.3	Hyperacetylated and citrullinated Histone H3.3	109
4.2	Type 2 Diabetes Mellitus	111
4.2.1	Study of the effects of over-nutrition diet on GLUT4 transporter	112
4.2.2	Murine model for GLUT4-HNE	112
References		114
Ringraziamenti		119

Abstract

A biomarker is a biological characteristic that is objectively measured and evaluated as an indicator of biological or pathological processes or as a response to a therapeutic intervention. Biomarkers in basic and applied research as well as in clinical practice have become so common that their presence in clinical trials is now accepted almost without question. In the case of specific biomarkers, that have been well characterized and repeatedly shown to correctly predict relevant clinical outcomes across a variety of treatments and populations, this use is entirely justified and appropriate.

Multiple Reaction Monitoring-Mass Spectrometry (MRM-MS) exploits the unique capability of three quadrupoles to act as mass filters and to selectively monitor a specific molecular ion of the analyte and one or several fragment ions generated from the analyte by collisional dissociation. High sensitivity and selectivity allow peptide quantification and biomarker identification in complex biological samples.

Chronic obstructive pulmonary disease (COPD) causes tissue destruction in lungs of patients and breathing problems, leading finally to death for insufficient respiratory ability. No treatment or diagnostic methods are available nowadays. The increasing number of patients with COPD has raised the need for therapy and the identification of a biomarker, in particular to prevent Acute Exacerbations of COPD (AECOPD). AECOPD has been associated with an accelerated decline in pulmonary function, a decrease in quality of life and an increase in morbidity and mortality. Histone 3.3 (H3.3) is elevated in the extracellular milieu in the lung and in the bronchoalveolar fluid. Also, neutrophil extracellular traps (NETs) release H3.3 during AECOPD. Collectively these data suggest that H3.3 is likely to be elevated in the plasma during AECOPD and is probably related to the number of exacerbations and the progression of the disease. Comparison of peptide of H3.3, in non-smoker and different GOLD stage patients with different number of exacerbation per year, showed a correlation with the state of the pathology making H3.3 a promising biomarker for COPD as a mirror of lungs destruction.

Obesity-linked insulin resistance greatly increases the risk for type 2 diabetes (T2D). Knowledge of how obesity promotes insulin resistance remains incomplete. In adipose tissue oxidative stress causes the extensive oxidation and carbonylation of numerous proteins,

including GLUT4 carbonylation (GLUT4-HNE) near the glucose transport channel, which likely results in loss of GLUT4 activity. The significant difference of GLUT4-HNE amount between obese non-diabetic and obese pre-diabetic and diabetic subjects, in different fat tissue subtypes, suggests that the initial T2D event is caused by an oxidative stress that produces GLUT4-HNE triggering insulin-resistance. These findings propose GLUT4-HNE as an early biomarker for insulin resistance syndrome and T2D progression. The same GLUT4-HNE trend is found in mice fat tissue, indeed, ob/ob and HFD mice have higher amount of GLUT4-HNE compared with control mice. In addition, we assume that physical exercise decreases the amount of GLUT4-HNE. The mouse could be, therefore, a good model for Diet Induced Obesity study including GLUT4-HNE analysis, making possible experimentations of other drugs or alternative insulin treatments in the future.

Riassunto

Un biomarker è una caratteristica biologica che viene oggettivamente misurata e valutata come un indicatore dei processi biologici o patologici o come una risposta ad un intervento terapeutico. I biomarker nella ricerca di base e applicata e nella pratica clinica sono diventati così comuni che la loro presenza negli studi clinici è ora accettata quasi senza dubbio. Nel caso di biomarker specifici, che sono stati ben caratterizzati e ripetutamente verificati nel prevedere correttamente i risultati clinici rilevanti all'interno di una varietà di trattamenti e popolazioni, questo utilizzo è completamente giustificato e appropriato.

La Multiple Reaction Monitoring-Mass Spectrometry (MRM-MS) sfrutta la capacità unica di tre quadrupoli di agire come filtri di massa e di monitorare selettivamente uno specifico ione molecolare dell'analita e uno o più ioni-frammento generati dall'analita mediante dissociazione collisionale. L'alta sensibilità e selettività permettono la quantificazione del peptide e l'identificazione del biomarker in campioni biologici complessi.

La BroncoPneumopatia Cronica Ostruttiva (BPCO) provoca distruzione tissutale nei polmoni dei pazienti e problemi di respirazione, portandoli infine a morte per insufficienza respiratoria. Oggi non sono disponibili né trattamenti né metodi diagnostici. Il numero crescente di pazienti con BPCO ha aumentato la necessità di terapia e l'identificazione di un biomarker, in particolare per prevenire le esacerbazioni acute della BPCO (EABPCO). EABPCO è stata associata ad un accelerato declino della funzionalità polmonare, alla diminuzione la qualità della vita e all'aumento della morbidità e mortalità. L'istone H3.3 (H3.3) è elevato nell'ambiente extracellulare nel polmone e nel fluido broncoalveolare. Inoltre, le trappole extracellulari neutrofili (NETs) rilasciano H3.3 durante l'EABPCO. Insieme, questi dati suggeriscono che è probabile che H3.3 sia elevato nel plasma durante EABPCO e presumibilmente sia correlato con il numero di esacerbazioni e la progressione della malattia. Il confronto del peptide di H3.3, in pazienti non fumatori e in pazienti con diverse categorie GOLD e con diversi numeri di esacerbazioni l'anno, ha mostrato una correlazione con lo stato della patologia che ha reso H3.3 un biomarker promettente per la BPCO come specchio di distruzione dei polmoni.

La resistenza all'insulina legata all'obesità aumenta notevolmente il rischio per il diabete di tipo 2 (T2D). La conoscenza di come l'obesità promuova la resistenza all'insulina rimane

incompleta. Nel tessuto adiposo lo stress ossidativo provoca un'estesa ossidazione e carbonilazione di numerose proteine, compresa la carbonilazione di GLUT4 (GLUT4-HNE) vicino al canale di trasporto del glucosio, che probabilmente provoca la perdita di attività GLUT4. La differenza significativa del livello di GLUT4-HNE tra i soggetti obesi non-diabetici e i soggetti obesi pre-diabetici e diabetici, in diversi sottotipi di tessuto grasso, suggerisce che l'evento iniziale di T2D è causato da uno stress ossidativo che produce GLUT4-HNE causando insulino-resistenza. Questi risultati suggeriscono GLUT4-HNE come biomarker precoce per la sindrome di resistenza all'insulina e la progressione a T2D. Lo stesso andamento di GLUT4-HNE si trova nel tessuto adiposo murino, infatti, i topi ob/ob e HFD hanno una quantità maggiore di GLUT4-HNE rispetto ai topi di controllo. Inoltre, ipotizziamo che l'esercizio fisico riduce la quantità di GLUT4-HNE. Il topo potrebbe essere, perciò, un buon modello per lo studio Diet Induced Obesity incluso l'analisi GLUT4-HNE, consentendo di sperimentare in futuro altri farmaci o trattamenti alternativi o coadiuvanti l'insulina.

Section 1: Introduction

1.1 Biomarkers in medicine

1.1 Biomarkers in medicine

1.1.1 Definition, role and criteria

According to the Food and Drug Administration (FDA), the following terms, definitions and characteristics are proposed to describe biological measurements in therapeutic development and assessment.

Biological marker (biomarker): A characteristic that is objectively measured and evaluated as an indicator of normal biological processes, pathogenic processes, or pharmacologic responses to a therapeutic intervention.

From a biochemical point of view, a biomarker is often a protein, or a panel of proteins and their Post Transcriptional Modifications or metabolites the presence or quantitative characteristics of which are measured commonly using methods based on antibodies [1]. Biomarkers may have the greatest value in early efficacy and safety evaluations such as *in vitro* studies in tissue samples, *in vivo* studies in animal models and early-phase clinical trials to establish “proof of concept”. Biomarkers have many other valuable applications in disease detection and monitoring of health status. These applications include the following:

- use as a diagnostic tool for the identification of those patients with a disease or abnormal condition (e.g. elevated blood glucose concentration for the diagnosis of diabetes mellitus),
- use as a tool for staging of disease or classification of the extent of disease (e.g. prostate-specific antigen concentration in blood used to reflect extent of tumor growth and metastasis),
- use as an indicator of disease prognosis (e.g. anatomic measurement of tumor reduction of certain cancers),
- use for prediction and monitoring of clinical response to an intervention (e.g. blood cholesterol concentrations for determination of the risk of heart disease).

Clinical endpoint: A characteristic or variable that reflects how a patient feels, functions, or survives. Clinical endpoints are distinct measurements or analyses of disease characteristics observed in a study or a clinical trial that reflect the effect of a therapeutic intervention. Clinical endpoints are the most credible characteristics used in the assessment of the benefits and risks of a therapeutic intervention in randomized clinical trials.

Surrogate endpoint: A biomarker that is intended to substitute for a clinical endpoint. A surrogate endpoint is expected to predict clinical benefit (or harm or lack of benefit or harm) based on epidemiologic, therapeutic, pathophysiologic or other scientific evidence.

Surrogate endpoints are a subset of biomarkers. Although all surrogate endpoints can be considered biomarkers, it is likely that only a few biomarkers will achieve surrogate endpoint status. It is important to point out that the same biomarkers used as surrogate endpoints, in clinical trials, are often extended to clinical practice in which disease responses are similarly measured. The use of biomarkers as surrogate endpoints in a clinical trial requires the specification of the clinical endpoints that are being substituted, class of therapeutic intervention being applied and characteristics of population and disease state in which the substitution is being made (Figure 1) [2].

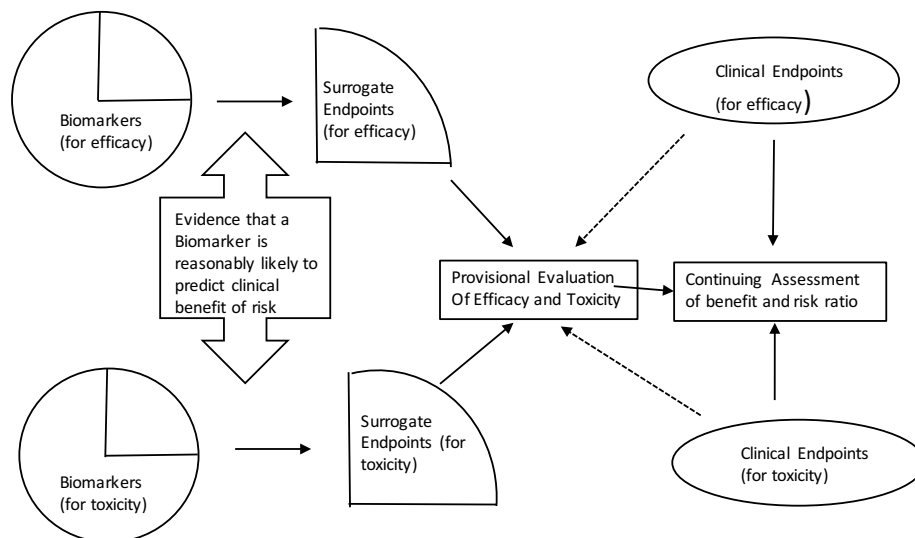


Figure 1. Conceptual model of the relationship of biomarkers, surrogate endpoints, and the process of evaluating therapeutic interventions.

To have a protein classified as an ideal biomarker, several criteria have to be met in order to enable unbiased diagnosis, particularly in patients without specific symptoms:

1. It has to be highly specific toward the given disease and highly sensitive,
2. The assay for the biomarker should be easily performed and standardized by trained healthcare professionals,
3. Readability of the test results should be transparent and clear for clinicians [1].

The projects shown in this thesis involved the study in particular of Prognostic and Predictive biomarkers. The distinction between prognostic and predictive biomarkers lies in the fact that a prognostic marker is a single molecular trait or signature of traits that separate different patient populations with respect to the risk of a disease in the absence of treatment (risk for cancer recurrence), whereas a predictive biomarker is the one that distinguishes patient populations with respect to the risk of a disease in response to a particular treatment [2]. During the last 10–15 years, proteomic technology has developed to accommodate the growing demand for biomarker research using biospecimens collected from tissue, blood and other biofluids. Innovative approaches including protein microarrays, aptamer arrays, bead-based flow cytometry and Mass Spectrometry (MS) to identify and sequence proteins in a high-throughput and quantitative manner have furthered our understanding in molecular mechanisms involved in diseases. Furthermore, depletion of high-abundance proteins from plasma and/or multi-dimensional chromatographic fractionation coupled with MS has expanded the dynamic range of detection for low abundance proteins in serum and plasma. A triple quadrupole (TQ) operated in the multiple reaction monitoring (MRM)-MS mode show exceptional levels of sensitivity and selectivity when coupled to LC. This level of specificity cannot be attained with any other bioanalytical technique employed for biomarker analysis [3].

1.2 Chronic Obstructive Pulmonary Disease

Chronic Obstructive Pulmonary Disease (COPD) represents an important public health challenge and is a major cause of chronic morbidity and mortality throughout the world. COPD is currently the fourth leading cause of death in the world (Figure 2) but is projected to be the 3rd leading cause of death by 2030 [WHO]. COPD is associated with significant economic burden, in the European Union the cost is estimated to be €38.6 billions while in the United States \$32 billions [9]. COPD exacerbations account for the greatest proportion of the total COPD burden on the health care system. Not surprisingly, there is a striking direct relationship between the severity of COPD and the cost of care.

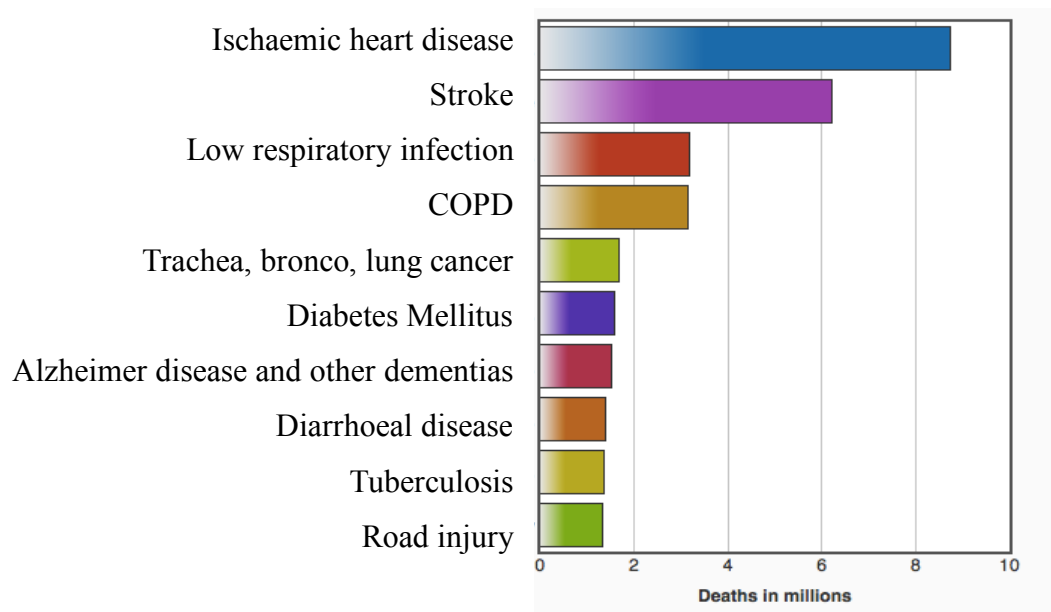


Figure 2. Top 10 cause of death globally in 2015, COPD death 3.17 million

1.2.1 Definition

Chronic Obstructive Pulmonary Disease is a common, preventable and treatable disease that is characterized by persistent respiratory symptoms and airflow limitation that is due to airway and/or alveolar abnormalities usually caused by significant exposure to noxious

particles or gases. The chronic airflow limitation characteristic of COPD is caused by a mixture of small airways disease (obstructive bronchiolitis) and parenchymal destruction (emphysema). The relative contributions of which vary from person to person. Worldwide, the most commonly found risk factor for COPD is tobacco and marijuana smoking. Outdoor, occupational and indoor air pollution are other major COPD risk factors. COPD is the result of a complex interplay of long-term cumulative exposure to noxious gases and particles, combined with a variety of host factors including genetics, airway hyper-responsiveness and poor lung growth during childhood [10].

1.2.2 Risk Factors

The prevalence of COPD is often directly related to the prevalence of tobacco smoking, although in many countries outdoor, occupational and indoor air pollution are major COPD risk factors. The risk of developing COPD is related to the following factors:

- **Tobacco smoke**, including cigarette, pipe, cigar, water-pipe and other types of tobacco smoking is popular in many countries, as well as environmental tobacco smoke. Cigarette smoking (CS) in particular is by far the most commonly encountered risk factor for COPD. Cigarette smokers have a higher prevalence of respiratory symptoms and lung function abnormalities: such as a decline, over years, in Forced Expiratory Volume in 1 second (FEV₁) and a greater COPD mortality rate than non-smokers. Age at starting smoke, total pack smoked per year and current smoking status are predictive for COPD [11]. Not all smokers develop clinically significant COPD, which suggest that genetic factors must modify each individual's risk [12]. Passive exposure to cigarette smoking may also contribute to respiratory symptoms and COPD [13].
- **Indoor air pollution**, from biomass fuel used for cooking and heating in poorly vented dwellings, this risk factor particularly affects women in developing countries [14],
- **Occupational exposures**, including organic and inorganic dusts, chemical agents and fumes are under-appreciated risk factors for COPD [15]. COPD does not have a clinical

subcategory that is clearly identified as occupational, largely because the condition develops slowly. Consequently, a diagnosis of “occupational COPD” is rarely made by clinicians; this situation is in sharp contrast to occupational asthma, which is more frequently recognized. Despite these difficulties, an impressive body of literature accumulated over the past two decades demonstrates the link between specific occupational exposures and the development of COPD. Longitudinal studies of the effects of occupational exposures and COPD have been performed in coal and hard-rock miners, tunnel, concrete-manufacturing and non-mining industrial workers in Paris. In these studies, moderate smoking and occupational exposures had approximately comparable effects on COPD risk [15]. Community-based studies from China, France, Italy, the Netherlands, New Zealand, Norway, Poland, Spain and the US have demonstrated increased relative risks for respiratory symptoms and/or chronic airflow limitation consistent with COPD, as well as, the excess annual decline in FEV₁ is associated with occupational exposure to dusts, gases and fumes. [15].

- **Outdoor air pollution:** although it appears to have a relatively small effect in causing COPD compared with that of cigarette smoking, air pollution from fossil fuel combustion, primarily from motor vehicle emissions in cities, is associated with decrements of respiratory functions [16,17],
- **Genetic factors,** such as severe hereditary deficiency of alpha-1 antitrypsin [18],
- **Lung growth and development,** any factor that affects lung growth during gestation and childhood (low birth weight, respiratory infections, etc.) has the potential to increase an individual’s risk of developing COPD [19],
- **Socioeconomic status,** there is strong evidence [WHO report] that the risk of developing COPD is related to socioeconomic status. In particular it is not clear the reason why the middle-income economies are more affected (Figure 3a), whether this pattern reflects exposures to indoor and outdoor air pollutants, crowding, poor nutrition, infections or other factors related to socioeconomic status,

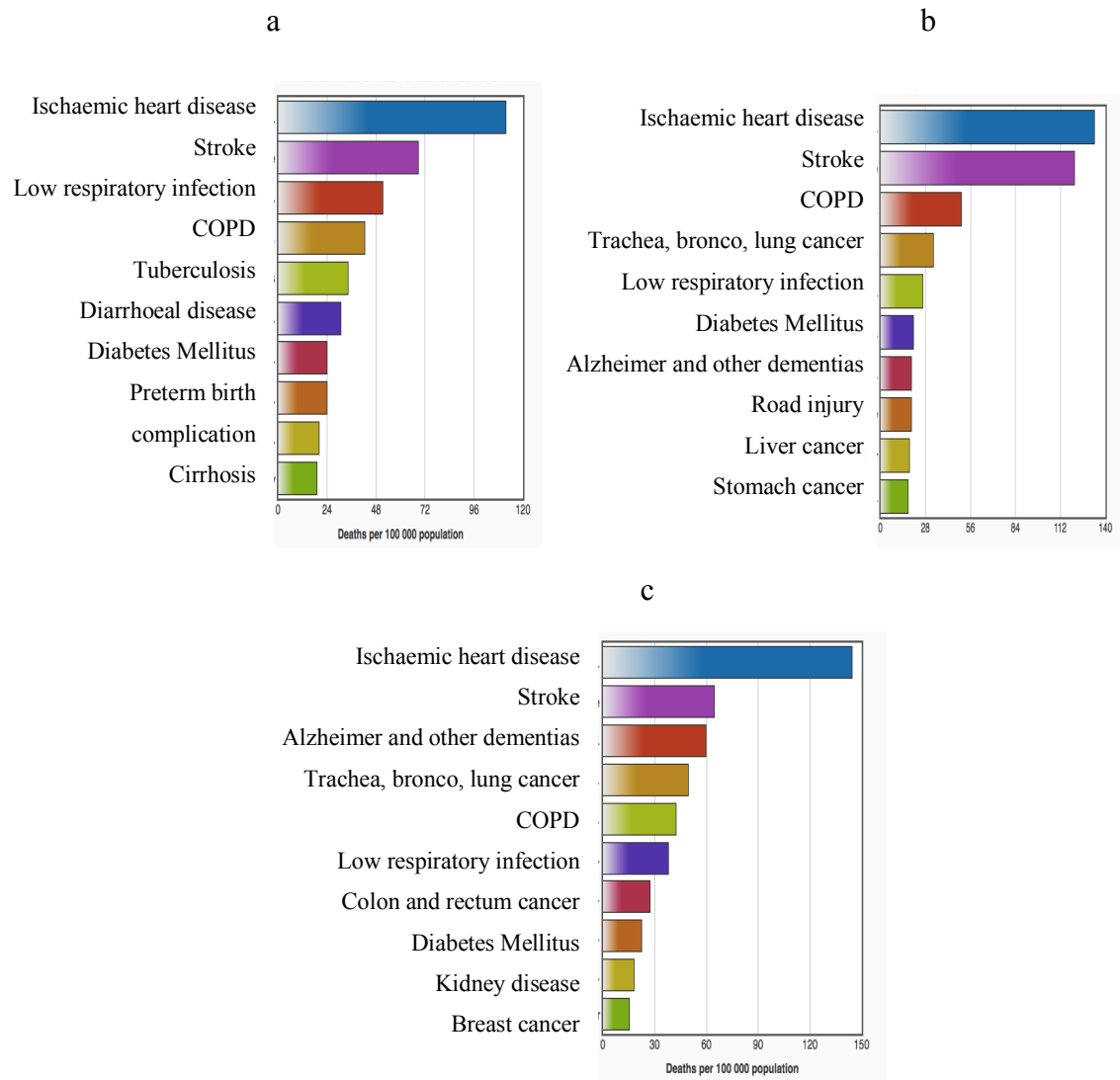


Figure 3. Top 10 causes of death by economy income group in 2015, a. lower-middle income economies, b. upper-middle economies, c. high-income economies (WHO)

- **Asthma and airway hyper-reactivity**, asthma may be a risk factor for the development of airflow limitation and COPD [20],
- **Infections**, bacteria and virus may contribute to the pathogenesis and progression of COPD. Bacterial colonization associated with airway inflammation may also play a significant role in exacerbations. A history of severe childhood respiratory infection has been associated with reduced lung function and increased respiratory symptoms in adulthood [19,21].

1.2.3 Pneumo-histopathology of COPD

Pathological changes characteristic of COPD are found in proximal airways, peripheral airways, lung parenchyma and pulmonary vasculature [22] (Figure 4).

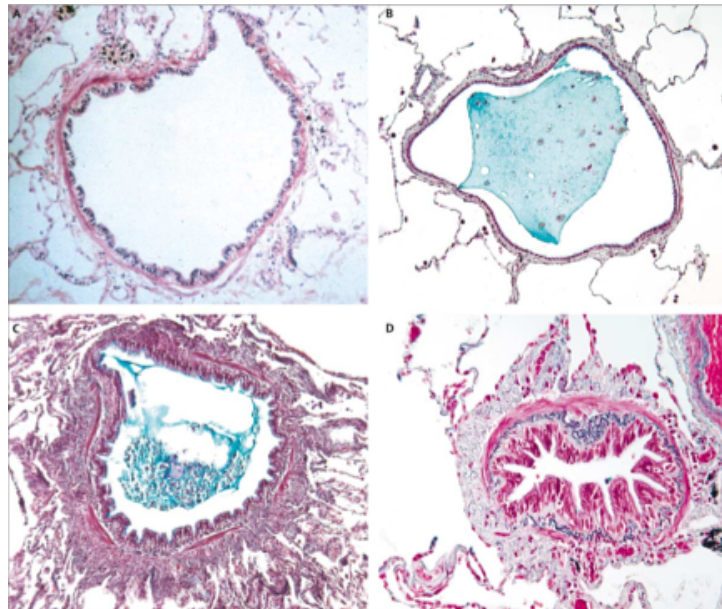


Figure 4. Small airway obstruction, a. Normal small airway. b. Small airway containing plug of mucus with relatively few cells. c. Acutely inflamed airway with thickened wall in which the lumen is partly filled with an inflammatory exudate of mucus and cell. d. Airway surrounded by connective tissue, which appears as if it might restrict normal enlargement of the lumen and unfolding of the epithelial lining that occurs with lung inflammation [22].

Smoking and other inhaled irritants cause inflammatory response in the peripheral airways and lung parenchyma [23]. The origin of pathology of COPD could be an abnormal inflammatory response in concert with the oxidative stress, both of them caused by inhaled noxious agents. The activated macrophages release inflammation mediators and chemotactic factors, including tumor necrosis factor- α (TNF- α), interleukin IL-6, interleukin IL-8, monocyte chemotactic peptide (MCP)-1, leukotriene LTB₄ and reactive oxygen species, and secrete proteolytic enzymes (especially MMP-9, MMP-12) whose action contributes to the establishment of pulmonary emphysema [23].

Macrophage numbers are increased in the lungs of patients with COPD. These macrophages are derived from circulating monocytes, which migrate to the lungs in response to

chemoattractants such as CCL2 (also known as MCP1) acting on CCR2, and CXCL1 acting on CXCR2 [22]. Neutrophils are recruited to the airways, under the influence of secreted chemotactic factors such as IL-8, LTB-4 and CXCL1 [23]. Neutrophils are also increased in the sputum of patients with COPD and this correlates with severity of the disease [24]. Neutrophils secrete serine proteases, including neutrophil elastase (NE), cathepsin G, proteinase-3 [23] and matrix metalloproteinase (MMP-8 and MMP-9), which may contribute to alveolar destruction [24]. Remarkable roles in COPD inflammation are played by dendritic and epithelial cells. Dendritic cells initiate the immune response activating a variety of inflammatory and immune cells including macrophages, B and T-lymphocytes and neutrophils [23]. Airways and alveoli epithelial cells, triggered by smoking, are the major source of inflammatory mediators and proteases, these cells secrete various factors such as TNF- α , the TGF- β , interleukins IL-1b and IL-8, GM-CSF (granulocyte-macrophage colony stimulating factor) [23] and IL-6 [24], which cause activation of fibroblasts and small airways fibrosis. The epithelial cells contribute to the defence of the body through the production of mucus which traps bacteria and through substances, such as defensins and cationic proteins, which have antimicrobial properties [23].

Adaptive immunity is also involved in the immune mechanisms of COPD. The number of pulmonary CD8⁺ T cells increases in the higher stages of airflow limitation and emphysema, during that phase they release proteolytic enzymes which cause structural cell death via apoptosis and/or necrosis [23,24]. In contrast, lungs of stable COPD patients are populated by CD4⁺ Th1 and Th17 cells, which produce IFN- γ , IL-17A and IL-17F, respectively. IL-17 promotes neutrophil accumulation at the site of injury increasing the release of granulocyte growth factors (G-CSF, GM-CSF) [24].

In general, CS contains a wide variety of toxic molecules that can trigger innate and adaptive immunity [23]. The inflammatory and structural changes in the airways increase with disease severity and persist on smoking cessation. The inflammation in the respiratory tract of COPD patients appears to be an amplification of the normal inflammatory response of the respiratory tract to chronic irritants such as cigarette smoke. Lung inflammation is further amplified by oxidative stress and an excess of proteinases in the lung. Together these mechanisms lead to the characteristic pathological changes in COPD (Figure 5).

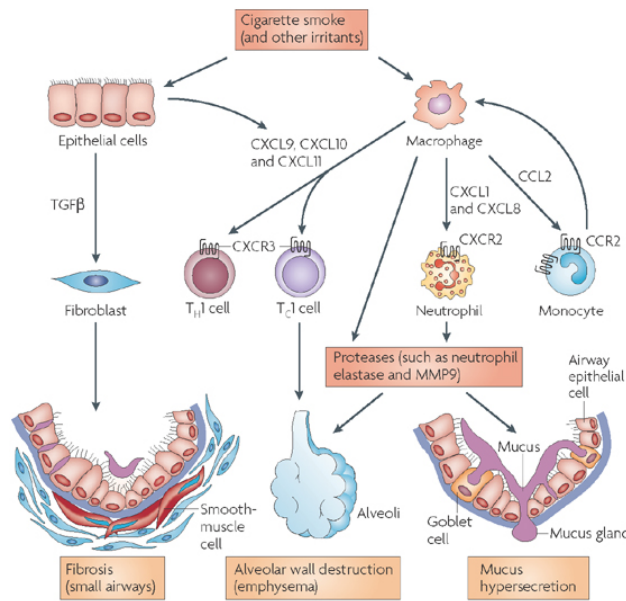


Figure 5: Inflammatory and immune cells involved in COPD [24].

Oxidative stress is considered an important amplifying mechanism in COPD. Patients have evidence of oxidative stress in the lungs, blood and skeletal muscle because mitochondrial dysfunctions lead to excessive production of reactive oxygen species (ROS) resulting in harmful effects: lipids, proteins and DNA damages [23]. Oxidative stress is further increased in the exacerbations [GOLD Report].

ROS, in patients with COPD, are produced by inflammatory (neutrophils, macrophages) and structural cells (epithelial cells) activated into the airways. This event leads to alteration of the airways and parenchyma resulting into bronchoconstriction and increase of inflammatory responses [23]. Furthermore, oxidative stress triggers NF-κB and histone acetyltransferase activation, promoting the expression of multiple inflammatory genes and down-regulation of anti-proteases, including α₁- antitrypsin, resulting in acceleration of the breakdown of elastin in lung parenchyma [23] (Figure 6).

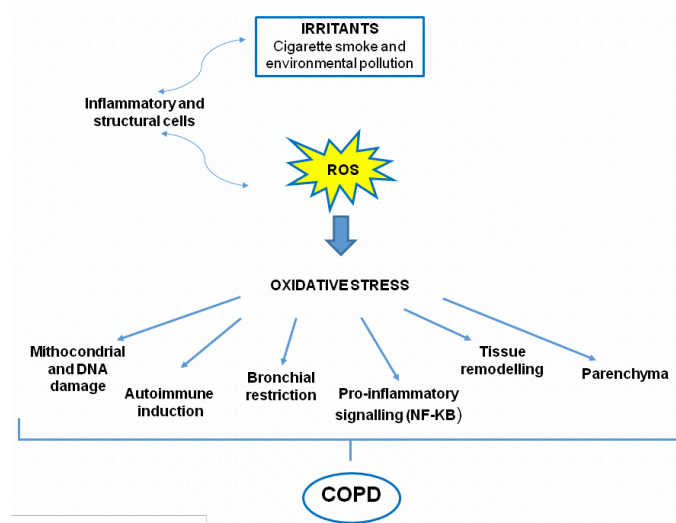


Figure 6. Oxidative stress in COPD. Both oxidants generated from inhaled oxidants (cigarette smoke) and inflammatory cells in the lungs contribute to a burden of ROS, which drives many features of COPD. [23]

An important role in the pathology of COPD is the histones release from neutrophil and apoptotic cells. Histones have recently been demonstrated to function also as endogenous danger signals or DAMPs () when they translocate from the nucleus to the extranuclear space. H1, H2A, H2B, H3 and H4 are frequently detected at the cell surface or cytoplasm of immune cells, cerebellar neurons, Schwann cells and microglia in response to stress. Levels of circulating histones as well as nucleosomes are increased in patients with cancer, inflammation and infection, suggesting an extracellular role in human disease [25].

Histones are released from activated neutrophil by extracellular traps (NETs) in response to microbial infection. Extracellular traps are networks of extracellular fibres composed of neutrophil chromatin components and other antimicrobial factors, which capture and degrade invading microorganisms. Moreover, increased release of NET can lead to a unique form of immune cell death termed as “NETosis”. In addition to NETosis-mediated histone release, apoptotic or necrotic cells can release histones that are usually associated with impaired phagocytosis (Figure 7a). Extracellular histones have been considered as potential mediators of lethal systemic inflammatory diseases including infection and COPD (Figure 7b) [25].

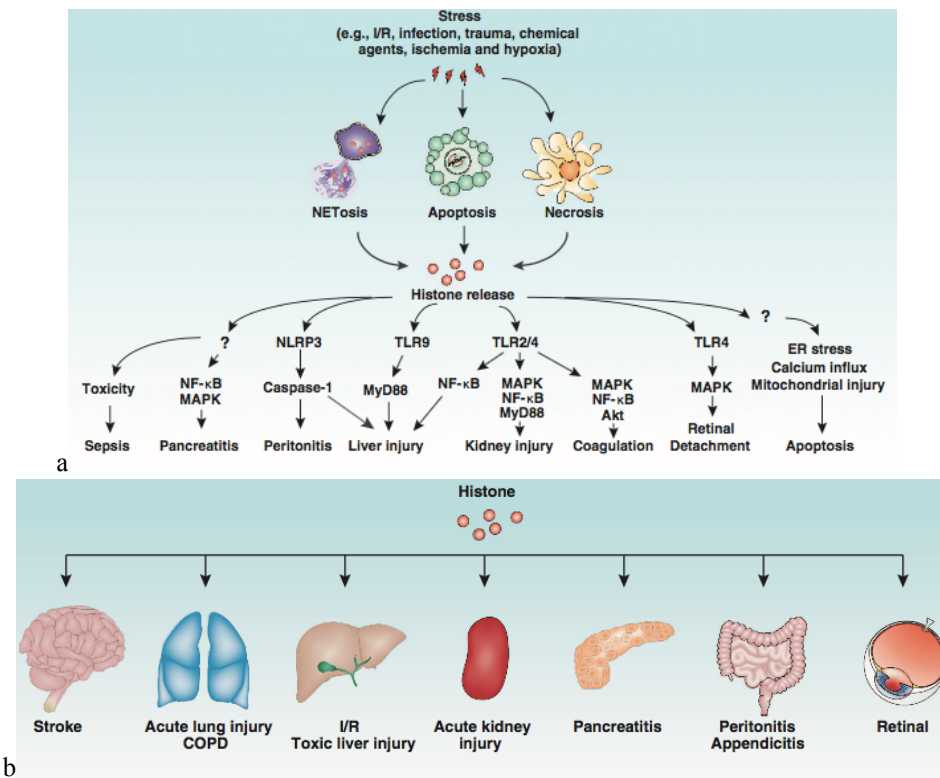


Figure 7. a. Release and activity of histones in response to stress. b. Histone-mediated tissue injury and disease. [25]

Apoptotic cells are defined by two major morphological characteristics: chromatin condensation and DNA fragmentation. Nuclear components are generally not released during apoptosis. However, increasing evidence indicates that cells undergoing apoptosis have the ability to release nuclear substances to the extracellular space. These nuclear substances include histone, HMGB1, DNA and possibly other nuclear proteins [25]. Histones are also involved in a self-sustaining cascade of apoptosis, which facilitates progression of COPD. In particular, hyperacetylated H3.3 is resistant to proteasomal degradation, which causes H3.3 accumulation in the extracellular space. Extracellular H3.3 binds to lung structural cells and induces apoptosis through several mechanisms, including induction of calcium influx, enhancement of the endoplasmic reticulum unfolded protein response and elevation of mitochondrial toxicity (Figure 7a). In contrast, the use of H3-neutralizing antibodies can protect against H3.3-mediated lung injury. These findings suggest that H3.3 released by apoptotic cells induces further apoptosis in lung cells, which establishes a vicious cycle [7].

1.2.4 Histone acetylation and deacetylation: importance in COPD

COPD involves inflammation with the coordinate expression of multiple inflammatory genes in the lungs. These inflammatory genes code for the expression of cytokines, chemokines, enzymes that synthesize inflammatory mediators, inflammatory mediator receptors and adhesion molecules, resulting in a coordinated influx and activation of inflammatory cells. Many of these inflammatory genes are regulated by proinflammatory transcription factors, including NF- κ B and activator protein (AP)-1 [26]. These transcription factors orchestrate, amplify and perpetuate the inflammatory response and form the molecular basis of chronic inflammation. Modification of core histones, around which DNA is wound within the chromosomes, plays a critical role in regulating the expression of all genes and in determining which genes are activated and which genes are repressed. Chromatin is made up of nucleosomes, consisting of DNA associated with an octamer of two molecules each of the core histone proteins (H2A, H2B, H3 and H4). In the resting cell, DNA is wound tightly around these basic core histones, excluding the binding of the enzyme RNA polymerase II. When pro-inflammatory transcription factors, such as NF- κ B, are activated, they bind to specific recognition sequences in DNA and subsequently interact with large co-activator molecules, such as CREB-binding protein (CBP), p300 and p300/CBP-associated factor (PCAF) [26]. These coactivator molecules act as molecular switches that control gene transcription and all have intrinsic Histone Acetyltransferase (HAT) activity. Each core histone has a long terminal, which is rich in lysine residues that may be acetylated, thus changing the electrical charge of the core histone. This results in acetylation of core histones, thereby reducing their charge, which allows the chromatin structure to transform from the resting closed conformation to an activated open form. Thus, this allows binding of TATA and RNA polymerase II, which initiates gene transcription [26]. While acetylation of histones is associated with gene induction, the removal of acetyl groups by Histone Deacetylase (HDAC) is associated with repacking of chromatin and a lack of gene expression or gene silencing. In COPD, there is a marked reduction in HDAC activity in the lung parenchyma, and this decrease is correlated with disease severity [26]. The reduction in HDACs is

selective for the isoform 2 in the peripheral lung. In patients with very severe disease, GOLD IV, there is a 95% reduction in the expression of HDAC2. Reduced HDAC activity is also related to resistance to the anti-inflammatory effects of corticosteroids, a characteristic feature of COPD. HAT activity is increased and HDAC2 activity is reduced in lungs of rats exposed to cigarette smoke, which show increased NF- κ B activation and expression of inflammatory genes [26]. Inflammatory diseases may be due to increased HAT, in asthma, decreased HDAC, in COPD, or a combination of both (Figure 8). Alveolar macrophages from normal smokers also show a reduction in HDAC activity and expression of HDAC2. This is correlated with an increase in release of TNF- α and IL-8 in response to an inflammatory stimulus and there is a further reduction in HDAC and HDAC2 in alveolar macrophages from COPD patients [26].

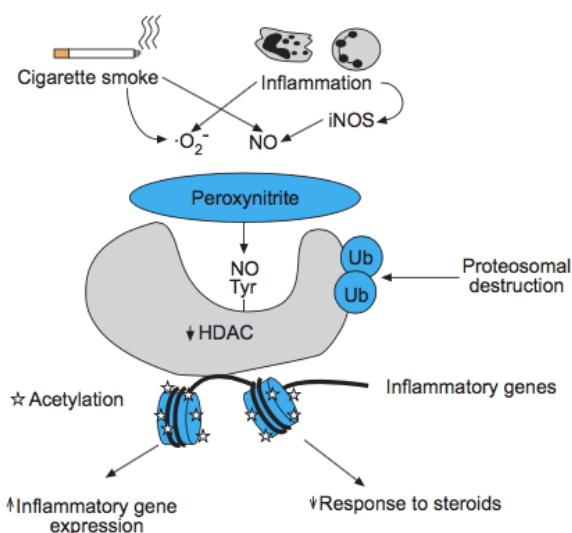


Figure 8. Possible mechanism of reduction in HDAC2. HDAC2 is inactivated by peroxynitrite, generated by an interaction of nitric oxide generated by inflammation and CS and superoxide anions. Peroxynitrite nitrates tyrosine residues on HDAC2 and this may block enzymatic activity and also mark the enzyme for destruction. The loss of HDAC2 leads to amplification of the inflammation and resistance to corticosteroids [26].

Previous studies using the Western blot analysis and chromatin immunoprecipitation (ChIP) assays demonstrated increased acetylation of histones 3 and 4, which was attributed to the decreased HDAC expression and activity [26]. Barrero *et al* [7] investigated whether H3.3 might be differentially acetylated in COPD. This study confirmed a previously reported COPD hyperacetylation, identifying the specific residues as Lys 10, 15, 19 and 24 and

previously unreported C-terminal acetylation at Lys 116 (Figure 9). The same study confirmed the effect of acetylation on proteasome degradation, Western blots show that hyperacetylated H3.3 is less sensitive to degradation by 20S proteasomes than H3.3 from the control cells. Probably the minor H3.3 sensitivity to proteasome degradation helps to account for the increase in lung H3.3 and induce apoptosis of airway epithelial cells and lung endothelial cells.

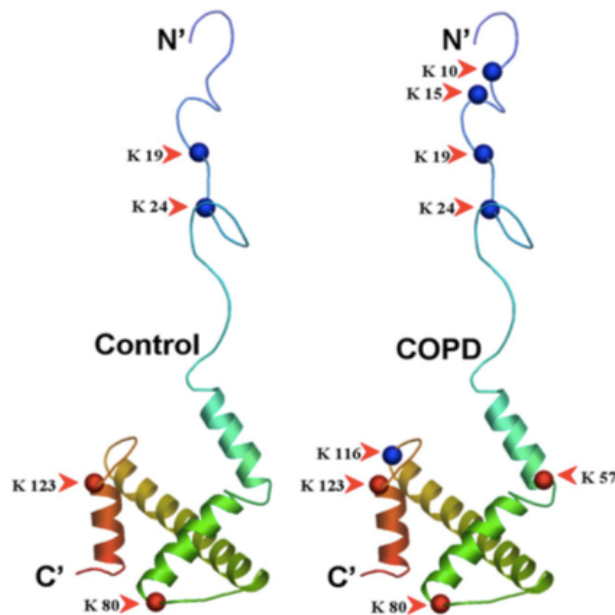


Figure 9. Ribbon diagram of histone H3.3 showing a comparison of acetylated (blue spheres) or ubiquitylated (red spheres) residues in GOLD IV-COPD patients and ex-smokers subjects (Control), as identified by mass spectroscopy [7].

1.2.5 Chronic bronchitis and Emphysema in COPD

The more familiar terms “chronic bronchitis” and “emphysema” are included within the COPD diagnosis and are the two major pathologic outcomes in COPD [WHO report], it is important to describe these aspects.

Chronic bronchitis

Chronic Bronchitis (CB) is defined by chronic cough and sputum production for at least 3 months per year for two consecutive years. CB has numerous clinical consequences, including an increased exacerbation rate, accelerated decline in lung function, worse health-related quality of life and possibly increased mortality. Mucous metaplasia, a process in which mucus is overproduced in response to inflammatory signals, is the pathologic foundation for CB. Mucus hypersecretion by goblet cells develops as a consequence of cigarette smoke exposure, infections or inflammatory cell activation of mucin gene transcription via activation of the epidermal growth factor receptor (EGFR). This is increased by difficulty in clearing secretions because of poor ciliary function, distal airway occlusion and ineffective cough secondary to respiratory muscle weakness and reduced peak expiratory flow [27]. There are both in vitro data and indirect clinical evidence supporting the role of Th17 inflammation in mucous metaplasia development in COPD. IL-17 is a potent inducer of IL-6 production by bronchial epithelial cells and both IL-6 and IL-17 are strong inducers of Muc5AC and Muc5B, the two major airway mucins, by lung epithelial cells [27] (Figure 10, upper panel)

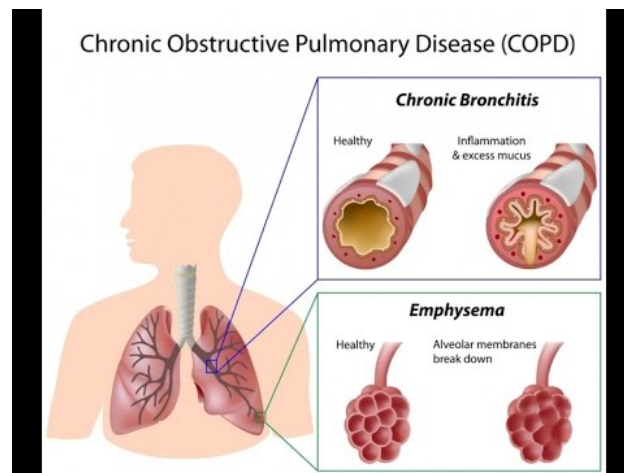


Figure 10. Morphologic features of Chronic Bronchitis and Emphysema. [Blogs.biomedcentral.com]

Emphysema

The lesions produced by emphysema were first described by Laennec and are defined by an abnormal and permanent enlargement of distal air space at the terminal bronchium,

accompanied by destruction of the walls without obvious fibrosis. *Centrilobular* emphysema is characteristic of smoking patients with COPD. The typical aspect is the lobules pathohistology: the proximal central portions of the acini, formed by the respiratory bronchioles, are involved, while distally alveoli are spared. Thus, within the same alveoli and lobule coexist emphysematous zones and normal zones. Lesions are more common and usually more severe in the upper lobes, particularly in the apical segments. It is common to find inflammation around bronchi and bronchioles and the distal part of the alveoli may also be affected in severe emphysema [28]. These injuries are the result of the destructive effects of high proteolytic activity, in fact, in smokers neutrophils and macrophages accumulate in the alveoli. Accumulated neutrophils are activated and release their granules content rich in cellular proteases (EN, proteinase 3 and cathepsin G), which causes tissue lesions [27]. Cigarette smoking also increases macrophages production of metalloproteases involved in the tissues destruction. This pathological destruction of the actual "respiratory" part of the lung is accompanied by a progressive reduction in stiffness making it more easily collapsable and thus aggravating the bronchial obstruction to the passage of the air with further accentuation of the patient's respiratory discomfort (Figure 10 lower panel).

1.2.6 Pathophysiology of COPD

Now there is a good understanding of how the underlying disease process in COPD leads to the characteristic physiologic abnormalities and symptoms. There are different features whose characterize the COPD pathophysiology:

- **Airflow limitation and air trapping**, the extent of inflammation, fibrosis and luminal exudates in small airways is correlated with the reduction and the accelerated decline of FEV₁ and FEV₁/FVC indexes in COPD patients [29]. This peripheral airway obstruction progressively traps air during expiration, resulting in hyperinflation. Although emphysema is more associated with gas exchange than with reduced FEV₁, it does contribute to air trapping during expiration. Hyperinflation reduces inspiratory capacity

such that functional residual capacity increases, particularly during exercise and this results in dyspnoea and limitation of exercise capacity [GOLD Report].

- **Gas exchange abnormalities**, result in hypoxemia and hypercapnia (hematic $\text{CO}_2 > 45$ mmHg) and have several mechanisms in COPD. In general, gas transfer worsens as the disease progresses. The severity of the emphysema correlates with arterial PO_2 and other markers of ventilation perfusion (V_A/Q) imbalance. Peripheral airway obstruction also results in a V_A/Q imbalance and combines with ventilator muscle impaired function in severe disease to reduce ventilation, leading to CO_2 retention. The abnormalities in alveolar ventilation and a reduced pulmonary vascular bed further worsen the V_A/Q abnormalities.
- **Mucus hypersecretion**, resulting in a chronic productive cough is a feature of chronic bronchitis and is not necessarily associated with airflow limitation. Not all patients with COPD have symptomatic mucus hypersecretion. When present it is due to mucus metaplasia with increased number of goblet cells and enlarged submucosal glands in response to chronic airway irritation by CS or other noxious agents.
- **Pulmonary hypertension**, mild to moderate pulmonary hypertension may develop late in course of COPD and is due to the hypoxic vasoconstriction of small pulmonary arteries, eventually resulting in structural changes. There is an inflammatory response in vessels, similar to that seen in the airways, and evidence for endothelial cell dysfunction. The loss of pulmonary capillary bed in emphysema may also contribute to increased pressure in pulmonary circulation. Progressive pulmonary hypertension may lead to right ventricular hypertrophy and eventually to right-side cardiac failure.
- **Systemic features**, it is increasingly recognized that COPD involves several systemic features, particularly patients with severe disease and these have a major impact on survival and comorbid diseases. Cachexia is commonly seen in patient with severe COPD. There may be a loss of skeletal muscle mass and weakness as a result of increased apoptosis or muscle disuse. Patients with COPD also have increased likelihood of having osteoporosis, depression and chronic anaemia [30]. Increased concentration of

inflammatory mediators and ROS may mediate some of these effects. There is an increased risk of cardiovascular diseases correlated with an increase in C-reactive protein (CRP).

- **Acute Exacerbations:** is an event characterized by a sudden worsening of the patient's respiratory symptoms and leads to a hospitalization and to a change in treatment, more details in paragraph number 1.2.7.

1.2.7 Acute Exacerbations aetiology

An exacerbation of COPD is an acute event characterized by a worsening of the patient's respiratory symptoms that is beyond normal day-to-day variations and leads to a change in medication. Acute Exacerbations of COPD (AECOPD):

- Negatively affect a patient's quality of life,
- Have effects on lung function that take several weeks to recover from,
- Accelerate the rate of decline of lung function,
- Are associated with significant mortality, particularly if requiring hospitalization,
- Have high socioeconomic costs.

Mortality reaches 40% at 1 year after discharge and 49% at 3 years after hospitalization [Gold Report]. Prevention, early detection and prompt treatment of exacerbations are vital to reduce the burden of COPD.

Predictor factors

Predictors for frequent exacerbations include various clinical factors such as daily cough, wheeze and sputum production, as well as, frequency of exacerbations in the previous year [31]. Recent published study showed that COPD smokers with chronic bronchitis had exacerbations 1.6–1.9 times more frequently than those without [31]. This suggests that factors predisposing to chronic bronchitis also predispose to exacerbation, possibly due to

reduced mucociliary clearance that facilitates bacterial invasion of mucosa. Indeed, excess production of mucus, which characterizes chronic bronchitis, has been shown to provide a site for bacterial adherence and it is associated with increased mortality from bacterial infection. In addition, saliva and serum levels of lysozyme have been studied in patients with chronic bronchitis. Patients with two or more exacerbations over 12 months had significantly lower serum levels of lysozyme, lysozyme activity and ability of saliva to aggregate non-typeable *Haemophilus influenzae* than those with less than two exacerbations [31].

Symptoms and causes

Understanding the aetiology of exacerbations requires that potential mechanisms of these episodes are related to the key symptoms:

- **Increased breathlessness**, one possible cause for these symptoms could be the increased metabolic/cationic state associated with pyrexia that rises oxygen demand and may increase hydrogen ion concentrations stimulating the respiratory centre to increase tidal volume and respiratory rate [31]. Another potential mechanism for this change in airflow would be the airway narrowing by bronchospasm which could be mediated by endothelin-1. In addition to promoting bronchial hyper responsiveness, endothelin-1 may stimulate mucus secretion, promote airway oedema and smooth muscle proliferation, as well as upregulate production of cytokines. The concentration of this peptide, which is produced by the bronchial epithelium, alveolar macrophages and pulmonary endothelium is increased in sputum. Infiltration of the airway wall with inflammatory cells could also contribute to airflow limitation. During exacerbation, biopsy studies have shown that the inflammation becomes more marked with recruitment of eosinophils and an increase in the population of CD4⁺ lymphocytes. Furthermore, sputum studies have shown increased neutrophil content and increased protein leakage from serum to sputum which also occurs during mucoid exacerbations that may lead to oedema of the airway wall. The presence of sputum in the airways would be expected to reduce its airway calibre and this effect would be enhanced if the viscosity of the sputum increased. Gas exchange deteriorates during exacerbations through worsening V/Q matching.

- **New or increased sputum purulence**, a major finding in airway secretions during exacerbations is associated to an increase in neutrophils [31]. Neutrophil degranulation results in release of elastase and other proteinases which may cause epithelial damage, reduce ciliary beat frequency, stimulate mucus secretion by goblet cells and increase the permeability of the bronchial mucosa, resulting in airway oedema and protein exudation into the airway. Another potential mechanism which may explain many of the features of exacerbation is eosinophil recruitment. Biopsy studies have shown 30 folds higher numbers of eosinophils in bronchial mucosa during exacerbations [32] and serum levels of eosinophilic cationic protein are higher in patients with exacerbations than in those with stable COPD [31]. Although this suggests an “asthmatic profile”, the observed eosinophils are not degranulated (as they would be in asthma) and are not associated with increased IL-5 expression. The relative importance of the eosinophilia remains to be determined, but several eosinophil products may cause inflammatory damage to the airway (eosinophil peroxidase, major basic protein, eosinophil cationic protein, metalloproteinases and cysteinyl leukotrienes) and, together with histamine, can also cause bronchospasm. The presence of eosinophils in airway secretions can contribute to sputum purulence which is a feature of some exacerbations [31].

- **Increased sputum production**, is given as a result of the previous mechanisms.

Causes

Exacerbations of COPD can be precipitated by several factors: bacteria, viruses and environmental agents account for the vast majority of episodes of exacerbation. In a recent study of patients admitted to hospital with severe exacerbations, 78% of patients had evidence of viral or bacterial infection. However, many patients suffer from exacerbations where no specific causes can be identified [32].

Bronchoscopic studies have shown that at least 50% of patients have bacteria in their lower airways during exacerbations of COPD [32], but a significant proportion of these patients also have bacteria colonizing their lower airways in the stable phase of the disease. Systemic and mucosal immune responses to non-typeable *Haemophilus influenzae*, *Moraxella*

catarrhalis and *Streptococcus pneumoniae* develop in the majority of exacerbations associated with isolation of these bacteria from sputum [32]. The acquisition of bacterial strains that are new to the patient is associated with exacerbations of COPD [32]. On the other hand, approximately 50% of exacerbations are associated with upper respiratory tract virus infections and infection with rhinovirus, respiratory syncytial virus and influenza. The presence of an upper respiratory tract infection leads to a more severe exacerbation and a longer symptom recovery time. Increased symptoms induced by virus-associated exacerbations appear to last longer than bacterial exacerbations [32]

Peaks of air pollution can also precipitate exacerbations of COPD and increase hospitalizations and mortality [33]. However, the cause of about one-third of severe exacerbations of COPD cannot be identified. Some patients appear particularly prone to suffer exacerbations of COPD whereas others do not.

In addition to infections and exposure to pollutants, exacerbations of respiratory symptoms (especially dyspnoea) in patients with COPD may be due to different mechanisms that may overlap in the same patients. Conditions that may mimic and/or aggravate exacerbations, including for example pneumonia, pulmonary embolism, pneumothorax and pleural effusion need to be considered [34].

The AECOPD are classified as Mild, Moderate or Severe, sometimes associated with acute respiratory failure.

1.2.8 Stages of COPD

COPD should be considered in any patient who has dyspnoea, chronic cough or sputum production and/or history of exposure to risk factors for the disease. A detailed medical history of a new patient who is known, or suspected, to have COPD is essential. Spirometry is required to make the diagnosis in this clinical persistent airflow limitation and thus of COPD in patients with appropriate symptoms and significant exposures to noxious stimuli. Spirometry is the most reproducible and objective measurement of airflow limitation, it is a non-invasive and readily available test. Spirometry consists in two indexes:

- Forced expiratory volume (FEV₁) that measures how much air a person can exhale during the first seconds of the forced breath measured in liters,
- FEV₁/FVC that represents the ratio between the forced vital capacity (total amount of air that can be forcibly be blown out after full inspiration, measured in liters) and forced expiratory volume.

According to GOLD initiative, a collaboration between the US National Institutes of Health (NIH) and the World Health Organization (WHO) the COPD patients are classified as follows:

Stage I (GOLD I): Mild COPD - Characterized by mild airflow limitation, chronic cough and sputum production may be present.

Stage II (GOLD II): Moderate COPD - characterized by a worsening airflow limitation, shortness of breath, exertion and cough sputum production.

Stage III (GOLD III): Severe COPD - characterized by a further worsening of airflow limitation, greater shortness of breath, reduced exercise capacity, fatigue and repeated exacerbations that almost always have an impact on patients' quality of life.

Stage IV (GOLD IV): Very Severe COPD - characterized by severe airflow limitation and respiratory failure is defined as an arterial partial pressure of O₂ (PaO₂) less than 8.0kPa. Respiratory failure may also lead to effects on the heart such as *cor pulmonale* and elevation of the jugular venous pressure. At this stage, quality of live is appreciably impaired and exacerbations may be life threatening.

The FEV₁ and FEV₁/FVC are indicated in the following table.

GOLD GROUP	STAGE	FEV ₁ (predicted)	FEV ₁ /FVC
GOLD I	MILD	≥80%	< 0.70%
GOLD II	MODERATE	50% ≤ FEV ₁ <80%	< 0.70%
GOLD III	SEVERE	30% ≤ FEV ₁ <50%	< 0.70%
GOLD IV	VERY SEVERE	<30 or <50% with chronic respiratory failure	< 0.70%

Table 1. Classification of airflow limitation severity in COPD based on FEV₁ and FEV₁/FVC

1.2.9 COPD biomarkers: state of art

A crucial aspect in the study for a COPD treatment is the characterization of a biomarker that reflects the presence, severity or state of a disease. Furthermore, the natural history of COPD is marked by episodes of deterioration, exacerbations of COPD, which lead to increased morbidity and mortality. An ERS/ATS Task Force published in 2008 has described Acute Exacerbation (AECOPD) as one of the clinical outcomes of COPD that should be used for the assessment of patients and for defining the impact of treatment interventions. Sampling methods elaborated during the last decades offer an innovative basis for the identification of pulmonary biomarkers. These techniques may be totally non-invasive, semi-invasive or invasive [4]. For COPD the only biomarkers currently widely used in drug trials is lung function testing, FEV₁ and FEV₁/FVC. Although FEV₁ and FEV₁/FVC are easy to obtain and reproducible they don't inform about underlying disease activity, don't separate out phenotypes of COPD, are not specific to COPD and are unresponsive to some therapies that clearly improve survival [5].

Non-invasive sampling

Exhaled biomarkers (EB)

Breath analysis is considered to be a valuable non-invasive technique for sampling volatile biomarkers. Fractional exhaled nitric oxide (FeNO) is the only exhaled biomarker studied in AECOPD. Electronic nose, a recently developed “omics” technique that provides a “breathprint” of exhaled volatile organic compounds, has not been studied yet during AECOPD. Although, in stable COPD FeNO is derived predominantly from the periphery of the lung, in AECOPD it appears to be produced homogeneously in the central and peripheral airways. The lack of data uniformity for this biomarker may be attributed to different study designs and confounding factors, such as smoking or inhaled corticosteroids, which are known to influence FeNO levels [4].

Exhaled breath condensate (EBC)

Exhaled breath is saturated with water vapour which can be condensed by cooling and used to sample a wide range of mediators. EBC samples the entire respiratory tract but newer techniques allow fractionated sampling and provide the ability to collect condensate from different parts of the respiratory tract. EBC collection is a promising sampling method but several methodological issues hamper its clinical use. Only a few studies have focused on EBC biomarkers of AECOPD and so far no study has assessed the course of biomarkers between baseline and the onset of AECOPD. EBC pH, one of the most validated EBC biomarkers, has been assessed only by one study which found no correlations with pulmonary function tests and arterial blood gas parameters [4]. NO-related products have not yet been evaluated in this context, whereas for hydrogen peroxide published data showed correlations with dyspnoea but no correlations with the clinical status or the pulmonary function tests. Isoprostanes and leukotrienes, are arachidonic acid metabolites that have also been measured in EBC samples. Definite conclusions cannot be drawn based on published evidence because controversial [4]. Despite the abovementioned problems of traceability, pulmonary sampled cytokines have been extensively studied in the context of AECOPD. Of interest is the rather distinct pattern of TNF- α . The measurement of cytokines in lower respiratory tract infections

and inflammatory conditions is not sufficiently useful. This is mainly due to short plasma half-life, rapid turnover, presence of blocking factors, and compartmentalised production in the lung. Therefore, acute phase proteins and the so-called hormokines seem to be more reliable, owing to their longer plasma half-life, fewer variations in daily levels and stability in vivo and *ex vivo* [6].

Spontaneous sputum (SS)

Most of the SS biomarkers studied during AECOPD were evaluated for their associations with the clinical severity and the causal diagnosis such as Neutrophil elastase (NE) and some antimicrobial. Published studies report that in AECOPD sputum myeloperoxidase (MPO) and IL-8 are associated with sputum colour and purulence. Moreover, MPO has been associated with the sputum leucocyte count, IL-8 with sputum bacterial load and the macrophages count and LTB4 concentration has been associated with the overall chemotactic activity of sputum. Again, these studies aren't sufficiently useful as predictor biomarkers [4].

Semi-invasive sampling

Induced sputum (IS)

IS is used in clinical practice for microbiological and cell count studies, whereas measurement of inflammatory biomarkers is increasingly implemented in research. Several biomarkers have been measured in the supernatants of IS, notably IL-6, IL-8 and TNF- α , but methodological issues influenced the measurement making these studies inconclusive [4].

Invasive sampling

Broncho alveolar lavage (BAL)

BAL from bronchoscopy permits the study of cellular and biochemical components present in the epithelial lining fluid. So far only a few studies assessed simultaneously BAL and other airway sampling techniques in AECOPD. Based on current evidence, the clinical usefulness of BAL biomarkers is rather limited. BAL biomarkers may illustrate the underlying mechanisms of AECOPD, but methodological issues such as low sample numbers or sample

manipulation techniques have been considered to be confounding factors limiting the statistical significance of the results [4].

Biomarkers of bronchial biopsies obtained during AECOPD

Biomarkers expressed in biopsies obtained during AECOPD have been studied, but associations with clinical variables or outcomes have not been sufficiently assessed [4].

Inflammation biomarker

An acute phase reactant extensively evaluated in clinical situations is C-reactive protein (CRP). Its levels are increased in the presence of localised bacterial and viral infections, and also in chronic inflammatory conditions [6]. Another promising inflammatory mediator is neopterin, it is a 2-amino-4-hydroxy pteridine synthesised by macrophages and monocytes after induction by interferon- γ secreted by T-lymphocytes. It has been reported to act as a mediator of cell immunity against intracellular pathogens, such as viruses, parasites and intracellular bacteria. The soluble form of the triggering receptor expressed on myeloid cells (sTREM)-1 is expressed on neutrophils, mature monocytes and macrophages, its levels being increased during sepsis, and not during non-infectious inflammatory conditions [6].

Procalcitonin, Adrenomedullin, Copeptin and Endothelin-1 are also known as hormokines, they can follow either a classical hormonal expression, or under specific inflammatory and infectious conditions show a cytokine-like behaviour. From natriuretic peptides family, two biomarkers are also candidates: Atrial Natriuretic Peptide, and Brain Natriuretic Peptide [6].

Extracellular histones have been reported as a hallmark for different diseases such as sepsis and trauma-induced lung injury. In COPD, histones are involved in a self-sustaining cascade of apoptosis, which facilitates progression of chronic obstructive pulmonary disease [7]. Increased H3.3 levels were detected in BALF and blood of GOLD 4 patients [7]. At the base of the mechanism that lead to histones' release, there can be the role for apoptotic and necrotic cells in the lungs as well as the activated neutrophils that led to neutrophil extracellular traps (NETs) release, all factors correlated with inflammatory aspects. Therefore, the clarification of histones involvement and role in the origination and propagation of the disease is a promising approach for diagnosis and treatment of COPD [7].

1.3 Type 2 Diabetes Mellitus

Diabetes mellitus (DM) is probably one of the oldest diseases known. It was first reported in Egyptian manuscript and Indian physicians about 3000 years ago. The term “diabetes” was first used in 230 B.C. from the Greek Apollonius da Menfi. The term “Mellitus” or “Honey” was added by British John Rolle in the late eighteenth century. Effective treatment was not developed until the first half of the 20th century, when in 1921 Frederick Banting and Charles Herbert Best discovered the insulin. Type 2 Diabetes makes up about 90% of cases of diabetes, with the other 10% due primarily to diabetes mellitus type 1 and gestational diabetes [WHO report, Figure 11].

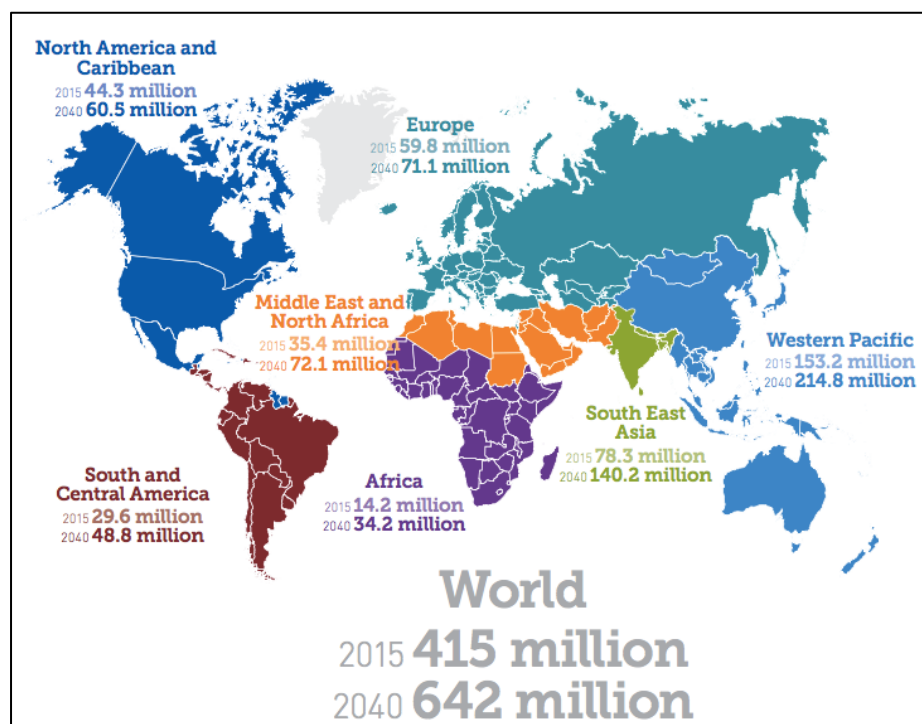


Figure 11. Estimated number of people with diabetes worldwide and per region in 2015 and 2040 [IFD Diabetes Atlas 7th].

1.3.1 Definition

Diabetes, according WHO, is a chronic disease that occurs either when the pancreas does not produce enough insulin or when the body cannot effectively use the insulin it produces. Type 2 Diabetes (T2D) comprises the majority of people with diabetes around the world and is largely the result of excess body weight and physical inactivity. Symptoms include excessive excretion of urine (polyuria), thirst (polydipsia), constant hunger, weight loss, vision changes and fatigue. Until recently, this type of diabetes was seen only in adults but it is now also occurring increasingly frequently in children and pets.

1.3.2 Risk Factors and Diagnosis

- **Obesity**, the major potentially modifiable risk factor for T2D, exists an exponential relationship between Body Mass Index (BMI) and the risk of T2D. Obesity has been found to contribute to approximately 55% of cases of type 2 diabetes [35]; chronic obesity leads to increased insulin resistance that can develop into type 2 diabetes, most likely because adipose tissue (especially that in the abdomen around internal organs) is a source of several chemical signals, hormones and cytokines, to other tissues.
- **Diet**, the composition of dietary fat intake is linked to diabetes risk; decreasing consumption of saturated fats and trans fatty acids while replacing them with unsaturated fats may decrease the risk. Sugar sweetened drinks appear to increase the risk of T2D both through their role in obesity and potentially through a direct effect [36].
- **Early life**, research also suggests intrauterine growth restriction or prenatal undernutrition (macro and micronutrient) as another probable factor [37].
- **Stress**, different forms of emotional stress, depression anxiety and anger/hostility, are associated with an increased risk for the development of T2D [38].
- **Sleep**, reduction in sleep is associated with a significant increase in the incidence of type 2 diabetes [39].

- **Genetic**, more than 36 genes have been found that contribute to the risk of T2D, all of these genes together still only account for 10% of the total genetic component of the disease [40]. There are a number of rare cases of diabetes that arise due to an abnormality in a single gene (monogenic) [41].
- **Age**, one of the main drivers of the occurrence of type 2 diabetes, people from 40/45 to 65 years old have a higher predisposition [42].
- **Ethnicity**, there seems to be an excess genetic risk of diabetes in certain ethnic groups such as South Asians, Afro-Americans and the indigenous people of certain regions, for example the Aborigines in Australia. However, it is not so much the genetic predisposition per se, as the influence on this genetic predisposition that explains the relatively recent increase in diabetes prevalence in these groups [42].
- **Socioeconomic factors**, two out of every three diabetes patients live in urbanized areas, and those in the lower socio-economic classes are disproportionately affected, possible because these classes are rising in the countries where recent urbanization and economic growth have most drastically changed lifestyle and longevity.
- **Sedentary**, has heavy effects on glucose metabolism and on the risk of becoming obese [42].

Diagnosis

Blood glucose values are normally maintained in a very narrow range, usually below 100 mg/dL in fasting condition or <110 before lunch and <120 before bedtime. The diagnosis of diabetes is established when an increase in blood glucose is observed with any of the following criteria [43]:

- A random blood sugar > 200 mg/dL, with classic signs and symptoms,
- A fasting plasma glucose (FPG) < 126 mg/dL in more than one occasion,
- An abnormal oral glucose tolerance test (OGTT) in which the glucose is > 200 mg/dL

Individuals with blood glucose lower than 100 mg/dL or less than 140 mg/dL after OGTT are considered euglycemic. However, those with fasting blood glucose greater than 100 but less than 126 or OGTT values greater than 140 but less than 200 are considered to have an impaired glucose tolerance (IGT) (table 2).

	Mg/DL	Fasting	After Eating	2-3 hours After Eating
Normal		80-100	170-200	120-140
Impaired Glucose		101-125	190-230	140-160
Diabetic		126+	220-300	200 plus



Table 2. Blood glucose chart showing the ranges of glycaemia for normal (green), pre-diabetic (yellow) and diabetic (red) patients in fasting, post prandial and IGT test conditions.

When the body processes sugar, glucose in the bloodstream naturally attaches to haemoglobin. The amount of glucose that combines with this protein is directly proportional to the total amount of sugar that is in the system at that time. Because red blood cells in the human body survive until 120 days before renewal, measuring glycated haemoglobin (or HbA1c) can be used to reflect average blood glucose levels over that duration, providing a useful longer-term gauge of blood glucose control. If the blood sugar levels have been high the HbA1c will also be elevated [43].

1.3.3 Insulin mechanism of action and GLUT4 transporter

Normal glucose metabolism is closely regulated by three related mechanisms: production of glucose from the liver, glucose uptake by peripheral tissues, in particular skeletal muscle, and insulin action on glucose and counter-regulating hormones such as glucagon. Insulin and glucagon have opposite regulatory effects on glucose homeostasis. During fasting, low levels of insulin and elevated glucagon facilitate gluconeogenesis and liver glycogenolysis by lowering glycogen synthesis and thus preventing hypoglycaemia [27]. Therefore, plasma glucose levels in fasting plasma are mainly determined by the production of hepatic glucose. After a meal, insulin levels increase and glucagon levels decrease in response to glucose

intake. Insulin promotes the absorption and use of glucose in tissues. Skeletal muscle together with adipose tissue are the most responsive sites of insulin for the use of post prandial glucose and is also crucial for preventing hyperglycaemia and maintaining the glucose homeostasis [27].

Insulin release regulation

The insulin gene is expressed in the β -cells of pancreatic islets. Pre-proinsulin is synthesized in the rough endoplasmic reticulum from insulin mRNA and transported to the Golgi apparatus. A series of proteolytic cleavages subsequently generate mature insulin and the cleavage of peptide C. Both insulin and peptide C are then accumulated in secretory granules and secreted after physiological stimulation [27]. The most important stimulus to synthesis and release of insulin is the glucose. An increase in blood glucose causes glucose uptake in the pancreatic β -cells favoured by a glucose transporting channel, insulin-independent, GLUT-2. Glucose metabolism through glycolysis generates ATP, causing an increase in cytoplasmic ATP/ADP ratio, this inhibits ATP-responsive K^+ activity on β -cell membrane, leading to depolarization of the membrane and Ca^{2+} extracellular intake through the channels of Ca^{2+} voltage-dependent [27]. The consequent increase in Ca^{2+} intracellular stimulates the secretion of insulin, stored in the cell granules β (figure 12) [27].

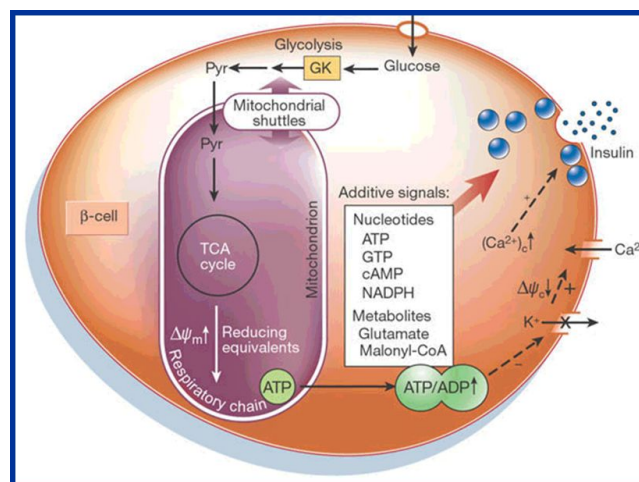


Figure 12. Schematic mechanism of insulin release after glucose intake.

Insulin is one of the most powerful anabolic hormone known, with multiple effects of inducing synthesis and promoting growth. Its main metabolic function is to increase the rate of glucose transport within certain cells of the body. These are represented by striated muscle cells and adipocytes, representing about 2/3 of the total body weight. In muscle cells, glucose is then stored as glycogen or oxidized to generate ATP [27]. In adipose tissue, glucose is stored mainly in the form of lipids. In addition to promoting synthesis, insulin also inhibits lipid degradation in adipocytes. Likewise, insulin promotes the capture of aminoacids and protein synthesis and inhibits the degradation of proteins. Thus, the anabolic effects of insulin are attributable to the increased synthesis and reduced degradation of glycogen, lipids and proteins. Insulin binding to its receptor activates a complex cascade of phosphorylation and protein dephosphorylation that culminates in the metabolic and mitogenic effects described above. The insulin receptor is a tetrameric protein composed of two subunits α and two β [27]. The cytosolic domain of subunit β possesses tyrosine kinase activity. By binding the insulin to the extracellular domain of the subunit α activates the tyrosine kinase of subunit β causing both the receptor's auto-phosphorylation and the phosphorylation of signal transduction elements downstream. The metabolic effects of insulin are mainly mediated by phosphatidylinositol-3-kinase (PI-3K). The PI-3K-dependent signal mediates many of the cellular effects of insulin (Figure 13) [27].

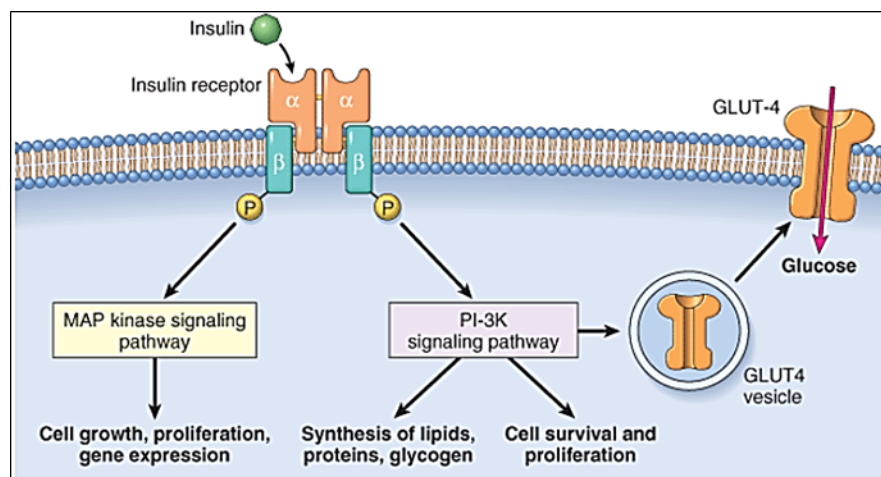


figure 13. Effects of insulin on cell activity and on GLUT4 membrane exposition.
[usmle.biochemistryformedics.com/mechanism-of-action-of-insulin/]

GLUT4 also known as solute carrier family 2, facilitated glucose transporter member 4, is a protein encoded, in humans, by the *SLC2A4* gene. GLUT4 is one of 13 members of the GLUT family of facilitative transmembrane hexose transporters, each of which has a distinct affinity and specificity for particular hexoses, as well as unique tissue distribution, subcellular localization and physiological function [44]. The structure comprises 12 transmembrane domains (Figure 14), and characteristic sequences in both its COOH and NH₂ terminal domains are important determinants of its intracellular localization and trafficking [45]. N-terminal sequence contains a potentially critical phenylalanine residue, as well as dileucine and acidic motifs in the COOH terminus, these motifs likely govern kinetic aspects of both endocytosis and exocytosis in a continuously recycling trafficking system [45].

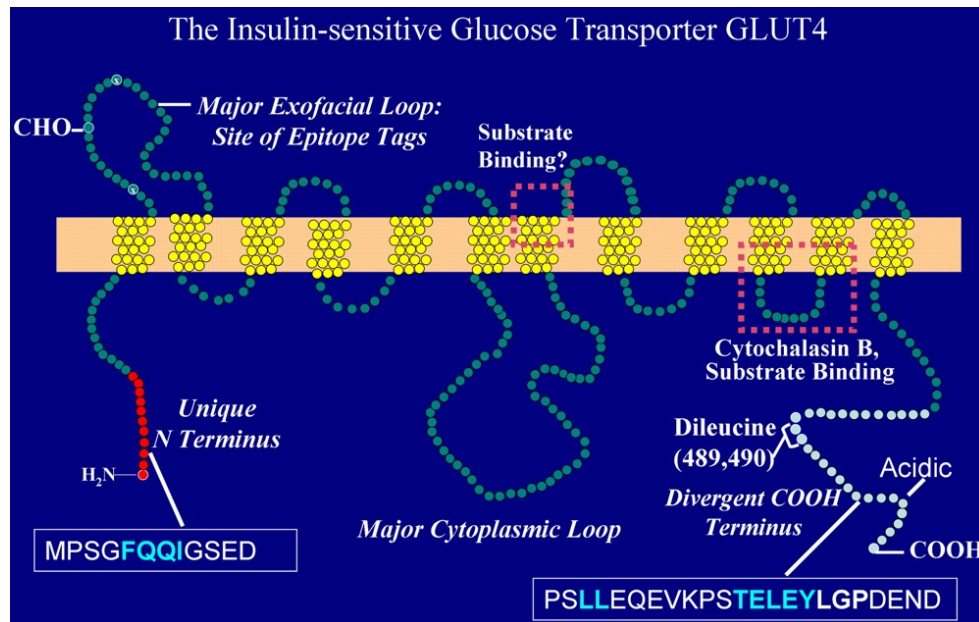


Figure 14. Structural Features of the Insulin-Regulated GLUT4 Glucose Transporter Protein. [45]

GLUT4 is a high affinity glucose transporter that is predominantly expressed in muscle cells and adipocytes. In the absence of insulin, the majority of GLUT4 is distributed between endosomes, the *trans*-Golgi network (TGN) and heterogeneous tubule– vesicular structures that consist of endosomal sorting intermediates and specialized GLUT4 storage vesicles (GSVs). In the absence of insulin, only ~5% of the total transporter pool is found on the cell surface [46]. Exclusion of GLUT4 from the cell surface depends on efficient sorting and sequestration into GSVs that do not cycle to the plasma membrane in the absence of

stimulation but translocate there in response to insulin or exercise, which results in a tenfold increase in glucose uptake [46]. The failure of GLUT4 to translocate to the plasma membrane in response to insulin is an early step in the development of insulin resistance and type 2 diabetes mellitus.

About 90% of insulin-stimulated glucose uptake occurs in skeletal muscle. Although adipose tissue accounts for only 10% of insulin-stimulated glucose uptake, this process is important for controlling whole body energy homeostasis, as adipocytes serve as a cellular 'rheostat' that senses the energy status and responds by secreting numerous hormones, cytokines and chemokines that regulate metabolism in muscle, liver and brain [46]. GLUT4 delivery to the cell surface requires its mobilization from intracellular membrane compartments, recognition of GLUT4-containing vesicles at the plasma membrane and finally fusion of these two membranes. Insulin signaling coordinates these steps by engaging a series of small GTPases. Active GTPases interact with multiple components of the trafficking machinery to confer directionality and specificity in membrane flow. In addition to small GTPases, insulin signaling directly targets motor proteins, membrane tethers and fusion regulating proteins, which suggests that insulin acts at multiple steps in the GLUT4 trafficking itinerary to increase the concentration of the transporter on the surface of the cell [46]. The insulin signaling pathways acutely upregulate GLUT4 surface levels largely by increasing exocytosis of GLUT4 storage vesicles (GSVs). However, there is evidence that insulin might also affect other stages of GLUT4 trafficking, including endocytosis, sorting in the endosomal system and the formation of GSVs [46]. The recruitment of GSVs can occur by PI3K-dependent insulin pathway or by APS-insulin signal pathway. GSV exocytosis can be separated into three distinct processes:

1. **Translocation**, insulin stimulates the accumulation of GLUT4-containing vesicles at the periphery of the cell within 5 minutes of exposure to the hormone. Whether insulin regulates GSV movement on cytoskeletal tracks is still debated [46].
2. **Targeting**, the vesicles are initially recognized by the destination membrane. In adipocytes, GSV targeting to lipid rafts on the cell surface is important for efficient insertion of GLUT4 into the plasma membrane. After stimulation of cells with insulin, the level of

GLUT4 increases in the plasma membrane several minutes before GLUT4 is exposed extracellularly. A crucial component of the GLUT4 targeting machinery is the exocyst, an octameric complex, that assembles at sites of exocytosis and tethers exocytic vesicles to the plasma membrane [46].

3. **Fusion**, GSV fusion with the plasma membrane is driven by the assembly of SNARE complexes. The activated insulin receptor phosphorylates the fusion regulatory protein of SNARE, MUNC18C, which then stimulates GSV fusion [46].

1.3.4 Pathology and pathophysiology of T2D

Hyperglycaemia, is a common effect of uncontrolled diabetes and over time leads to serious damage to many of the body's systems, especially the nerves and blood vessels. Type 2 diabetes is a chronic and progressive disease caused by various pathological mechanisms such as impaired insulin secretion, increased peripheral insulin resistance, and increased hepatic glucose production, resulting in increased concentrations of glucose in blood [47]. The morbidity associated with long-term diabetes of any type results from numerous serious complications that interest the medium and large calibre muscle arteries (macroangiopathy), as well as the target organ capillaries (microangiopathy). Macroangiopathy causes in diabetics an accelerated atherosclerosis, leading to a greater risk of myocardial infarction, stroke and lower limb gangrene [27]. The effects of microangiopathy are more severe in the retina, kidneys and peripheral nerves, causing, respectively, retinopathy, nephropathy and diabetic neuropathy. Diabetes is the first cause of blindness and terminal renal failure in the Western hemisphere, as well as contributing considerably to the annual incidence of cardiovascular events. Most experimental and clinical data suggest that complications of diabetes are a consequence of metabolic disorders of hyperglycaemia in particular. Two major multicentre trials for the study of the effects of glycaemic levels on long-term complications, Diabetes Control End Complication Trial and United Kingdom Prospective Diabetes Study have clearly demonstrated that progression of microvascular complications is delayed by strict control of hyperglycaemia [27]. At least three distinct metabolic pathways

appear to be implicated in the pathogenesis of complications of diabetes. Even if it is not established what is the prevalent one. These routes are as follows:

- **Formation of final products of advanced glycosylation**, the final products of advanced glycosylation (AGE) are formed by the non-enzymatic reaction between the intracellular precursors of glucose-derived carbonyl compounds and the amine protein group both intra and extra cell. AGE have various chemical and biological properties that are detrimental to both extracellular matrix components and target cells of diabetic complications. The receptor-AGE bond causes NF-kB factor activation and translocation, generating a variety of cytokines, growth factors, and other pro-inflammatory molecules [27].

- **Activation of protein kinase C (PKC)**, intracellular activation by calcium ions and the second messenger diacylglycerol (DAG) is an important signal transduction path in many cellular systems. Intracellular hyperglycaemia may stimulate the newly synthesized DAG from glycolysis intermediates and thus cause PKC activation. The secondary effects of PKC activation are numerous and include:

- production of VEGF (Vascular Endothelial Grow Factor) involved in neurovascularization characterized by diabetic retinopathy,
- increased activity of endothelin-1 vasoconstrictor and reduction of nitric oxide endothelial vasodilator synthesis (eNOS),
- production of pro-fibrogenic molecules such as TGF- β leading to an increased extracellular matrix deposit and basal membrane material,
- producing pro-coagulant molecule plasminogen activator inhibitor 1 (PAI-1) leading to reduced fibrinolysis and possible occlusive vascular episodes,
- pro- inflammation by the endothelium [27],

- **Intracellular hyperglycaemia with polyol pathway alteration**, in some tissues that do not require insulin for glucose transport hyperglycaemia leads to an increase intracellular glucose which is then metabolised by sorbitol aldose reductase, a polyol, and finally fructose. During this process, intracellular NADPH is used as a cofactor. The NADPH is also needed

as a cofactor of the glutathione reductase enzyme to regenerate reduced glutathione (GSH). GSH is one of the major antioxidant mechanisms in cells, and a reduction in GSH levels increases cellular susceptibility to oxidative stress. In the presence of prolonged hyperglycaemia, progressive overexpression of intracellular NADPH from the aldose-reductase compromises the regeneration of GSH [27].

Insulin resistance and prediabetes

In insulin resistance, muscle, fat, and liver cells do not respond properly to insulin and thus cannot easily absorb glucose from the bloodstream [48]. As a result, the body needs higher levels of insulin to help glucose enter cells [27]. The β cells in the pancreas try to keep up with this increased demand for insulin by producing more of this hormone. As long as the beta cells are able to produce enough insulin to overcome the insulin resistance, blood glucose levels stay in the healthy range. Over time, insulin resistance can lead to type 2 diabetes and prediabetes because the β -cells fail to keep up with the body's increased need for insulin and the glucose builds up in the bloodstream. Although insulin resistance alone does not cause T2D, it often sets the stage for the disease by placing a high demand on the insulin-producing β -cells. Healthy lifestyle including control of body weight, change the diet and increase the physical activity prevents the insulin resistance onset [49]. The role of resistance insulin in type 2 diabetes pathogenesis can be more clearly assessed on the basis of the observations that:

- Insulin-resistance is often found 10-20 years before the onset of diabetes in predetermined subjects [27],
- In prospective studies, insulin resistance is more important predictor of succession in diabetes mellitus [27].

Obesity-linked insulin resistance greatly increases the risk for type 2 diabetes but exactly how obesity promotes insulin resistance and other associated problems remains incompletely understood [50]. Genetic defects of the receptor and the insulin regulation pathway and obesity have, so far, been considered the responsible for insulin resistance.

Previously, by Professor Merali's group [50], it has been shown that healthy men supply ~ 6000 kcal/day [~ 50% carbohydrates, ~ 35% fat and ~ 15% protein] for 1 week has produced rapid growth by weight and rapid onset (after 2 or 3 days) of insulin resistance and oxidative stress at systemic level and fat tissue. In adipose tissue, oxidative stress causes a large oxidation and carbonylation of numerous proteins, including GLUT4 carbonylation close to the glucose transport channel (R246, R265 and K264), which is likely to cause a GLUT4 loss activity. These findings suggest that the initial occurrence of insulin resistance can be the overactive oxidative stress resulting in inactivation of GLUT4, at least in part, by oxidation and carbonylation [50].

1.3.5 Type 2 Diabetes biomarkers: state of art

Haemoglobin A1c (HbA1c) as a Biomarker in Diabetes

The use of HbA1c as a diagnostic criterion for diabetes ($\geq 6.5\%$) and pre-diabetes (5.7-6.4%) was recently added to the standards of care by the American Diabetes Association (ADA) based on the recommendations of the International Expert Committee. The consensus recognized several advantages of HbA1c test in comparison to fasting plasma glucose levels test. Specifically, HbA1c is viewed as a better standardized assay than glucose, a better index of overall glycaemic exposure and as less subject to biological variability, pre-analytic instability, prandial status, and acute stress. The epidemiological evidence on the role of age, race, genetics, and physiology that are biological determinants of the HbA1c-blood glucose relationship further limits the assumption that HbA1c is a consistent measure of mean blood glucose [8].

Metabolic Biomarkers in Diabetes: Glycation, Oxidation and Carbonyl Stress

The discovery of HbA1c and its identification as a glycated form of haemoglobin, opened a field of diabetes research that has since been growing for over forty years: the chemistry of glycation (non-enzymatic glycosylation) and its consequences, including the role of advanced glycation end-products (AGEs), free-radical damage mediated by reactive oxygen

species and lipoxidation. Modification of many types of biomolecules (not only proteins, but also phospholipids and nucleic acids in both intra- and extra-cellular locations), is mediated by reactive intermediate products formed as a result of carbohydrate and lipid oxidation. In diabetes, increased substrate for these oxidative reactions (resulting from hyperglycaemia and dyslipidaemia) and increased oxidative stress accelerate the molecular damage, yielding altered species that may serve as both markers and mechanisms of disease. The binding of AGEs with cellular receptors activates pathways that have been implicated in the pathogenesis of vascular complications in diabetes. Serum levels of soluble receptors of AGE products have been proposed as predictive biomarkers of risks of coronary heart disease in type 2 diabetic patients [8].

Biomarkers of Vascular Function in Diabetes

The endothelium has numerous functions: acting as a structural barrier between the circulation and the tissue, as a source of growth factors and angiogenic and anti- angiogenic factors, controlling thrombosis and fibrinolysis, mediating inflammation and mediating vascular tone. In diabetes, all of these functions are perturbed: basement membranes are thickened, permeability is altered, angiogenic/antiangiogenic balance is disturbed (with increases in either cell proliferation or cell death), thrombosis and platelet activation are increased, inflammation is enhanced, vascular tone is altered and there is injury mediated by accumulation of lipids in the sub-endothelial space. These functional effects may precede measurable structural changes, providing chances for functional biomarker development [8].

Tissue Biomarkers in Diabetes: Skin and Retina

Recently, non-invasive means to measure fluorescence of skin collagen, the surrogate measure of cumulative glycoxidative damage in skin, have been developed. This technique, which obviates the need for skin biopsy, is under intensive evaluation as a means to screen for the presence of undiagnosed diabetes and to determine susceptibility for complications of diabetes. It represents a new form of biomarker which detects tissue damage independent of changes in short-lived plasma proteins or urine. Another opportunity for new biomarker development is the retina [8]. Diabetic retinopathy is the most frequent cause of blindness in

adults in the developed world. The retinal microcirculation and associated measures of serum lipoproteins may be used as biomarkers in the treatment of early-stage diabetic retinopathy.

Previously, by Professor Merali's group [50], it has been shown that healthy men supply ~6000 kcal/day (~50% carbohydrates) for 1 week has produced a rapid onset of insulin resistance and oxidative stress at systemic and fat tissue level. In adipose tissue, oxidative stress causes a large oxidation and carbonylation of numerous proteins, including GLUT4 carbonylation close to the glucose transport channel, which is likely to cause a GLUT4 loss activity. These findings suggest that the initial occurrence of insulin resistance can be the overactive oxidative stress resulting in inactivation of GLUT4 [50]. GLUT4 carbonylation level could be an early biomarker for insulin resistance and progression to T2D.

1.3.6 Animal Models of Obesity

By the beginning of the twentieth century, the use of animal modelling had increased dramatically and, while some individuals still questioned the ethics of their use, animal modelling, particularly in rodents, had become an essential method of demonstrating biological significance. Through the efforts of many forward-thinking individuals the genetic variability- problem was addressed via inbreeding of mice to the point that genetically identical mice became available for experimental use. If natural models were not available or feasible, the ability to manipulate the genome of a model species allowed for the creation of animals uniquely susceptible or resistant to a certain model [51].

The incidence of obesity continues to climb worldwide, making it imperative that animal models sharing characteristics of human obesity and its co-morbidities be developed in the quest for novel preventions and/or treatments. While there is a clear and well-documented genetic component for the tendency to become obese, most instances of human obesity are nonetheless considered to be polygenic, resulting from the integrated activity of numerous genes each of which carries only a small risk factor on its own. Animal models of obesity can therefore be partitioned into different categories, the major ones being based on mutations or manipulations of one or a few individual genes vs. those in genetically intact

animals exposed to obesogenic environments such as being maintained on high-fat diets [52]. Because food intake has high face validity when considering possible factors influencing body adiposity, most characterizations of animal models include assessments of intake as well as of body fat, plasma leptin, insulin and glucose, and other related parameters. It is therefore important to understand the basics of the controls of food intake and how they might relate to obesity [52]. Diet- induced models of obesity (DIO) are often used to study polygenic causes of obesity. DIO animals are believed to mimic better the state of common obesity in humans than most of the genetically modified models and may be the best choice for testing prospective therapeutics [52].

Leptin and Lep^{ob}/Lep^{ob} mouse, the “obese” mouse

Animals with a defect in the leptin-signaling pathway in the hypothalamus of the brain develop a morbidly obese phenotype. The models include animals that lack leptin production and/or that are insensitive to leptin due to leptin receptor mutations or extreme leptin resistance. Mutations are spontaneous (e.g., Lep^{ob}/Lep^{ob} mouse; Lep^{db}/Lep^{db} mouse) or genetically engineered. Animals with mutations that lie downstream of the leptin-sensing neurons in the hypothalamus are also included. A spontaneous mutation leading to the markedly obese phenotype in the Lep^{ob}/Lep^{ob} mouse has been recognized since the 1950s [52]. Today, the ob gene is one of the most-studied genes in obesity research. A single-base spontaneous mutation of the ob gene prevents the secretion of bioactive leptin because leptin synthesis is terminated prematurely. Leptin is mainly synthesized in white adipocytes and its secretion is directly proportional to the amount of stored triglyceride. Leptin deficiency has also been observed in rare cases of human obesity. Phenotypically, the lack of leptin leads to marked, early-onset obesity characterized by hyperphagia, reduced energy expenditure, insulin resistance associated with hyperglycemia and hyperinsulinemia and hormone dysregulation [52]. Obesity in Lep^{ob}/Lep^{ob} mice is one of the few forms of obesity that can be treated effectively by the administration of exogenous leptin. Leptin normalizes all known phenotypic defects in Lep^{ob}/Lep^{ob} mice including obesity, symptoms of the metabolic syndrome and reproductive function [52].

Aim of the thesis

Chronic Obstructive Pulmonary Disease (COPD) and Type 2 (T2D) Diabetes are two of the most important public health challenges and major causes of morbidity and mortality throughout the world. The increasing number of patients with COPD and T2D has raised the need for therapies and identification of biomarkers, in particular to prevent respectively, exacerbations of COPD and T2D progression. This work of thesis is focused on the identification and validation of reliable biomarkers for these two diseases using Multiple Reaction Monitoring-Mass Spectrometry (MRM-MS). This technique exploits the unique capability of three quadrupoles to act as mass filters and to selectively monitor a specific molecular ion analyte and one or several fragment ions generated from the analyte by collisional dissociation. The a highly sensitivity and selectivity allow peptide quantification and biomarker identification in complex biological samples.

Section 2: Materials and Methods

2.1 Chronic Obstructive Pulmonary Disease

2.2 Type 2 Diabetes Mellitus

2.1 Chronic Obstructive Pulmonary Disease

2.1.1 Patients demographic data

The samples analysed for COPD project are plasma from two cohorts of GOLD II-III-IV subjects. More demographic data available in table 3a and b.

A: First cohort (n=20)

Age (years)		N/A
Male %		55
Current smoking %		N/A
FEV ₁		1.032±0.48
FVC		2.60 ± 0.80
FEV ₁ /FVC		0.33 ± 0.07
Oxygen %		70%
GOLD stage	# GOLD II	4
	# GOLD III	7
	# GOLD IV	9

B: Second cohort (n=67)

Age (years)		66 ± 7.5
Male %		81
Current smoking %		22
FEV ₁		1.18 ± 0.56
FVC		2.74 ± 0.94
FEV ₁ /FVC		0.43 ± 0.13
Oxygen %		62.7
GOLD stage	# GOLD II	16
	# GOLD III	24
	# GOLD IV	23

Table 3. Patient demographic data and classification according GOLD standards.

The blood samples were collected twice, the first time during the enrolment in the experiment and the second after 12 months. After the draws, plasmas were then separated from the corpuscular part and stored at -80°C. The samples were then statistically analysed to confirm the conformance to the general trends found and characterizing the COPD patients. This examination was important in evaluating the compliance with the COPD characteristics of the two cohorts submitted to experiments (Figure 15).

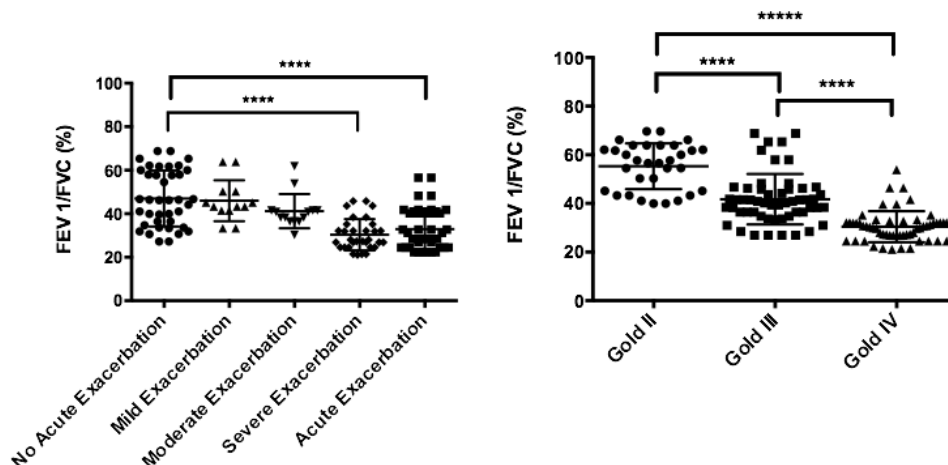


Figure 15. General overview on analysed patients. Patients were grouped according to the severity of experienced exacerbations (a) or to GOLD classification (b) and correlate with their FEV₁/FVC ratio.

2.1.2 Plasma samples preparation

Plasma samples were mixed with same volume of FASP buffer (4% SDS, 100 mM Tris, 100 mM DTT, all from Sigma-Aldrich) and incubated at room temperature for 20 minutes. After heating at 55°C for 5 minutes, samples were put in a 50 KDa cutoff centrifugal filter (Amicon Ultra, Millipore) and centrifuged for 10 minutes at 10000Xg. Samples were washed several times with 8M urea buffer, each time with 10 minutes centrifuge at 10000Xg. The collected volumes were transferred in a 10 KDa cutoff centrifugal filter (Amicon Ultra, Millipore) to concentrate the samples. Plasma proteins were then carboxymethylated and digested first with 0.5µg of Lys-C overnight at room temperature then with Trypsin (Promega) for 4 hours at 37°C. The digested proteins were collected dried and resuspended with 100µL of buffer A

(0.1% Formic Acid). Prior to MS analysis, all samples were desalted and concentrated with StageTip clean-up method according to *Rappsilber et al.*, [53].

StageTips

The mass spectrometric (MS) analysis of proteins has become a major technology in the investigation and understanding of biological processes. The interface between protein digestion and MS analysis is crucial for the overall quality and sensitivity of the analysis and the robustness of the proteomic workflow. Peptides can be concentrated and cleaned in a single step through their binding to a small quantity of reversed-phase material and eluted in organic solution ready for MS analysis. Commercial tips such as the ZipTips (Millipore), in addition to their high costs, have limitations for high-sensitivity work owing to recovery problems and large elution volumes [53]. Furthermore, their capacity is limited and can't be adjusted according to the need. StageTips combine the flexibility and low price of self-made tools with the ease-of-use, recovery, reproducibility and robustness typical for mass-manufactured devices [53].

StageTips were made by placing a small portion of Empore material (3M) in an ordinary pipette tip (Figure 16). Empore disks have chromatographic beads immobilized in a Teflon meshwork. From the commercially available large sheet, a small disk was stamped out using a blunt-ended tip. Peptides are retained and eluted with high efficiency, high capacity and high reproducibility [53]. Cleaning the peptides on a StageTip ensures stability of the liquid chromatography–tandem mass spectrometry (LC–MS/MS) system by removing impurities such as gel pieces and aggregates, thus preventing those from clogging the column.

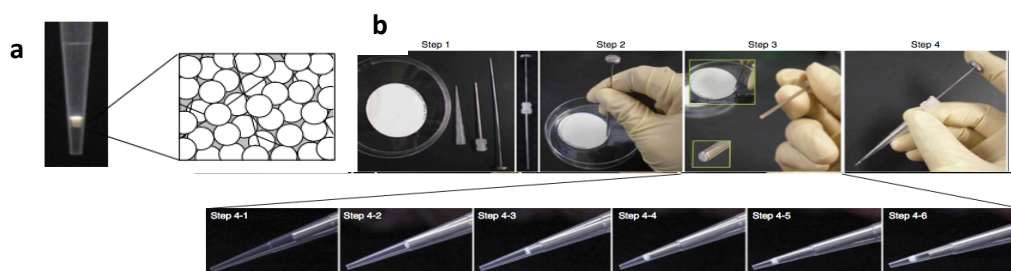


Figure 16. Schematic representation and production of StageTips extraction: panel (a) the chromatographic beads for micro-purification are embedded in a Teflon mesh and are held in place solely by the tapering of the vessel. (b) Step-by-step manufacture of a StageTip [53].

Once prepared the StageTips the samples are ready to be desalted and concentrated, the StageTips protocol includes 3 main steps: Activation, Cleaning and Elution.

In the “activation” step the membranes of each StageTip were conditioned with 50µL of 100%Acetonitrile (ACN) and rinsed twice with 50µL of Buffer A, each step is followed by a 2000Xg centrifugation. In the next phase of “cleaning” the samples were loaded into StageTips and centrifuged at 2400Xg. The flow-through were loaded again on top of the correspondent StageTip in order to recover as sample as possible. After rinsed twice with 50µL of Buffer A, to avoid aspecific bounds, the samples were ready for the last step, the “elution”. The peptides bounded are eluted adding 50µL of Buffer B’ (85% ACN e 15% Buffer A) and 50µL of 100% ACN. After elution the samples are dried, resuspended with 10µL of Buffer B’ and 90µL of Buffer A and loaded in a 96 well plate for the HPLC-MS analysis.

2.1.3 Chromatographic Separation

Chromatography is a technique by which a mixture sample is separated into components. Although originally intended to separate and recover (isolate and purify) the components of a sample, today, complete chromatography systems are often used to both separate and quantify sample components.

The term, "chromatography" was coined by the Russian botanist, Tswett, who demonstrated that, when a plant extract was carried by petroleum ether through a column consisting of a glass tube packed with calcium carbonate powder, a number of dyes were separated, as shown in figure 17. He named this analysis method "Chromatography" after “*chroma*” and “*graphos*”, which are Greek words meaning “colour” and “draw”, respectively.

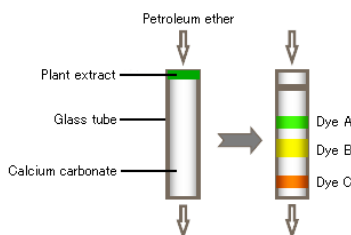


Figure 17. Diagram showing Tswett's experiment. [hitachi-hightech.com]

Liquid chromatography (LC), which is one of the forms of chromatography, is an analytical technique that is used to separate a mixture in solution into its individual components. As indicated by Tswett, the separation relies on the use of two different “phases”, one of which is held stationary while the other moves over it. LC is the generic name used to describe any chromatographic procedure in which the mobile phase is a liquid. The separation occurs because, under an optimum set of conditions, each component in a mixture will interact with the two phases differently relative to the other components in the mixture. High-Performance/Pressure Liquid Chromatography (HPLC) is the term used to describe LC in which the liquid mobile phase is mechanically pumped through a column that contains the stationary phase. The speed of a migrating sample component depends on whether the component has an affinity for the stationary or mobile phase. This affinity appears via various actions: adsorption, partition, ion exchange, etc. Components that have a higher affinity for the mobile phase compared with the stationary phase migrate more rapidly, while components that have a higher affinity for the stationary phase are eluted from the column later. The order and resolution of the components emerging from the column depend on the type of selected stationary and mobile phases.

Chromatography is based on the principal that under the same conditions, the time between the injection of a component into the column and the elution of that component is constant. This characteristic is used to perform qualitative or quantitative analysis.

Principles of Chromatography

Chromatography is described and measured in terms of four major concepts: capacity, efficiency, selectivity and resolution. To obtain the best possible separation, the efficiency of chromatographic system must be optimized in order to minimize band broadening. The column should have the capacity to retain the solutes and it should have the appropriate selectivity to resolve the analytes of interest.

Capacity

For effective liquid chromatographic separations, a column must have the capacity to retain samples and the ability to separate samples components efficiently. The capacity factor k'_R ,

of a column is the direct measure of the strength of the interaction of the sample with the packing material and is defined by the expression:

$$k'_R = \frac{t_R - t_0}{t_0} = \frac{V_R - V_0}{V_0}$$

where t_R is the time for a specific solute to reach the detector and t_0 is the time taken for non-retained species to reach the detector. V_R is the volume of solution that is pumped through the detector before a specific peak is eluted and V_0 is the volume of solvent pumped through the detector between the time of injection and the appearance of the non-retained species.

Selectivity

The selectivity of a chromatographic system is a measure of the difference in retention times between two given peaks and describes how effectively a chromatographic system can separate two compounds. Selectivity is usually defined in terms of α , where:

$$\alpha = \frac{t_2 - t_0}{t_1 - t_0} = \frac{V_2 - V_0}{V_1 - V_0} = \frac{k'_2}{k'_1}$$

The selectivity of a column is primarily a function of the packing material, although the chromatographer has some control using the mobile phase or temperature. The value for α can range from unity (1), when $t_2=t_1$, to infinity if the first component of interest is eluted in the void volume. The most powerful approach to increasing α is to change the composition of the mobile phase.

Efficiency

The efficiency of a column is the number that describes peak broadening as a function of retention, and it is described in terms of the number of theoretical plates, N . The plate model supposes that the chromatographic column contains a large number of separate layers, called *theoretical plates*. Separate equilibrations of the sample between the stationary and mobile phase occur in these "plates". The analyte moves down the column by transfer of equilibrated mobile phase from one plate to the next. The plates help us understand the processes at work in the column, they also serve as a way of measuring column efficiency,

either by stating the number of theoretical plates in a column, N (the more plates the better), or by stating the plate height; the *Height Equivalent to a Theoretical Plate* (the smaller the better).

The number of theoretical plates that a real column possesses can be found by examining a chromatographic peak after elution;

$$N = \frac{5.55 t_R^2}{w_{1/2}^2}$$

where $w_{1/2}$ is the peak width at half-height.

Resolution

Resolution is a term used to describe the degree of separation between neighbouring solute bands or peaks. It is affected by selectivity (α), efficiency (N) and capacity (k') of the column. The resolution equation describes the relationship between those factors and indicates how can be manipulated in order to improve the resolution between two peaks.

$$R = \frac{1}{4} \frac{\alpha - 1}{\alpha} \left(N^{\frac{1}{2}} \right) \frac{k'}{1 + k'}$$

HPLC C18 Reverse Phase

The HPLC employed for the projects described in this thesis is based on two separation principles:

Partition mode

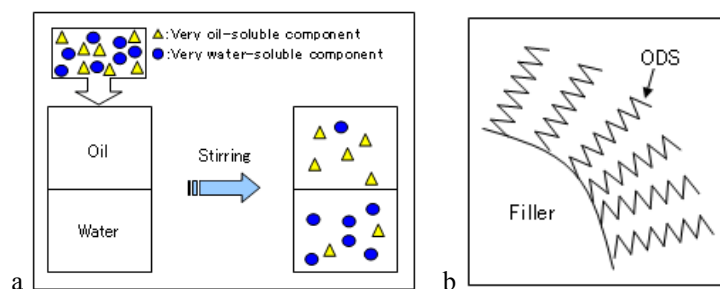


Figure 18. a. pattern diagram illustrating partition mode, b surface of an ODS filler.

In partition chromatography, the stationary phase is a non-volatile liquid which is held as a thin layer (or film) on the surface of an inert solid. The mixture to be separated is carried by a gas or a liquid as the mobile phase. The solutes distribute themselves between the moving and the stationary phases, with the more soluble component in the mobile phase reaching the end of the chromatography column first. Under these conditions, the solutes are said to be in an isotropic environment. In the partitioning model of retention, the stationary phase plays a more important role in the retention process.

Partition chromatography is one of the most useful biochemical lab procedure of high use, biochemistry and chemistry researchers use it to separate different biomolecules such as proteins, carbohydrates, and lipids. Partition chromatography involves in differences in the retention factor (K) as well as distribution coefficient (K_d) of the analytes.

Reversed Phase

Reversed Phase chromatography, the most widely used chromatographic mode, is used to separate molecules in solution on the basis of their hydrophobicity. As the name suggest, reversed-phase (RP) is the reverse of the normal-phase chromatography in the sense that it involves the use of a non-polar stationary phase and polar mobile phase. As a result, a decrease in the polarity of the mobile phase results in a decrease in solute retention. While biomolecules strongly adsorb to the surface of a reversed phase matrix under aqueous conditions, they desorb from the matrix within a very narrow window of organic modifier concentration.

Modern reversed-phase typically refers to the use of chemically bonded stationary phases, where a functional group is bonded to silica. Occasionally, however, polymeric stationary phases such as polymethacrylate or polystyrene, or solid stationary phases as porous graphitic carbon, are used. The most common stationary phase in RP chromatography are those in which a functional group is chemically attached to a silica support. The most popular bonded phase are the alkyl groups, such as -CH₃, (-CH₂)₃CH₃, (-CH₂)₇CH₃, (-CH₂)₁₇CH₃, phenyl (-C₆H₅) groups, cyano [(-CH₂)₃CN] groups and amino [(-CH₂)₃NH₂] groups, with a retention increasing exponentially with a chain length (Figure 19).

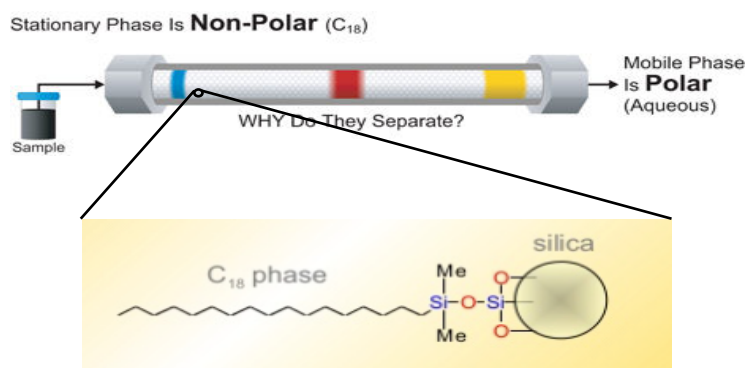


Figure 19. A reversed-phase column, in detail the chemical composition of the stationary phase. [Waters]

The particle size of the bead, as measured by its diameter, has important consequences for the size of the chromatographic bed which can be usefully packed, and for the efficiency of the separation. The larger particle size media are generally used for large scale preparative and process applications due to their increased capacity and lower pressure requirements at high flow rates. Small scale preparative and analytical separations use smaller particles since separation efficiency.

The mobile phase in reversed phase HPLC usually consists of water/aqueous solution (commonly an aqueous buffer) and an organic modifier. Chromatographically, in reversed phase HPLC water is the “weakest” solvent. As water is most polar, it repels the hydrophobic analytes into the stationary phase more than any other solvent, and hence retention times are long – this makes it chromatographically “weak”. When the organic modifier is added, and as this is less polar, the (hydrophobic) analyte is no longer as strongly repelled into the stationary phase, will spend less time in the stationary phase, and therefore elute earlier. This makes the modifier chromatographically “strong” as it speeds up elution/reduces retention. As progressively more organic modifier is added to the mobile phase, the analyte retention time will continue to decrease. The common organic modifiers are detailed below (Figure 20). The Snyder polarity index value gives a measure of the polarity of the solvents. The ϵ° values are also shown which give a measure of relative elution strength (the values quoted are for elution on C18).

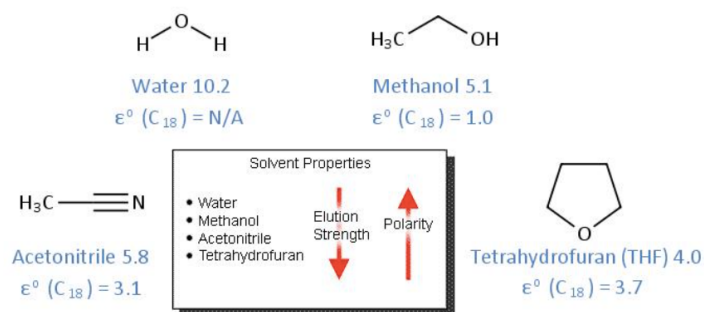


Figure 20. Typical solvents used in reversed phase HPLC

Solvent selection may be one of the most important parameters in an HPLC separation due to the effect it can have on the selectivity. In fact, selectivity may be the most effective tool for optimizing resolution. Changing the organic modifier within a mobile phase can alter the selectivity of the separation as well as the retention characteristics.

2.1.4 Parameters selected for the HPLC in COPD project

The chromatographic separation was achieved with a Dionex Ultimate 3000 SRLCnano HPLC system (Thermo Scientific) coupled to a TSQ Quantum Ultra (Thermo Scientific) triple quadrupole. The LC separation of the 5 μL injected samples was carried out on a C18 column Acclaim PepMap[®] RSLC column (Thermo Scientific). Elution was performed at a flow rate of 0.300 $\mu\text{L}/\text{min}$ with 0.1% (v/v) formic acid as Buffer A and acetonitrile containing 0.1% (v/v) formic acid as Buffer B. The separation was performed keeping a 5% concentration of Buffer B for 10 minutes and starting a linear shallow gradient from to 30% B in 22.5 minutes, to allow a good separation of the peptides of interest, followed by a steep gradient, from 30 to 90% of Buffer B, in 5.5 minutes. The washing step was executed with 90% B for 7 minutes and the column re-equilibration with Buffer A for 14 minutes. The entire cycle was 50 minutes long (Figure 21).

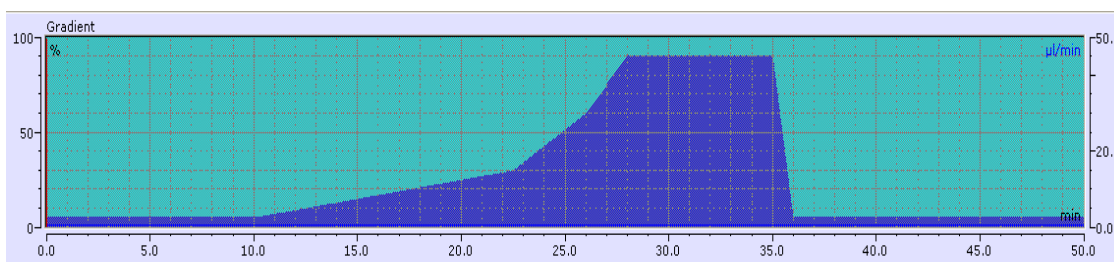


Figure 21. Schematic representation of the gradient of Buffer B during the HPLC separation.

Each analysis was preceded by a blank in order to prepare the column and every 5 samples was made a blank to clean the column avoiding accumulation of un-eluted peptides. In this case the physical parameters were maintained the same while the gradient was modified to promote a “deep” cleaning of the column. The gradient was accomplished at a flow rate of (0.400 $\mu\text{L}/\text{min}$). The blank was performed keeping a 5% concentration of Buffer B for 3 minutes and starting a linear gradient from 5% B to 90% B in 7 minutes. The 90% concentration of Buffer B was maintained for 15 minutes followed by column re-equilibration with Buffer A for 18 minutes. The entire cycle was 45 minutes long.

2.1.5 Mass Spectrometry (MS) Analysis

Mass spectrometry's characteristics have raised it to an outstanding position among analytical methods: unequalled sensitivity, detection limits, speed and diversity of its applications. In analytical chemistry, the most recent applications are mostly oriented towards biochemical problems, such as proteome, metabolome, high throughput in drug discovery and metabolism and so on. Other analytical applications are routinely applied in pollution control, food control, forensic science, natural products or process monitoring. Other applications include atomic physics, reaction physics, reaction kinetics, geochronology, inorganic chemical analysis, ion–molecule reactions, determination of thermodynamic parameters (G° , K_a , etc.) and many others [54].

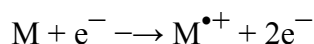
Mass spectrometry is an indispensable analytical tool in chemistry, biochemistry, pharmacy, and medicine, it's employed to help explore single cells or other planets. Structure elucidation

of unknowns, environmental and forensic analytics, quality control of drugs, flavours and polymers: they all rely to a great extent on mass spectrometry.

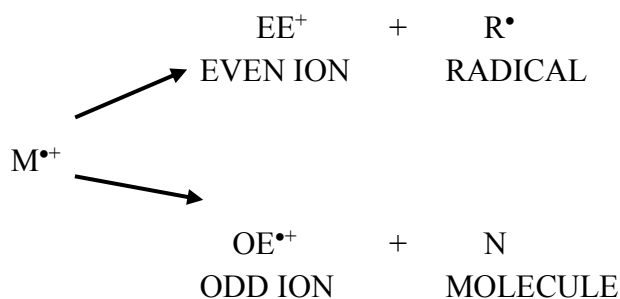
From the 1950s to the present mass spectrometry has changed tremendously and still is changing. The pioneering mass spectrometrists had a home-built rather than a commercial instrument. This machine, typically a magnetic sector instrument with electron ionization, delivered a few mass spectra per day, provided sufficient care was taken of this delicate device. Nowadays, the output of mass spectra has reached an unprecedented level. Highly automated systems are able to produce even thousands of spectra per day and a large number of ionization methods and types of mass analyzers has been developed and combined in various ways.

Principles

The first step in the mass spectrometric analysis of compounds is the production of gas-phase ions of the compound, *molecular ion*, for example by electron ionization:



This molecular ion ($M^{\bullet+}$) normally undergoes fragmentations. Because it is a radical cation with an odd number of electrons, it can fragment to give either a radical and an ion with an even number of electrons, or a molecule and a new radical cation.



These two types of ions, *fragment ions*, have different chemical properties. Each primary product ion derived from the molecular ion can, in turn, undergo fragmentation, and so on. All these ions are separated in the mass spectrometer according to their mass-to-charge ratio, and are detected in proportion to their abundance. Ions provide information concerning the

nature and the structure of their precursor molecule. In the spectrum of a pure compound, the molecular ion, if present, appears at the highest value of m/z (followed by ions containing heavier isotopes) and gives the molecular mass of the compound.

Mass spectrum

A mass spectrum is the two-dimensional representation of signal intensity (ordinate) versus m/z (abscissa). The intensity of a peak, usually called signal, directly reflects the abundance of ionic species of that respective m/z ratio which have been created from the analyte within the ion source. The mass-to-charge ratio, m/z , is dimensionless by definition, because it calculates from the dimensionless mass number, m , of a given ion, and the number of its elementary charges, z . The number of elementary charges is often, but by far not necessarily, equal to one. However, there can be conditions where doubly, triply or even highly charged ions are being created from the analyte depending on the ionization method employed. The distance between peaks on that axis has the meaning of a neutral loss from the ion at higher m/z to produce the fragment ion at lower m/z . Often, the peak at highest m/z results from the detection of the intact ionized molecule, the molecular ion $M^{\bullet+}$. The molecular ion peak is usually accompanied by several peaks at lower m/z caused by fragmentation of the molecular ion to yield fragment ions. Consequently, the respective peaks in the mass spectrum may be referred to as fragment ion peaks. The most intense peak of a mass spectrum is called base peak. In most representations of mass spectral data the intensity of the base peak is normalized to 100% relative intensity. This helps to make mass spectra more easily comparable. The normalization can be done because the relative intensities are independent from the absolute ion abundances registered by the detector [55].

The above spectrum (Figure 22) is presented as a bar graph or histogram. Such data reduction is common in MS and useful as long as peaks are well resolved. The intensities of the peaks can be obtained either from measured peak heights or more correctly from peak areas.

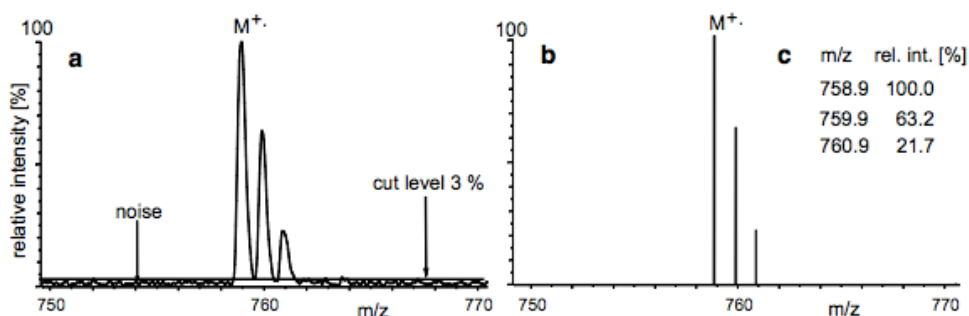


Figure 22. Three representations of the molecular ion signal in the field desorption mass spectrum of tetrapentacontane, $C_{54}H_{110}$; (a) profile spectrum, (b) bar graph representation, and (c) tabular listing [55].

Mass spectrometer

Obviously, almost any technique to achieve the goals of ionization, separation and detection of ions in the gas phase can be applied, and actually has been applied, in mass spectrometry. This leads to a simple basic setup having all mass spectrometers in common. A mass spectrometer consists of an ion source, a mass analyzer and a detector which are operated under high vacuum conditions. A closer look at the front end of such a device might separate the steps of sample introduction, evaporation and successive ionization or desorption/ionization, respectively, but it is not always trivial to identify each of these steps clearly separated from the others. Nowadays data system is added to the rear end which is used to collect and process data from the detector. Since the 1990s, data systems are also employed to control all functions of the instrument (Figure 23).

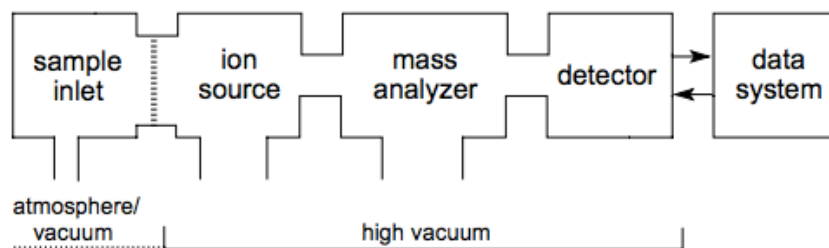


Figure 23. General scheme of a mass spectrometer. Often, several types of sample inlets are attached to the ion source housing. Transfer of the sample from atmospheric pressure to the high vacuum of the ion source and mass analyzer is accomplished by use of a vacuum lock.

Sample Inlet System, the introduction of the sample into the ionization chamber can be done either in the solid state using a probe, either liquid or gaseous, using a valve system that allows access to the ionization. The amount of product needed to record a spectrum is in the order of micrograms / nanograms. It is possible to use the output of a GC or HPLC system as input of the mass spectrometer. These techniques, GC-MS and HPLC-MS, are extremely useful in analysing product mixes [55].

Ion source, if a molecule is invested in a vapour phase by a bundle of electrons with significant kinetic energy, it can have its positive or negative ionization impact. The sample is ionized into a special ionization chamber, where the electron beam is produced from an ion source that varies according to the technique used. Generally, electrons are emitted by a hot tungsten or rhodium filament, and pass through a conduit, which creates the radius, in the central part of the chamber containing the gaseous sample. The fraction of electrons that does not hit the molecules is picked up by an electron trap, the molecules that are not ionized are removed from the high vacuum pump, while the ionized ones are accelerated and conveyed to the analyzer. The ionization system plays an essential role in mass spectrometry because it also depends on the number, nature and abundance of the molecular fragments that appear in the mass spectrum. For this reason, the techniques used are numerous and some of them give rise to particular variations in mass spectrometry. Among the various devices some allow only fragments to be analysed, while others also allow the detection of negative ions. In addition, some ionization techniques are definitely powerful, they operate at high energy and lead to a push fragmentation, while others operate at low energy producing fewer ions. Depending on the type of source used, the primary ionization of the sample is made in a variety of ways; the most used techniques are:

- Electronic Impact (E.I.)
- Chemical Ionization (C.I.)
- ElectroSpray Ionization (E.S.I.)

Mass analyzer, the analyzer allows differentiation of the generated ions based on their m/z ratio. The most common are:

- Magnetic Analyzer
- Double Focalization Analyzer
- Quadrupole Analyzer
- Ion Tripping Analyzer

Detector, as a collector and ion detector an electronic multiplier is commonly used, consisting of a series of cascade electrodes. When an ion arrives on the first electrode it emits a bundle of electrons that hit the second electrode, which in turn emits more electrons and so on. The result is a strong amplification of the signal which is then digitized and finally processed by the Spectrometer calculator for the presentation of the mass spectrum. Good mass accuracy can only be obtained from sufficiently sharp and evenly shaped signals that are well separated from each other. The ability of an instrument to perform such a separation of neighbouring peaks is called resolving power. It is obtained from the peak width expressed as a function of mass. The term resolution essentially describes the same; the small difference being that its definition is based on the resulting signals. The resolution R is defined as the ratio of the mass of interest, m , to the difference in masses, as defined by the width of a peak at a specific fraction of the peak height.

$$R = \frac{m}{\Delta m}$$

Two neighbouring peaks are assumed to be sufficiently separated when the valley separating their maxima is about 10 % of their intensity (Figure 24) [55].

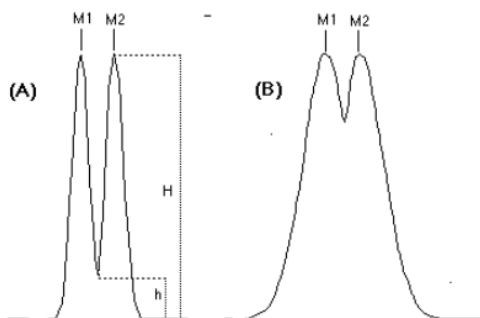


Figure 24. Two types of output spectra, in A two peaks well resolved, in B two peaks not resolved. [55]

2.1.6 Multiple Reaction Monitoring - MS (MRM-MS)

Taking into account that Multiple Reaction Monitoring – MS is the main technique common to both the studies it's necessary to dedicate a specific section.

In the past decade, the scientific community has seen an uptick in the use of mass spectrometry for the quantification of proteins and peptides in complex biological matrices. However, the technique that is most frequently used in quantitative assays, Multiple Reaction Monitoring, (MRM-MS) was first reported in 1979 during the introduction of the triple quadrupole (QqQ) mass spectrometer [58]. The ability to detect and quantify proteins or sets of proteins with high precision across multiple samples is an essential task in biological and biomedical research. Recently, MRM has emerged as a promising technique for such precise quantification of targeted proteins. Originally applied to the measurement of small molecules (such as metabolites or drugs), MRM is a mass spectrometry technique for the detection and quantification of specific, predetermined analytes with known fragmentation properties in complex backgrounds [57]. MRM is used most effectively in a liquid chromatography–coupled mass spectrometry (LC-MS) system, where a capillary chromatography column is connected in-line to the electrospray ionization source of the mass spectrometer. MRM exploits the unique capability of triple quadrupole (QqQ) mass spectrometers to act as mass filters and to selectively monitor a specific analyte molecular ion and one or several fragment ions generated from the analyte by collisional dissociation. The number of such fragment ions that reach the detector is counted over time, resulting in a chromatographic trace with retention time and signal intensity as coordinates (Figure 25).

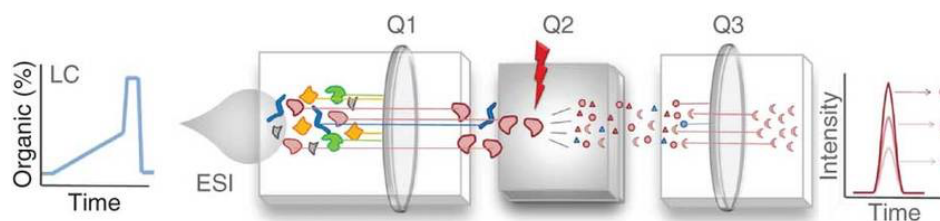


Figure 25 the multiple reaction monitoring technique. Molecular ions of a specific analyte are selected in Q1 and fragmented in Q2. A specific fragment ion from the target analyte (transition) is selected in Q3 and guided to the detector. On the right, chromatogram of the three transitions, corresponding to three different fragments of the target analyte, and the corresponding three MRM. [57]

Several such precursor–fragment ion pairs, termed MRM transitions, can be sequentially and repeatedly measured analysing chromatographic peak for each transition [55]. When applied to proteomics, MRM measures peptides produced by the enzymatic digestion of a proteome as surrogates of the corresponding proteins. Molecular ions within a mass range centred around the mass of the targeted peptide are selected in the first mass analyzer (Q1), fragmented at the peptide bonds by collision-activated dissociation (in q2) and one or several of the fragment ions uniquely derived from the targeted peptide are selected by the second analyzer (Q3). Integration of the chromatographic peaks for each transition supports the relative or, if heavy isotope–labelled reference standards are used, absolute quantification of the targeted peptide(s) resulting from the protein digestion and loaded on the LC-MS system. A suitably chosen set of MRM transitions therefore constitutes a specific assay to detect and quantify a target peptide and, by inference, a target protein in complex samples.

The application of MRM to proteomics has been slow and not without complications [57]. An MRM-based proteomic experiment starts with the selection of a target list of proteins, this step is followed by the selection of target peptides that optimally represent the protein set, the selection of a set of suitable MRM transitions for each targeted peptide and their validation, the optimization of other MRM assay parameters and, finally, the application of the assays to the detection and quantification of the proteins.

Selection of target proteins: the first step of a target proteomic experiment is the selection of a set of proteins of interest. Depending on the sensitivity and accuracy required, hundreds of proteins can be targeted in a single LC-MS analysis after the transitions have been optimized [57]. The selection of the protein set might be on the basis of previous experiment or scientific literature. In addition to the protein of interest, several “housekeeping” proteins should be selected as an invariant reference set to normalize the experimental variability.

Selection of the target peptides: Desirable target peptides are unique to the target protein and easily detectable by mass spectrometry (signature or proteotypic peptides). The specific mass spectrometry signal response of different tryptic peptides from the same protein can differ by as much as 100-fold in intensity. The choice of peptides with favourable mass spectrometry properties is thus crucial, as it determines the sensitivity of the assay. In an ideal

case, the target proteins are available as purified products and the mass spectrometry signal response of all their tryptic peptides can be directly tested via LC-MS [57]. Typically, only a few representative peptides per protein are targeted to infer the presence of a protein in a sample to determine its quantity [57]. In practice, the time required for assay development is significantly reduced if previous information is used to select those peptides that are most likely observed in the experiment and provide the strongest specific signals [57]. Alternatively, information from prior experiments conducted on natural proteomes (stored in, for example, PeptideAtlas, the Global Proteome Machine Database, genome annotating proteomic pipeline, Pride or Tranche) can be used to identify peptides that can be reproducibly detected and are thus likely associated with the most intense signals [57].

There are some indications to follow to maximize the performance of the experiment:

- **Uniqueness:** by selecting peptides for target MS analysis, it is essential to ensure that the peptides selected uniquely identify the target protein. The PeptideAtlas helps to distinguish between multiple splice isoforms and distinct genes by reporting the number of genome locations for observed peptides.
- **Post-translational modifications:** modified peptide cannot be detected by MRM unless specifically targeted. Quantitative differences observed in the analysis of unmodified peptide reflects either a true change in abundance of the target protein in the sample or the partial modification of the peptide. Therefore, for reliable quantification, at least two peptides should be monitored for each target protein.
- **Chemically induced modifications:** the introduction of artefactual modification due to the sample processing is a potential source of error quantitative MS experiment because a fraction of the target peptide might be converted into the modified form in an irreproducible and unpredictable manner. Therefore, care should be taken to avoid targeting peptides with a high propensity for artefactual modification. In particular, peptides containing methionine or tryptophan residues should be avoided. Furthermore, peptides containing glutamine and asparagine residues may be chemically unstable.
- **Cleavage sites:** peptides with missed cleavages or non-tryptic cleavage sites are frequently observed in analysis. Such peptides should not be targeted for absolute quantification, as the extent of these might be variable between samples. For example,

peptides with two neighbouring basic amino acids at either cleavage site of the protein sequence should be avoided, as those sites are predestined for high rate of missing cleavages.

Selection of MRM transitions: The quantification of a peptide by MRM requires the selection of specific m/z settings for the first and third quadrupole, which, in combination, results in a highly sensitive and selective detection of the peptide. The combination of m/z setting for the first and third quadrupole is referred to as “transition”. The m/z value of the first quadrupole is determined by the mass and the predominant charge state of a peptide. In the third quadrupole, a particular fragment ion of the peptide is selected. The intensities of individual fragments derived from one precursor ion differ substantially. To obtain a high-sensitivity assay, it is therefore essential to select transitions specific for the most intense fragments. Including transitions for all the major canonical fragments in the assay limits the analysis to a few peptides, as the total number of transitions per LC-MS run is limited. Therefore, commonly only the best 2–4 transitions per peptide are selected for quantitative assays. The selection of these transitions might be either on the basis of data from shotgun experiments or experimentally determined on the QqQ instrument. Shotgun experiments can be exploited to derive information about the predominant precursor charge state and the MS/MS fragmentation pattern of a targeted peptide. However, one needs to be aware that the ionization conditions can affect the charge state distribution. Similarly, the distribution of relative fragment ion intensities is dependent on the type of instrument used and the operating parameters.

Validation of transition: In spite of the high specificity of QqQ MRM analyses achieved by the two consecutive mass filtering stages, a particular precursor/fragment combination may not be specific for a peptide targeted in a complex sample. Unspecific signals may derive from other peptides with precursor/fragment ion pairs of similar masses. These peptides might have closely related sequences so that part of the transitions is identical. However, completely unrelated sequences might, by chance, result in mass pairs that are too close to be sufficiently filtered out in the quadrupoles. Such signals will usually be of lower intensity than the optimized transitions. However, if MRM is used to target peptides that are several orders of magnitude less abundant than the most abundant peptides, such unspecific signals

might still be well above the detection limit and often even more intense than the signal for the targeted peptide. The first step of validation is the parallel acquisition of several transitions for a targeted peptide. The presence of at least two product-ions representing the corresponding precursor ion, one for quantification and one for confirmation is needed for the transition validation. At the time of peptide elution, such transitions yield a perfect set of 'co-eluting' intensity peaks if they are derived from the same peptide. With each additional transition, the probability for a random match is markedly reduced, provided that perfect co-elution is observed. Another parameter for validation is the Retention Time, that characterizes a peptide and should be similar for all samples. The elution duration, also, is an index to see if the selected chromatographic method is optimal. The third characteristic for validation is the fingerprint, that is, the abundance of the ion-products, characteristic for each ion-precursor.

Quantification: Proteomics is gradually shifting from pure qualitative studies (protein identification) to large-scale quantitative experiments, prompted by the growing demand for protein biomarker qualification and verification in larger cohorts on one hand and the need for consistent quantitative data sets in systems biology to perform modelling on the other. Due to the difficulties inherent in analysing mixtures of intact proteins, most quantitative proteomic strategies rely on the use of peptides generated by enzymatic digestion as surrogates for targeted proteins. Liquid chromatography hyphenated to mass spectrometry (LC-MS and LC-MS/MS) has become the standard platform for quantitative proteomics as it has the capability of analysing a large number of peptides in complex biological samples. LC-MS also offers robustness and the ease of automation enabling high-throughput studies. By definition, a quantitative study requires the systematic determination of the amount of each component of interest present in a series of samples, including the replication of the analyses. Precise LC-MS quantification is routinely carried out using stable isotope dilution, in which internal standards (isotopically labelled synthetic peptides) are added to the samples prior to the LC-MS analysis. Often proteomic studies are focused on measuring changes in the level of expression of targeted proteins in different samples (control and disease samples). Such experiments are based on relative quantification, comparing the signal intensities

observed in different samples (after proper normalization to correct for instrument drifts and the sample amount injected). This method is referred to as a label-free quantification.

The development of tandem mass spectrometers, in particular triple quadrupole spectrometers, has revolutionized analytical chemistry. MRM is typically used to detect and quantify between ten and a few hundred peptides, but can in principle be used for thousands of peptides in one single assay. Typical applications of MRM assays include detection and quantification of serum proteins present at low (ng/ml) concentrations, which in combination with high reproducibility, selectivity (two levels of mass selection) and sensitivity (non-scanning mode) makes MRM a first choice for biomarker validation [59].

For this work, was used relative quantification, that is based on the signal intensities of specific MRM transitions. Upon establishment of the MRM assay, the individual samples were processed and analysed by LC-MS. Even though the label-free approach seems conceptually and experimentally simple, precise label-free quantification is challenging due to variations in signal intensities from one LC-MS analysis to the other and also within one LC-MS analysis: a peptide spiked into different backgrounds will result in different intensities depending on the sample and time of analysis [58]. In an attempt to control for these effects, normalization is performed in label-free quantitative proteomics with the assumption that the majority of protein/peptide concentrations in a sample are not changing. However, such normalization can only correct for global shifts and do not compensate local suppression or enhancement effects on individual peptides. Despite these limitations, label-free quantification can be successfully performed if the sample processing is well controlled and the samples are closely related in background and protein composition. As matrix effects become more pronounced with higher total peptide amounts injected, the injected sample amount should be kept low. In addition, it is essential that several peptides for each protein are quantified to avoid false conclusion owing to these effects [58].

2.1.7 Parameters selected for the MRM-MS in COPD project

In order to develop a MRM method, it is necessary to build a transition list of specific peptides. Multiple Reaction Monitoring was performed using a Quantum Ultra TSQ mass spectrometer (Thermo Scientific™) coupled with a Dionex Ultimate 3000 nanoLC system (Thermo Scientific™). The LC separation was carried out as described before. ESI was delivered using a stainless-steel emitter (ID 30 µM, 10 cm length, Thermo Scientific™). The MS analysis was carried out in a positive ionization mode, using an ion spray voltage of 2000V and a temperature of 200°C. The nebulizer and gas flow was set at 30 psi. The complete system was fully controlled by Xcalibur™ software (Thermo Scientific™). The sequence of clusterin (UniProt P10909, Figure 26A) and H3.3 (UniProt P84243, Figure 26B) were imported in the PinPoint software and digested in silico using the same software. The parent and the daughter ions were selected from a list according to calculated expected intensity signal. For sample quantification was used the internal standard peptide corresponding to residues 326-336 of clusterin. The method was initially tested with cells extract and then with plasma of healthy individuals with or without histones spikes. Using these standards to refine the method, MRM final signals satisfied the canonical criteria: reproducible retention time, at least 1 parent ion and 2 daughter ions (Figure 27a) and constant relative-intensity pattern of daughter ions (Figure 27b). Method development, mass analyses processing and protein quantification were performed using PinPoint 1.4 (Thermo Scientific).

A
MMKTLLLFVGLLLTWESGQVLGDQTVSDNELQEMSNQGSKYVNKEIQNAVNGVKQIKTLIEKTNEE
RKTLLSNLEEAKKKKEDALNETRESETKLKELPGVCNETMMALWEECKPCLKQTCMKFYARVCRSG
SGLVGRQLEEFNLQSSPFYFWMNGDRIDSLLENDRQQTHMLDVMQDHFSSRASSIIDELFQDRFFTR
EPQDTYHYLPFSLPHRRPHFFFPKSRIVRSLMPFSPYEPLNFHAMFQPFLEMIHEAQQAMD IHFHS
PAFQHPPTFE IREGDDRTVCREIRHNSTGCLRMKDQCDKCREILSVDCSTNNPSQAKLRRELDES
LQVAERLTRKYNELLKSYQWKMLNTSSLLEQLNEQFNWVSRLANLTQGEDQYYLRVTTVASHTSDS
DVPSGVTEVVVKLFDSDPITVTVPVEVSRKNPKFMETVAEKALQEYRKKHREE

B

MARTKQTARK[acet]STGGK[acet]APRK[acet]QLATK[acet]AARKSAPSTGGVKKPHRY
RPGTVALREIRRYQKSTELLIR[cit]KLPFQRLVREIAQDFKTDLRFAQSAAIGALQEASEAYLVG
LFEDTNLCAIHAK[acet]RVTIMPKDIQLARRIGERA

Figure 26. A. Clusterin sequence used for IS, B. Histone 3 fasta sequence. In red the modified residues and underlined the Clusterin peptide selected for IS.

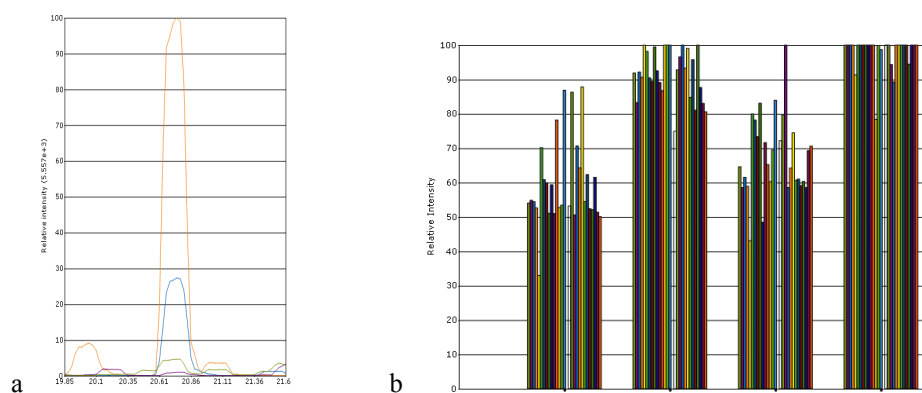


Figure 27. a. Chromatogram representing the relative abundance of the daughter ions of the H3.3 peptide detected and quantified by MRM-MS, on the abscissa the time on the ordinate the relative intensity. b Finger print of the relative intensity of the product ions of the H3.3 peptide and their abundance among 29 plasma samples.

The post-translational modifications of interest (citrullination and acetylation) were added to the peptides using the add & edit modifications tool.

The detailed MRM-MS method, with the m/z of precursor and product ions, is not fully described because the project is under confidential regulation till the publication.

2.1.8 Statistical Analysis

Experimental results are presented as mean \pm standard deviation of the mean (SDM). Significant variations and the p value in the data within groups were determined using non-parametric Kruskal-Wallis and Mann-Whitney tests. To determine whether H3.3 could be a good biomarker for COPD patients was used receiver operating curve (ROC) analysis with a 95% of Confidence Interval. All analyses were conducted using GraphPad Prism 6.0 (GraphPad Software, Inc.).

2.2 Type 2 Diabetes Mellitus

2.2.1 Patients demographic data

The first group analysed is a pool of healthy men, this set was analysed pre and post a hypercaloric diet composed by 50% carbohydrate, 35% fat, and 15% protein, demographic in table 4, from these patients was collect the fat tissue analysed for GLUT4 carbonylation.

Age (years)	50 ± 1.4
BMI (Kg/cm ²)	26 ± 1
HbA1C %	Below 5.7

Table 4. Study subjects: Age, BMI, body mass index; HbA1C.

The second set of samples is composed of male and female obese people (BMI ≥ 30), with an age between 19 and 58 years old (Table 5). The abdominal fat tissue of each patient was collected and analysed.

Age (years)		40 ± 11
BMI (kg/cm ²)		47 ± 9.5
HbA1C (%)		6 ± 0.95
Groups	# non-diabetic	7
	# diabetic	5
Gender	# male	2
	# female	9

Table 5 Study subjects: Age, BMI, HbA1A and classification according the illness status and the gender.

And the last samples, subcutaneous fat, come from obese male patients with an age between 31 and 71 years old. More demographic data available in table 6.

Age (year)		49 ± 11
BMI (Kg/cm ²)		48.4 ± 9.5
HbA1C(%)		6.8 ± 1.4
Groups	# non-diabetic	4
	# pre-diabetic	4
	# diabetic	11

Table 6. Study subjects: Age, BMI, body mass index; HbA1C and classification according the illness status.

2.2.2 Fat samples preparation

Extraction: Proteins were extracted from approximately 200mg of tissues using 400μL of Cell Permeabilization Buffer (Thermo Scientific™) and 4μL of Protease Inhibitor Buffer (Thermo Scientific™). Tissues were put in dry ice, then the homogenized for 1 min at 1000 rpm and proteins were separated by centrifugation at 13200Xg for 20 min at 4°C. The fat/oil fraction (upper) was transferred and kept at -80°C, while the cytoplasmic fraction (middle) was kept for the digestion step.

Digestion: 30μL of each sample were denatured with 10μL of DL-dithiotreitol (5mg/mL) at 37°C for 20 minutes and alkylated with 10μL of Iodoacetamide (12.5mg/mL) at 37°C for 20 minutes. Samples were diluted with 25mM NH₄HCO₃ (450μL). Trypsin digestion was performed in three stages: first digestion adding 15μL of Trypsin solution 1 (7.5μL (3.75μg) of Promega Trypsin solution + 7.5μL of 25mM NH₄HCO₃) to each sample and incubating overnight at 37°C, second digestion using 10μL of Trypsin solution 2 (8μL of 25mM NH₄HCO₃ + 2μL of Promega Trypsin solution (1μg)) to each sample and incubating at 37°C of 2 hours and the third step using again 10μL of Trypsin solution 2 to each sample and incubating at 37°C of 2 hours. 55μL of Formic Acid 10% were used to stop the digestion and ionize the peptides.

StageTips: Digested peptides were desalting and clean-up using the StageTips. The samples were passed two times through the tips, already activated, desalted twice with 50μL of

Buffer A and eluted with 50 μ L of Buffer B and 50 μ L of ACN 100%. Samples were dried in speed vacuum for 30 minutes and resuspended for the MRM analysis with 5 μ L of Buffer B' and 115 μ L of Buffer A.

2.2.3 Chromatographic and MRM-MS analysis

The chromatographic separation was achieved with a Dionex Ultimate 3000 SRLCnano HPLC system (Thermo Scientific™) coupled to a TSQ Quantum Ultra (Thermo Scientific™). The LC separation of the 5 μ L injected samples was carried out on a C18 column Acclaim PepMap® RSLC column from Thermo Scientific™. Elution was performed keeping a 5% concentration of Buffer B for 10 minutes and starting a linear shallow gradient from to 30% B in 22.5 minutes, to allow a good separation of the peptides of interest, followed by a steep gradient, from 30 to 90% of Buffer B, in 5.5 minutes. The washing step was executed with 90% B for 7 minutes and the column re-equilibration with Buffer A for 14 minutes. The entire cycle was 50 minutes long with a flow rate of 0.300 μ L/min.

Each analysis was preceded by a blank in order to prepare the column and every 5 samples was made a blank to clean the column avoiding an accumulation of un-eluted peptides.

For the detection of GLUT4 (UniProt 14672, Figure 28a) we selected some peptides, obtained from an *in silico* digestion library from Pinpoint software, and the relative parent and daughter ions were identified and used for the quantification. In this case we used the Human Heat shock 70KDa protein 1A/1B (UniProt P0DMV8-P0DMV9, Figure 28b) as internal standard (Figure 28). MRM analyses were performed with TSQ Quantum Ultra (Thermo Scientific™) triple quadrupole coupled to a Dionex Ultimate 3000 SRLCnano HPLC system (Thermo Scientific™). The LC separation was carried out as described before and ESI was delivered using a stainless-steel emitter (ID 30 μ M, 10 cm length, Thermo Scientific™). Pinpoint™ 1.4 (Thermo Scientific™) software was used for method development and the optimization of the mass spectrometer parameters. The MS analysis was carried out in a positive ionization mode, using an ion spray voltage of 2000V and a

temperature of 200°C with the nebulizer and gas flow set at 30 psi. The complete system was fully controlled by Xcalibur™ software (Thermo Scientific™).

A

MPSGFQQIGSEGEPPQQRVTGTLVLAVFSAVLGSLQFGYNIGVINAPQKVIEQSYNETWLGRQGP
EGPSSIPPGLTTLWALSVAIFSVGGMISSFLIGIISQWLGRKRAMLVNNVLAVLGGSLMGLANAA
ASYEMLILGRFLIGAYSGLTSGLVPMYVGEIAPTHLRGALGTNLQLAIVIGILIAQVLGLESLLGT
ASLWPLLLGLTVLPALLQLVLLPFCPEsprlyIIQNLEGPARKSLKR[GluSa]LTGWADVSGVL
AELKDEK[HNE]R[GluSa]KLERERPLSLLQLLGSRTHRQPLIIAVVLQLSQQLSGINAVFYYST
SIFETAGVGQPAYATIGAGVVNTVFTLVSVLLVERAGRRTLHLLGLAGMCGCAILMTVALLLLERV
PAMSYVSIVAIFGFVAFFEIGPGPIPWFIVAELFSQGRPAAMAVAGFSNWTSNFIIGMGFQYVAE
AMGPYVFLLLFAVLLLGFFIFTFLRVPETRGRTFDQISAAFHRTPSLLEQEVKPSLELEYLGPDEND

B

MAKAAAIGIDLGTTYSCVGVFQHGKVEIIANDQGNRTTPSYVAFTDTERLIGDAAKNQVALNPQNT
VFDAKRLIGRKFGDPVQSDMKHWPVQVINDGDKPKVQVSYKGETKAFYPEEISSMVLTKMKEIAE
AYLGYPVTNAVITVPAYFNDSQRQATKDAGVIAGLNLRIINEPTAAAIAYGLDRTGKGERNVLIF
DLGGGTFDVSIILTIDDGIFEVKATAGDTHLGGEDFDNRLVNHFVEEFKRKHKKDISQNKRAVRRLR
TACERAKRTLSSSTQASLEIDSLFEGIDFYTSITRARFEELCSDLFRSTLEPVEKALRDAKLDKAQ
IHDLVLVGGSTRIPKVQKLLQDFFNGRDLNKSINPDEAVAYGAAVQAAILMGDKSENVQDLLLLDV
APLSLGLTAGGVMTALIKRNSTIPTKQTQIFTTYSNQPGLVLIQVYEGERAMTKDNNLLGRFELS
GIPPAPRGVPQIEVTFDIDANGILNVTATDKSTGKANKITITNDKGRLSKEEIERMVQEAKEYKAE
DEVQREVRSAKNALESYAFNMKSAVEDEGLKGKISEADKKKVLDKCQEVISWLDANTLAEKDEFEH
KRKELEQVCNPIISGLYQGAGGPGPGGFGAQGPKGGSGSGPTIEEVD

Figure 28. A. Human GLUT4 fasta sequence, B. Human Heat Shock Protein sequence used for IS. In red the modified residues, underlined the HSP1a/1b used as IS

The detailed MRM-MS method, with the m/z of precursor and product ions, is not fully described because the project is under confidential regulation till the publication.

2.2.4 Statistical Analysis

Experimental results are presented as mean \pm standard error of the mean (SEM). Significant variations and the p value in the data within groups were determined using non-parametric Kruskal-Wallis and Mann-Whitney tests. All analyses were conducted using GraphPad Prism 6.0 (GraphPad Software, Inc.).

2.2.5 GLUT4 carbonylation in mice

The level of GLUT4-HNE was measured in mice with the aim to investigate if mouse could be a good model for future carbonylation studies and drug development projects. Furthermore, in US the animal diabetes is a growing problem so it's important to investigate this phenomenon also in animals for future treatments. For this experiment were used C57BL/6 mice. All the ethic and veterinary protocols and rules were adopted.

2.2.5.1 Animals and treatment

For this work the mouse (*Mus musculus*) was chosen as animal model because is small and easily to be maintained. Rodents are also generally mild-tempered and docile, making them easy for researchers to handle.

Most of the mice and rats used in medical trials are inbred so that, other than sex differences, they are almost identical genetically. This helps make the results of medical trials more uniform, according to the National Human Genome Research Institute. As a minimum requirement, mice used in experiments must be of the same purebred species. Rodents are used as models in medical testing is that their genetic, biological and behaviour characteristics closely resemble those of humans and many symptoms of human conditions can be replicated in mice and rats. "Rats and mice are mammals that share many processes with humans and are appropriate for use to answer many research questions", said Jenny Haliski, a representative for the NIH Office of Laboratory Animal Welfare. Rodents also make efficient research animals because their anatomy, physiology and genetics are well-understood by researchers, making it easier to tell what changes in the mice's behaviours or characteristics are caused by.

The C57BL/6 inbred strain, used for this work, was created by Dr. CC Little from the mating of female 57 with male 52 from Miss Abbie Lathrop's stock. C57BL/6 is one of the most versatile inbred mouse strains and is commonly used as the genetic background for transgenic

mouse models and for diet-induced obesity (DIO) study. In this experiment were also used some mice knock out for leptin (ob/ob mice) (Figure 29).



Figure 29. Picture of heterozygous and knockout for leptin mice. It's appreciable the different size.

C57BL/6 male mice were bought from Jackson laboratories, maintained under constant climatic conditions at 21°C with 12:12 h light–dark cycles, housed in group of four and given free access to food and water.

- Control (Chow) (n=14) received a standard laboratory diet, Chow diet, composed of 60% carbohydrates, 20% proteins and 10% lipids for 2 weeks from birth.
- High Fat Diet (HFD) (n=4) received a diet composed of 20% carbohydrates, 10% proteins and 60% lipids for 2 weeks from the birth.
- HFD & Exercise (n=4) received a diet composed of 20% carbohydrates, 10% proteins and 60% lipids for two weeks from the birth and subject to exercise in the second week of treatment.
- HFD & Control diet (n=4) received a diet composed of 20% carbohydrates, 10% proteins and 60% lipids and subject to exercise for 2 weeks from the birth and a Chow diet for 3 days.
- ob/ob mice (n=4) received a standard Chow diet.

At the end of the treatment the mice were fasted for 5 hours, after the starving each mouse was euthanized and some of the abdominal fat was taken and stored at -80°C.

2.2.5.2 Fat samples preparation

Extraction: Proteins were extracted from approximately 200mg of tissues using 400 μ L of Cell Permeabilization Buffer (Thermo Scientific™) and 4 μ L of Protease Inhibitor Buffer (Thermo Scientific™). Tissues were put in dry ice, then the homogenized for 1 min at 1000 rpm and proteins were separated by centrifugation at 13200Xg for 20 min at 4 C. The fat/oil fraction (upper) was transferred and kept at -80°C, while the cytoplasmic fraction (middle) was kept for the digestion step.

Protein quantification: Bio-Rad Protein Assay, based on the method of Bradford, is a simple and accurate procedure for determining concentration of solubilized protein. It involves the addition of an acidic dye to protein solution, and subsequent measurement at 595 nm with a spectrophotometer or microplate reader. Comparison to a standard curve provides a relative measurement of protein concentration. The Coomassie blue dye binds to primarily basic and aromatic amino acid residues, that the extinction coefficient of a dye-albumin complex solution is constant over a 10-fold concentration range. Thus, Beer's law may be applied for accurate quantitation of protein by selecting an appropriate ratio of dye volume to sample concentration. The Bio-Rad Protein Assay was executed as following:

- Bovine Serum Albumin (BSA) standard was reconstituted at the concentration of 1mg/ml and diluted 1:2 in order to obtain other 7 standards, which is representative of the protein solution to be tested: 0.5 mg/ml, 0.25 mg/ml, 0.125 mg/ml, 0.063 mg/ml, 0.031 mg/ml, 0.015 mg/ml and 0.007 mg/ml. The standards were conserved at -20°C.
- Each sample was diluted 1:10 with bi-distilled water.
- 10 μ L of each standard and sample solution was pipetted into the wells of a clean 96 wells plate in duplicate (table 7).
- 200 μ L of 1:4 diluted dye reagent were added to each well.

The plate was inserted in the plate reader, shaken and measured at 595 nm wavelength.

	1	2	3	4	5	6	7	8	9	10	11	12
A	ST 1	ST 1	smp 1	smp 1	smp 9	smp 9	smp 17	smp 17	smp 25	smp 25	smp 33	smp 33
B	ST 2	ST 2	smp 2	smp 2	smp 10	smp 10	smp 18	smp 18	smp 26	smp 26	smp 34	smp 34
C	ST 3	ST 3	smp 3	smp 3	smp 11	smp 11	smp 19	smp 19	smp 27	smp 27	smp 35	smp 35
D	ST 4	ST 4	smp 4	smp 4	smp 12	smp 12	smp 20	smp 20	smp 28	smp 28	smp 36	smp 36
E	ST 5	ST 5	smp 5	smp 5	smp 13	smp 13	smp 21	smp 21	smp 29	smp 29	smp 37	smp 37
F	ST 6	ST 6	smp 6	smp 6	smp 14	smp 14	smp 22	smp 22	smp 30	smp 30	smp 38	smp 38
G	ST 7	ST 7	smp 7	smp 7	smp 15	smp 15	smp 23	smp 23	smp 31	smp 31	smp 39	smp 39
H	ST 8	ST 8	smp 8	smp 8	smp 16	smp 16	smp 24	smp 24	smp 32	smp 32	smp 40	smp 40

Table 7. 96 wells plate map used for protein quantification, STD are the standards in decreasing dilution from 1mg/ml to 0.007mg/ml. smp. are the samples diluted 1:10

This step was introduced with the aim to standardize the analysis and process the same amount of proteins. This quantification helped us to understand the reproducibility of the method among the samples and standardize the analysis minimizing the variability of the samples. After obtained the concentration of the samples and decided the amount of proteins to process we proceeded with the digestion.

Digestion: Thirty microliters of each samples were denatured with 10 μ L of DL-dithiotreitol (5mg/ml) at 37°C for 20 min and alkylated with 10 μ L of Iodoacetamide (12.5mg/ml) at 37°C for 20 minutes. Samples were diluted with 25mM NH₄HCO₃ (450 μ L). Trypsin digestion was performed in three stages using: first digestion adding 15 μ L of Trypsin solution 1 (7.5 μ L (3.75 μ g) of Promega Trypsin solution + 7.5 μ L of 25mM NH₄HCO₃) to each sample and incubating overnight at 37°C, second digestion using 10 μ L of Trypsin solution 2 (8 μ L of 25mM NH₄HCO₃ + 2 μ L (1 μ g) of Promega Trypsin solution) to each sample and incubating at 37°C of 2 hours and the third step using again 10 μ L of Trypsin solution 2 to each sample and incubating at 37°C of 2 hours. 55 μ L of Formic Acid 10% were used to stop the digestion and ionize the peptides.

StageTips: Digested peptides were desalting and cleanup using the Stage Tips. Samples were passed two times through the tips, desalted with Buffer A and eluted with 50µL of Buffer B and 50µL of ACN 100%. Samples were dried in speed vacuum for 30 minutes and resuspended for the MRM analysis with 5µL of Buffer B' and 115µL of Buffer A.

2.2.5.3 Chromatographic and MRM-MS analysis

The chromatographic separation was achieved with a Dionex Ultimate 3000 SRLCnano HPLC system (Thermo Scientific™) coupled to a TSQ Quantum Ultra (Thermo Scientific™). The LC separation of the 5µL injected samples was carried out on a C18 column Acclaim PepMap® RSLC column from Thermo Scientific™. Elution was performed keeping a 5% concentration of Buffer B for 10 minutes and starting a linear shallow gradient from to 30% B in 22.5 minutes, to allow a good separation of the peptides of interest, followed by a steep gradient, from 30 to 90% of Buffer B, in 5.5 minutes. The washing step was executed with 90% B for 7 minutes and the column re-equilibration with Buffer A for 14 minutes. The entire cycle was 50 minutes long with a flowrate of 0.300µL/min.

Each analysis was preceded by a blank in order to prepare the column and every 5 samples was made a blank to clean the column avoiding an accumulation of un-eluted peptides.

For the detection of murine GLUT4 (UniProt 14142, Figure 30a) were selected some peptides and the relative parent and daughter ions for the quantification from Pinpoint in silico digestion library. In this case the IS used is Laminin (UniProt P02469, Figure 30b). MRM analyses were performed with TSQ Quantum Ultra (Thermo Scientific™) triple quadrupole coupled to a Dionex Ultimate 3000 SRLCnano HPLC system (Thermo Scientific™). The LC separation was carried out as described before and ESI was delivered using a stainless-steel emitter (ID 30 µM, 10 cm length, Thermo Scientific™). Pinpoint™ 1.4 (Thermo Scientific™) software was used for method development and the optimization of the mass spectrometer parameters. The MS analysis was carried out in a positive ionization mode, using an ion spray voltage of 2000V and a temperature of 200°C with the nebulizer and gas flow set at 30 psi. The complete system was fully controlled by Xcalibur™ software (Thermo Scientific™).

A

MPSGFQQIGSDDGEPPRQRTVTGLVLAVFSAVLGSLQFGYNIGVINAPQKVIEQSYNATWLGRQGGPGPDSIP
QGTLTTLWALSVAIFSVMGMISSFLIGIISQWLGRKRAMLANNVLAVLGGALMGLANAAASYEILILGRFLIG
AYSGLTSGLVPMYVGEIAPTHLRGALGTLNQLAIVIGILVAQVLGLESMLGTATLWPLLLALTIVLPALLQLIL
LPFCPESPRYLYIIRNLEGPARKSLKRLTGWADVSDALAELK [HNE] DEK [HNE] RKLERERPMSLLQLLGSR
THRQPLIIAVVLQLSQQLSGINAVFYYSSTIFESAGVGQPAYATIGAGVVNTVFTLVSVLLVERAGRRTLHLL
GLAGMCGCAILMTVALLLLERVPAISYVSIVAIFGFVAFFEIGPGPIPWFIWAELFSQGRPAAMAVAGFSNW
TCNFIVGMGFQYVADAMGPYVFLLFVALLLGFFIFTFLKVPETRGRTFDQISAAFRRTPSLLEQEVKPSLE
YLGPDEND

B

MGLLQVFAFGVLALWGTRVCAQEPEFSYGCAEGSCYPATGDLIGRAQKLSVTSTCGLHKPEPYCIVSHLQED
KKCFICDSRDPYHETLNPDSHLIENVVTTFAPNRLKIWWQSENGVENVTIQLDLEAEFHFTHLIMTFKTRPA
AMLIERSDDFGKAWGVYRYFAYDCSSFPGISTGPMKKVDDIICDSRYSDIEPSTEGEVIFRALDPAFKIEDP
YSPRIQNLLKITNLRIKFVKLHTLGDNLDSRMEIREKYYYAVYDMVVRGNCFCYGHASECAPVDGVNEEVEG
MVHGHCMCRHNTKGLNCELCMDFYHDLWPWPAEGRNSNACKKCNCEHSSSCHFDMAVFLATGNVSGGVCDNC
QHNTMGRNCEQCKPFYFQHPERDIRDPNLCEPCTCDPAGSENGGICDGYTDFSVGLIAGQCRCKLHVEGERCD
VCKEGFYDLAEDPYGCKSCACNPLGTIPGGNPCDSETGYCYCKRLVTGQRCDQCLPQHWGLSNDLDGCRPCD
CDLGGALNNSCEDSGQCSCPLHMIGRQCNEVESGYFTTLDHYIYEAEANLPGVIVVERQYIQDRIPSWT
GPGFVRVPEGAYLEFFIDNIPYSMEYEILIRYEPQLPDHWEKAVITVQRPGKIPASSRCGNTVPDDDNQVVS
SPGSRVVLPRPVCFEKGMNYTVRLELPQYTASGSDVESPYTFIDSLVLMPCYCKSLDIFTVGGSGDGEVTNSA
WETFQRYRCLENSRSVVKTPMTDVCNRIIFSISALIHQTGLACECDPQGSLSVCDPNGGQCQCRPNVVGRTC
NRCAPGTFGFGPNGCKPCDCHLQGSASAFCDAITGQCHCFQGIYARQCDRCLPGYWGFPSCQPCQCNHALDC
DTVTGECLSCQDYTTGHNCRCLAGYYGDP IIGSGDHCRPCPCPDGPDGSGRQFARSCYQDPVTLQLACVCDPG
YIGSRCDDCASGFFGNPSDFGGSCQPCQCHHNIDTTDPEACDKETGRCLKCLYHTEGDHCQLCQYGYGDALR
QDCRKCVCNYLGTVKEHCNGSDCHCDKATGQCSCLPNVIGQNCDCRCPNTWQLASGTGCGPCNCNAAHSFGPS
CNEFTGQCQCMGPGGRTCECQELFWGDPDVECRACDCDPRGIETPQCDQSTGQCVCVEGVEGPRCDKCTR
YSGVFPDCTPCHQCFALWD AII GELTNRTHKFLEKAKALKISGVIGPYRETVDSEKVKNEIKDILAQSPAAE
PLKNIGILFEEAEKLT KDVT EKMAQVEVKLTDTASQSNSTAGELGALQAEAESLDKTVKELAEQLEFIKNSDI
QGALDSITKYFQMSLEAEKRVNASTTDPNSTVEQSALTRDRVEDMLERESPFKEQQEEQARLLDELAKLQS
LDLSAVAQMTCTGTPPGADCESECGGPNCRTEDEGEKKCGGPGCGGLVTVAHSAWQKAMDFDRDVL SALAEVEQ
LSKMOVSEAKVRADAEKQNAQDVLLKT NATKEKVDKSNEDLRNLIKQIRNFLTEDSADLDSIEAVANEVLKMEM
PSTPQQLQNLTEDIRERVETLSQVEVILQQAAD IARAELLLEEAKRASKSATDVKVTADMVKEALEEAEKAQ
VAAEKAIKQADEDIQGTQNLTSIESETAASEETLTNASQRISKLERNEELKRKAAQNSGEAEYIEKVVS
KQNAADVKKTLDGELDEKYKKVESLIAQKTEESADARRKAELLQNEAKTL LAQANSKLQLEDLERKYEDNQK
YLEDKAQELVRLEGEVRSLLKDISEKVAVYSTCL

Figure 30. A. Murine GLUT4 fasta sequence, B. Laminin Protein sequence used for IS. In red the modified residues and underlined laminin peptide used as IS.

The detailed MRM-MS method, with the m/z of precursor and product ions, is not fully described because the project is under confidential regulation till the publication.

2.2.5.4 Statistical Analysis

Experimental results are presented as mean \pm standard error of the mean (SEM). Significant variations and the P value in the data within groups were determined using non-parametric Kruskal-Wallis and Mann-Whitney tests. All analyses were conducted using GraphPad Prism 6.0 (GraphPad Software, Inc.). Data used for the calculations derives from the mean of triple lecture of each sample.

Section 3: Results

3.1 Chronic Obstructive Pulmonary Disease

3.2 Type 2 Diabetes Mellitus

3.1 Chronic Obstructive Pulmonary Disease

3.1.1 Correlation between H3.3 peptide and FEV₁/FVC

The correlation between H3.3 with FEV₁/FVC was studied to prove the hypothesis that the release of H3.3 is connected with a worsening of COPD and is one of the cause and consequence of respiratory impairment. This correlation is important to show the consistency between the FEV₁/FVC index, already used in medicine as a diagnostic index for COPD, and the H3.3, the candidate biomarker. This study was developed plotting, for each patient, the FEV₁/FVC data (x axes) and the H3.3 amount (y axes), normalized. The graph below (Figure 31) displays that H3.3 level tends to increase with decreasing FEV₁/FVC capacity, showing that lung capacity impairment is linked with the release of H3.3 in the plasma. However, it has to be pointed out that a clear general correlation for COPD patients is hard to be establish because of several factors. Different factors, other than the severity of the pathology, contribute to the increase in H3.3 level leading to very heterogeneous populations. This effect is even amplified by the fact that AECOPDs have different possible causes and are not easy to be differentially diagnosed and can then cause higher variance in the analysis.

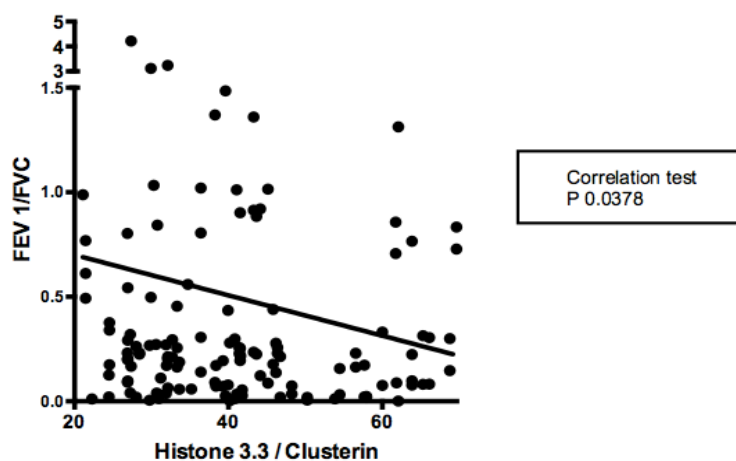
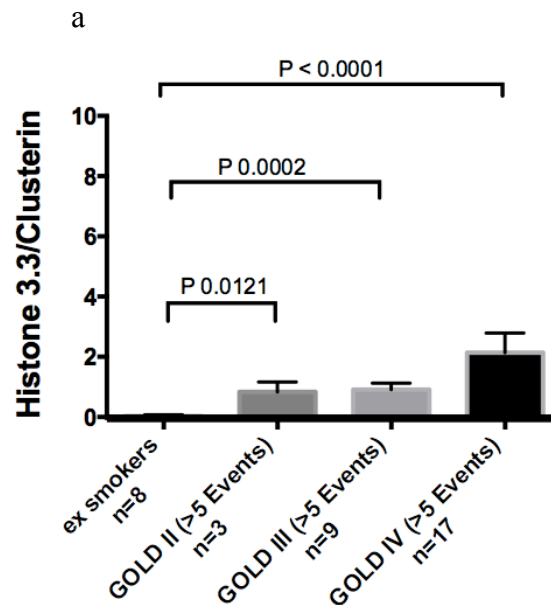
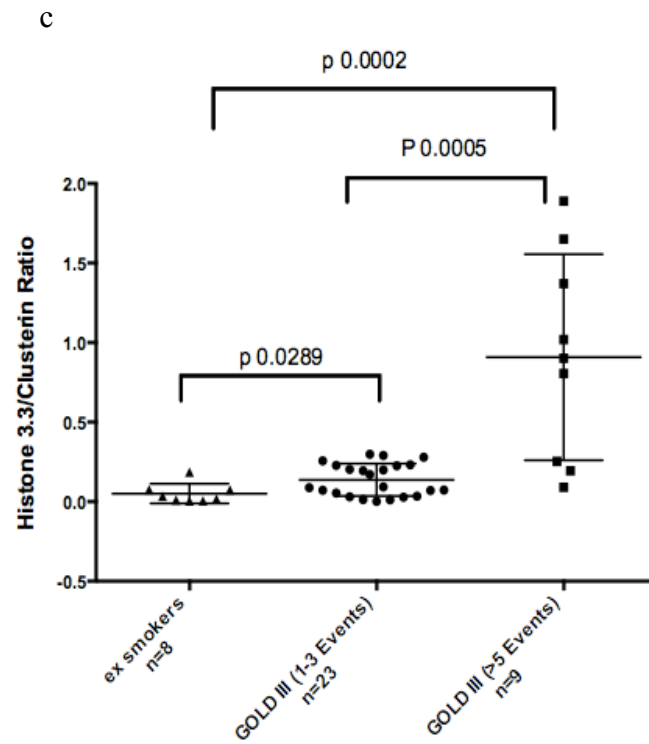
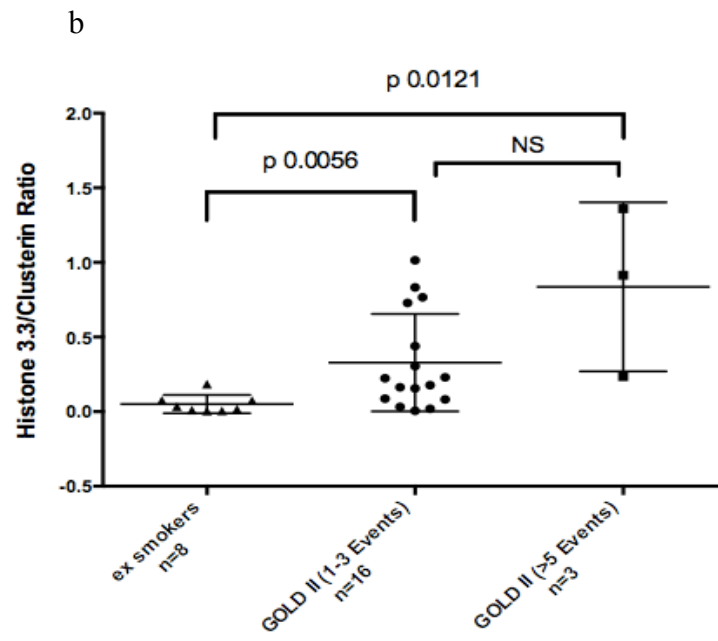


Figure 31. Correlation of H3.3 level with FEV₁/FVC ratio as indicator of pathology severity.

3.1.2 H3.3 increases in patients with most severe GOLD

To deepen the correlation of H3.3 levels with the disease, patients with rare AECOPD (1 to 3/year) were separately analyzed from patients that had more than 5 AECOPDs during the year. This classification is thus dependent on the GOLD stage. In figure 32b is shown the comparison of the H3.3 peptide amount in ex-smoker patients, used as control, and GOLD II patients, in c the same comparison with GOLD III patients and in d with GOLD IV patients. The higher level of circulating H3.3, reported in COPD patients, is more amplified in subjects with more >5 AECOPDs. p value between the control and the patients with >5 events, indeed, decreases with increasing of GOLD stage (GOLD II $p=0.0121$, GOLD III $p=0.0002$ and GOLD IV $p<0.0001$, Figure 32a).





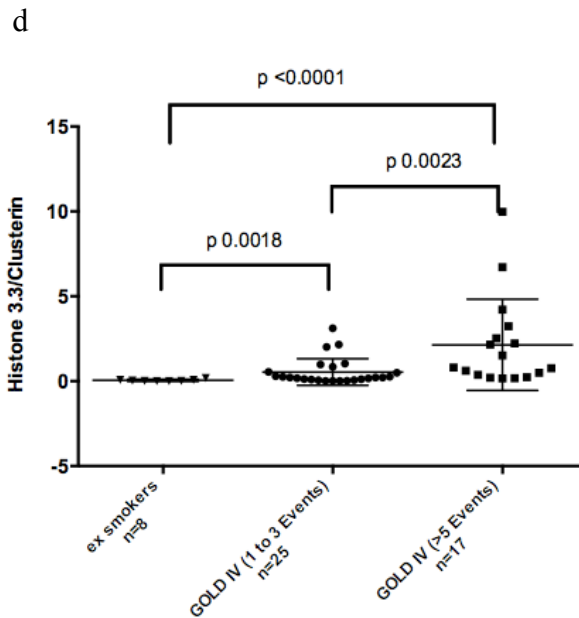
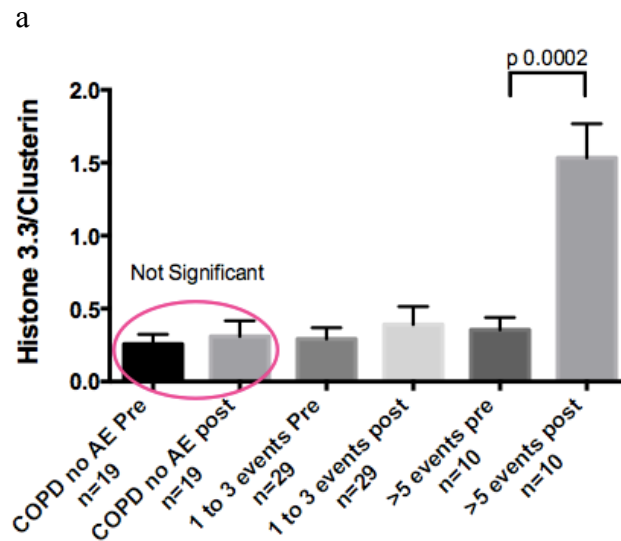


Figure 32. Total amount of H3.3. Amount of H3.3 for each GOLD stage in a, difference between non-smokers and patients with different number of AECOPD for GOLD II in b, GOLD III in c and GOLD VI in d.

Using a different classification of the patients, grouped according to the timing of blood draw (“pre” stands for time 0 and “post” for time 12) and the number of AECOPD per year, is possible confirm the hypothesis of a correlation between the amount of H3.3 and the worsening of the disease. The thesis supported is that not only the GOLD stage is important for COPD diagnosis, but also the AECOPD events in the year (Figure 33).



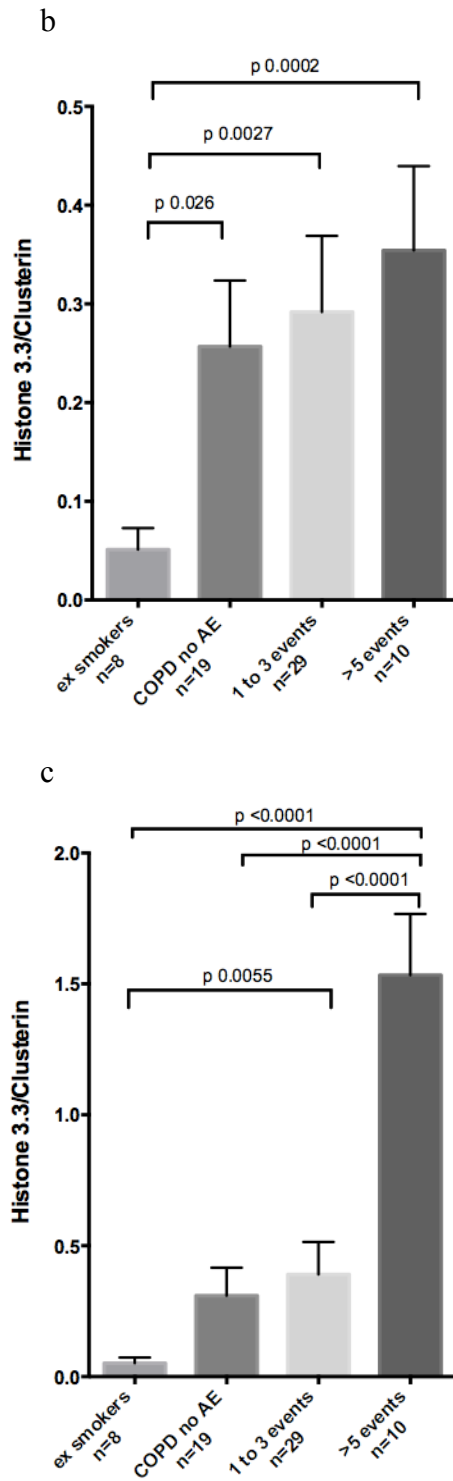
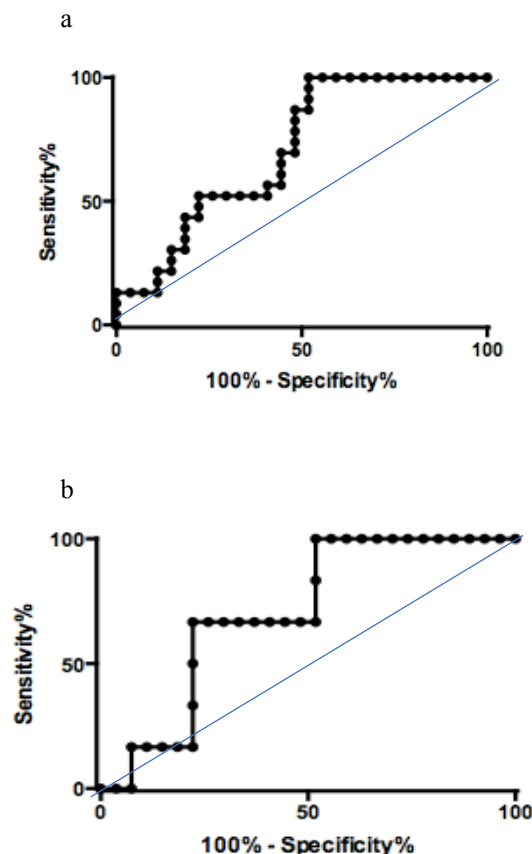


Figure 33. The graphs show the difference of H3.3 between ex-smokers, patients with no AECOPD and patients with a different number of AECOPD. In a the comparison between time 0 and time 12, in b the graphs represent the data regarding the level of H3.3 at time 0 and in c the same patients at time 12.

3.1.3 Evaluation of H3.3 as diagnostic biomarker

To determine whether H3.3 could be a good biomarker for COPD patients, receiver operating curve (ROC) was used (Figure 34). ROC curves provide a comprehensive and visually attractive way to summarize the accuracy of predictions. Each point on the curve represents the true-positive rate (Sensitivity) and false-positive rate (Specificity) associated with a particular test value. The AUC provides a useful metric to compare different tests. Whereas an AUC value close to 1 indicates an excellent diagnostic test, a curve that lies close to the diagonal (AUC = 0.5) has no information content and therefore no diagnostic utility.

The areas under the ROC curve (AUC) are good with an AUC of 0.707 for GOLD III and 0.585 for GOLD IV patients with 1 to 3 AECOPD/year, while the AUC of 0.707 for GOLD III and 0.88 for GOLD IV subjects with >5 exacerbations/years. With the exception of not frequent exacerbators GOLD IV patients the AUCs calculated are fair and acceptable.



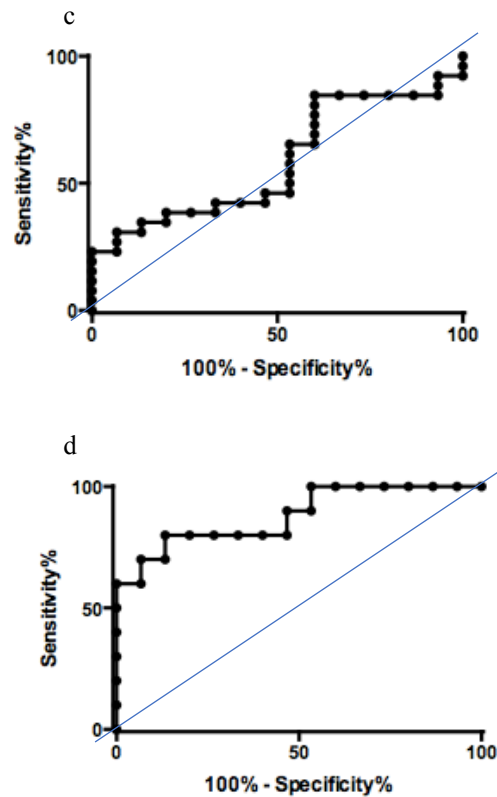


Figure 34. ROC curves of H3.3. ROC was used to differentiate patients with no AECOPD (control) from GOLD III 1-3 AE/year (A), GOLD III >5 AE/year (B), GOLD IV 1-3 AE/year (C) and GOLD IV >5 AE/year (D) The blue line marks the 50% threshold.

3.1.4 H3.3 peptide increases in proximity of AECOPD events.

Generally, patients with the same GOLD that experienced more than 5 AECOPD during the 12 months of follow up showed the higher increase in H3.3. On the light of these results, we deepen investigation about the increase in H3.3 level correlating H3.3 level with proximity to AECOPD event. We found that H3.3 levels were enhanced and almost doubled within 2 weeks from the exacerbation events (Figure 35). In order to identify a possible prognostic marker, we analyzed H3.3 levels before and after AECOPD; interestingly the increase in H3.3 levels occurred mainly before AECOPD, while after the event the protein amount tends to return stable within 2 weeks.

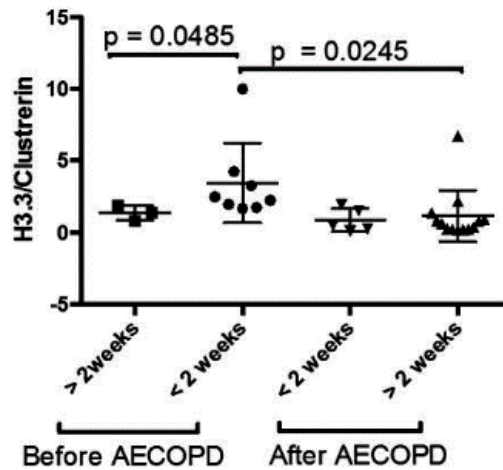


Figure 35. COPD patients were grouped according to the proximity to AECOPD events at the moment of blood withdrawal. From left to right the patients were more than 2 weeks distant before an AECOPD, less than 2 weeks before, less than 2 weeks after and more than 2 weeks after.

3.1.5 H3.3 and its role in the pathology

To clarify how H3.3 is involved in the pathology progression, we run more specific MRM analysis focused on post-transcriptional modification of H3.3. Indeed, it has been reported that H3.3 detected in BLAF is hyperacetylated [7]. On the other hand, H3.3 released from NETs that circulates in the blood propagating the inflammatory disease can be detected by the citrullination. So, we aimed at detecting acetylated and citrullinated H3.3 to differentiate the source of the protein and strengthen the theory of H3.3 as rational biomarker for COPD. We found that both acetylated and citrullinated H3.3 were present in the plasma, suggesting a picture of lung-initiated effect that is then amplified by circulating NETs. In particular, citrullinated H3.3 level gave the highest signal, consisting with an inflammatory situation as previously reported in the introduction (Figure 36).

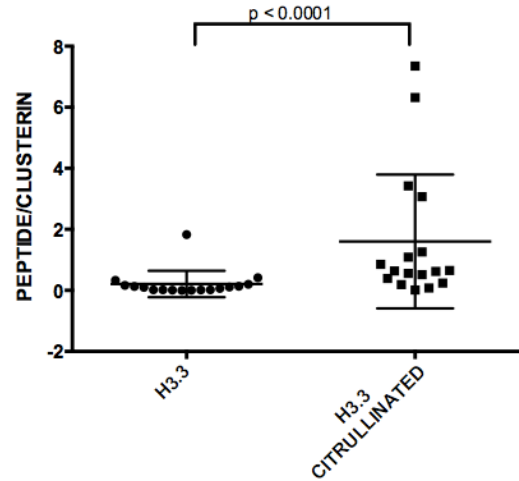


Figure 36. Amount of H3.3 and Citrullinated H3.3 in plasma sample of patients. H3.3 and H3.3cit data correspond to the same set of patients.

Acetylated H3.3 was detected in plasma of the same patient analyzed for H3.3 and classified according the GOLD stage. The results shown that the trend of the amount of hyperacetylated histones is consistent with the severity of the GOLD classification (Figure 37).

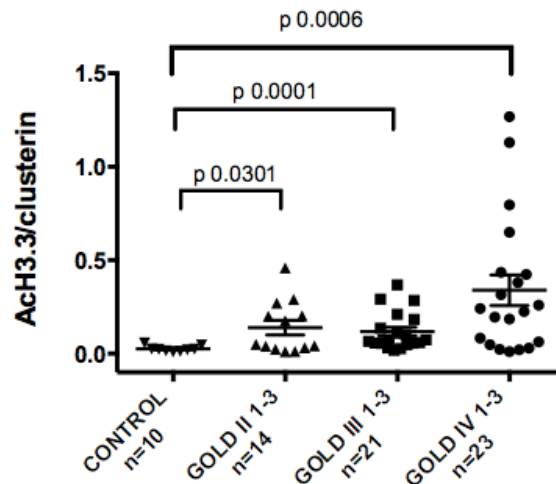


Figure 37. Amount of AcH3.3 in control people and in GOLD II, GOLD III and GOLD IV patients with 1-3 AE/year.

Also comparing the amount of AcH3.3 according to the time and the number of AECOPD is possible see that patients with 1 to 3 events have a higher level of acetylated histones. Interesting, patients with no AE during the year decrease the amount of AcH3.3 to levels not

statistically different from the control. It's also possible appreciate the impact of the abundance of the acetylated part on the total content of histones (Figure 38).

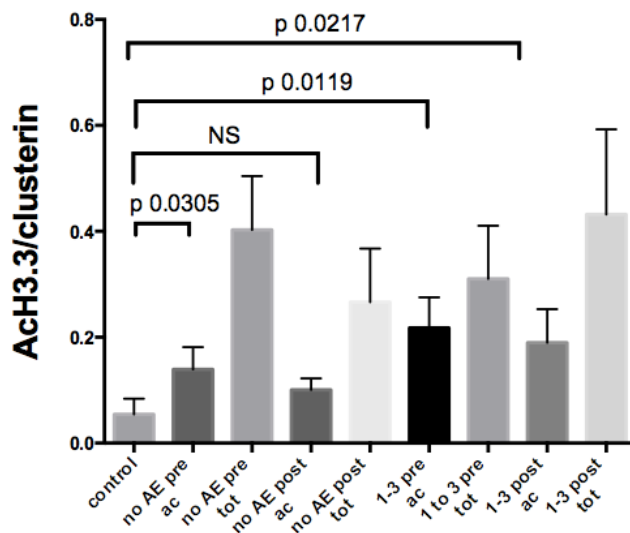


Figure 38. Time 0 (pre) and time 12 months (post) comparison of the levels of AcH3.3 in control, patients with no AE and patients with 1-3 events/year.

The results shown that the trend of the amount of hyperacetylated histones is consistent with the course of the disease, confirming the theory of the self-sustaining cascade of apoptosis in COPD progression.

3.2 Type 2 Diabetes Mellitus

3.2.1 Level of GLUT4-HNE after Over-nutrition Diet

Oxidative stress has already been implicated in the etiology of insulin resistance; in the previous work *Merali et al.* [50] hypothesized that connection between the oxidative stress and the insulin resistance are several GLUT4 post-translational modifications.

Six healthy people were fed for 7 days with 6206 ± 256 kcal/day of a common American diet consisting of 50% carbohydrates, 35% lipids and 15% protein, called Lean diet. After 7 days these patients gained weight, represented by adipose tissue, reaching a BMI between 25 and 29.9. Although not increasing Free Fatty Acids (FFAs) concentration and maintaining a fasting rate in the standard, a fast insulin-resistance was observed, as demonstrated by the homeostasis model of assimilation of insulin resistance (HOMA-IR). It was then investigated whether the development of this pre-diabetic syndrome could be attributed to pro-inflammatory cytokines derived from the FFAs. There was no significant change in adipose tissue in any of the mRNA coding for stress factors, therefore the proteomic screen in adipose tissue does not support the hypothesis that FFAs would induce, through pro-inflammatory cytokine, the initial development of overnutrition-induced insulin resistance. Obviously, this hypothesis does not exclude the role of FFAs in the pathogenesis of the disease. The analysis of fatty tissue proteomics showed an increase in ROS detoxification mechanisms such as superoxide dismutase 2 (SOD), catalase and glutathione peroxidase. This transcriptional profile has highlighted the idea that adipose tissue is a source of ROS production that overcomes the detoxification mechanism. The idea of a link between oxidative stress and extensive post-translational modifications was supported by the observation (with 2D electrophoresis gels) of an extensive ROS- mediated protein oxidation and carbonylation. Specifically, extensive GLUT4 carbonylation as well as adduction of HNE and glutamic semi-aldehyde in close proximity to the glucose transport channel. Carbonylation typically causes protein cross-linking and loss or alteration of protein function.

On the light of these evidences, the amount of GLUT4-HNE peptide, before and after the over-nutrition diet, was compared with the aim to verify the relative amount. The following graph (Figure 39) represents the mean \pm SEM of GLUT4-HNE measured in the cytosolic fraction of sub-cutaneous fat tissue of patients.

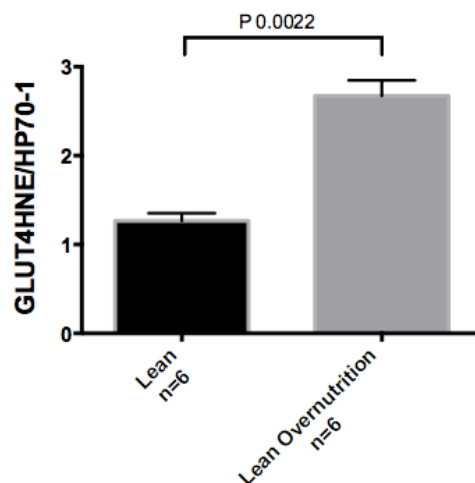


Figure 39. Comparison of the amount of GLUT4-HNE before (Lean) and after a high calorie diet intake (Lean Overnutrition) composed of 50% by carbohydrates.

The rising amount of GLUT4-HNE with the concomitant insulin resistance has meant a link between oxidative stress, carbonylation, GLUT4 inactivity, insulin resistance and therefore T2D.

3.2.2 Level of GLUT4-HNE in non-diabetic and diabetic subjects

After seeing the significant difference in GLUT4 carbonylation in sub-cutaneous fat tissue of those patients showing an insulin-resistance profile it was studied whether this difference is also present fat tissue coming from non-diabetic and diabetic people.

Many investigators have reported that abdominal adipose tissue is a major contributor to metabolic risk. Department of Internal Medicine, University of Texas, has examined the relationships between generalized and regional adiposity and insulin sensitivity in a group of non-diabetic men with varying degree of obesity, concluding that abdominal fat plays a major role in obesity related insulin resistance in comparison to sub-cutaneous fat [60].

Subsequently, by the same Department, were examined a similar relationship among men with non-insulin dependent diabetes mellitus and found that abdominal fat had a stronger correlation with insulin sensitivity than sub-cutaneous fat [60].

A mixed races pool of abdominal fat tissue samples from obese non-diabetic (control) and obese diabetic people was analyzed. The investigation of these samples has the purpose to observe whether the presence of GLUT4-HNE is transient and present only in insulin resistance syndromes or if it persists in the progression of the disease. The threefold increase of GLUT4-HNE, in figure 40, shown a significant difference between diabetic patients (black) and control (grey), showing a lower availability of functional GLUT4 in diabetic patients.

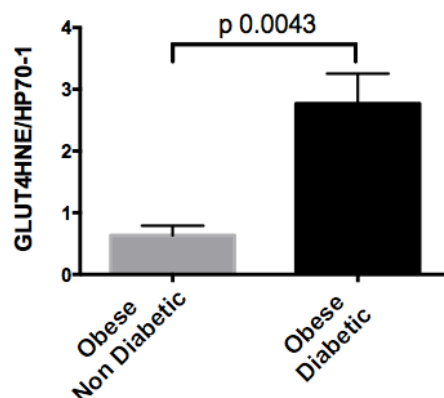


Figure 40. GLUT4-HNE level comparison between non-diabetic and diabetic people in abdominal fat tissue.

This result confirms the hypothesis about the central role of abdominal fat in insulin-resistance syndrome. GLUT4-HNE concentration, indeed, is higher in diabetic fat tissue. These patients, probably, slowly become diabetic through different stages:

Over nutrition => Oxidative stress => GLUT4-HNE => Insulin-resistance => Diabetes.

At this point was also necessary investigate subcutaneous fat coming from obese non-diabetic, obese pre-diabetic and obese diabetic people. The samples were processed, MRM-analyzed and statistically studied with the same methods and criteria used for the abdominal samples, according to material and methods. These steps were followed carefully and

rigorously in order to have the maximum accuracy for a good comparison, reducing as much as possible the variables.

In the following graphs (Figure 41) it's clear the difference between control (black), pre-diabetic (grey) and diabetic people (dark gray), indeed, obese pre-diabetic and obese diabetic have a double amount of GLUT4-HNE compared with obese non-diabetic control people. The presence of carbonylation in pre-diabetic patients strengthens the hypothesis according to which is the GLUT4 carbonylation the very first step to insulin-resistance and Type 2 Diabetes.

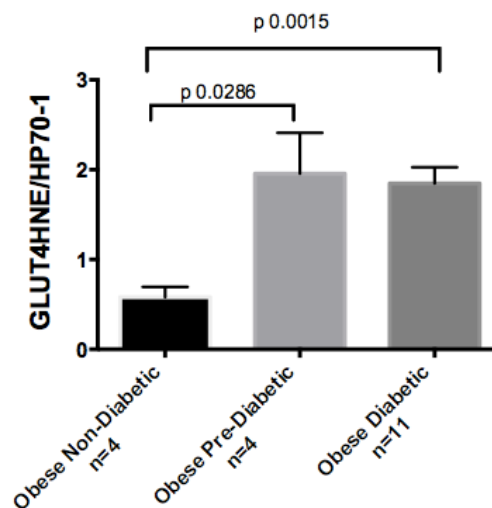


Figure 41. Comparison of GLUT4-HNE level, subcutaneous fat tissue, between healthy subjects, pre-diabetic and diabetic subjects, the bars represents the mean \pm SEM.

The presence of GLUT4-HNE also in subcutaneous fat pointed out the involvement of the whole fat tissue in appearance and progression of insulin-resistance.

3.2.3 Murine GLUT4-HNE level

In order to confirm if mouse could be a good model for the drug development able to mimic the human metabolism to design treatments of new drugs or other metabolism training, was studied the mice pattern of GLUT4-HNE in response to a DIO (Diet-induced obesity). The amount of GLUT4-HNE was analyzed among several dietary groups of mice. In the following picture (Figure 42) is possible to appreciate the statistical difference of the abundance of Carbonylated GLUT4. The subcutaneous fat tissue of HFD and ob/ob mice have a higher level of GLUT4-HNE than the chow diet mice (control).

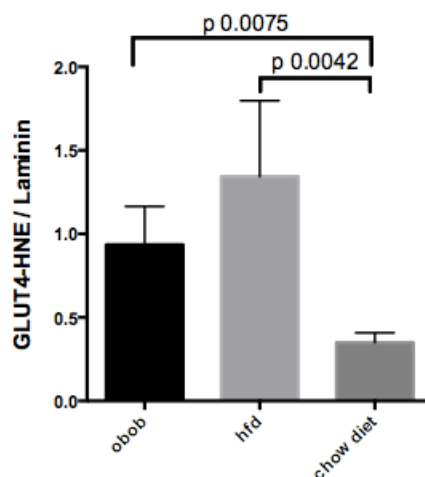


Figure 42. Comparison of GLUT4-HNE level in adipose tissue of ob/ob mice with a regular diet, HFD mice and mice with a regular diet.

Is possible to highlight that there is no difference between the ob/ob mice, obese *per se* and the HFD mice, induced to became obese. That means that genetic predisposition to obesity induce a tendency to carbonylation. This condition is difficult to treat only feeding mice with a standard diet.

Next step was to evaluate how reduce the level of GLUT4-HNE in mice with a HFD. In other words, the goal is to determine is possible to reverse the Carbonylation reaction. An interesting comparison was done studying the effect of physical exercise or diet in HFD mice. A bad lifestyle has always been corrected with physical exercise and health diet in pre-

diabetic and diabetic patients. To see how good is the physical exercise and a correct diet for GLUT4-HNE level, data from the mice subjected to exercise or diet were analyzed and compared to the previous results (Figure 43).

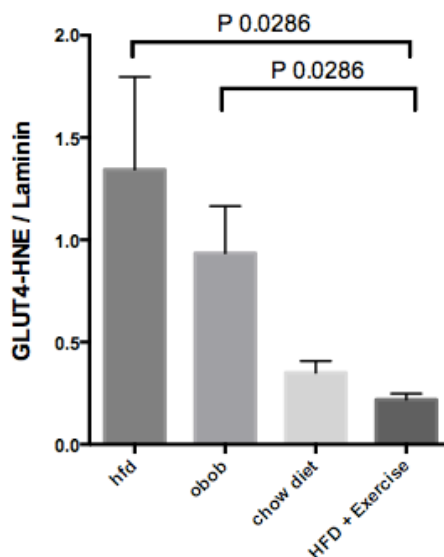


Figure 43. Comparison of GLUT4-HNE level in adipose tissue of HFD mice, ob/ob mice with a chow diet, chow diet mice and mice subjected HFD and exercise.

For the analysis in Figure 43 chow diet mice population is considered negative control and HFD and ob/ob are considered positive controls (the significant difference between them was already shown in figure 42). The graph shows how mice treated with exercise reach levels of GLUT4-HNE comparable with those of chow diet control mice. This data can underline the positive effect of and exercise on the regression of carbonylation. Regarding data from HFD mice subjected to a “correcting” chow diet was not possible to show a statistic because one of the samples was not good and was impossible to have a good MRM result.

Section 4: Conclusions

4.1 Chronic Obstructive Pulmonary Disease

4.2 Type 2 Diabetes Mellitus

A biomarker is a biological characteristic that is objectively measured and evaluated as an indicator of normal biological or pathological processes, or a response to a therapeutic intervention. The use of biomarkers in basic and clinical research as well as in clinical practice has become so commonplace that their presence in clinical trials is now accepted almost without question. In the case of specific biomarkers that have been well characterized and repeatedly shown to correctly predict relevant clinical outcomes across a variety of treatments and populations, this use is entirely justified and appropriate.

Multiple Reaction Monitoring - Mass Spectrometry (MRM-MS) exploits the unique capability of three quadrupoles to act as mass filters and to selectively monitor a specific analyte molecular ion and one or several fragment ions generated from the analyte by collisional dissociation. The a highly sensitivity and selectivity allow peptide quantification and biomarker identification in complex biological samples.

Chronic obstructive pulmonary disease and type 2 diabetes are two of the most important public health challenges and major cause of morbidity and mortality throughout the world. The increasing number of patients with COPD and T2D has raised the need for therapies and identification of biomarkers, in particular to prevent, respectively, exacerbations of COPD and T2D progression.

4.1 Chronic Obstructive Pulmonary Disease

COPD is described by extensive lung inflammation, cell apoptosis, and tissue destruction in a picture of progressive disease that leads to impairment of breath ability. Previously reported study pointed out that H3.3 is detected in BALF of patients, thus a better understanding of the H3.3 involvement would contribute to a better understanding of COPD disease progression and perhaps new approaches to treatment. COPD is characterized by episodes of acute exacerbation with frequency variation, with the tendency to cluster together, that frequently require hospitalization and repeated readmissions to hospital. These AECOPD are acute aggravation of the symptoms that often follow persistent elevated systemic inflammation. The most frequent causes of AECOPD are respiratory infections,

atmospheric pollution or exposition to cigarette smoke; however, in around one-third of cases the causes are not identified. The consequence of AECOPD is the acceleration of the decline of lung function and increased mortality of COPD patients, thus worsening patients' life quality and increasing death rate. Indeed, most of the morbidity and mortality in COPD relates to exacerbations. AECOPD accounts for a large proportion of the health care expenditure on the treatment of COPD, underlining the importance of research for strategies to prevent them. Patients that experience frequent exacerbations have significant airway and systemic inflammation even during the stable phase of the disease. It has been already reported that extracellular histones are involved in several inflammatory diseases and circulating core histones have been demonstrated to be mediators of trauma-associated lung injury and cytotoxic to lung cells. Different mechanisms have been reported or proposed to explain histones toxicity and their role in inflammation.

It seems reasonable to focus on Histone 3.3 as player in COPD due to its inflammation involvement and to try to correlate its extracellular level with the progression of the disease and with exacerbation occurrence. In this study, I tested this hypothesis by comparing plasma samples of COPD patients with different clinical situation, i.e. in different GOLD classification and with rare or frequent AECOPD. Internal normalization was done using abundant plasma protein, clusterin.

4.1.1 Correlation between FEV₁/FVC and H3.3 in plasma

FEV₁/FVC is one of the most used criteria to classify a COPD patient and it's a good parameter to describe the health status of lungs. This index however is not able to predict an event of exacerbations or cannot be performed if the patient is senseless. It is important, thus, understand if the amount of H3.3 in plasma is correlated with the FEV₁/FVC index to become a valid and reliable parameter to describe the pulmonary efficiency. The analysis shows a significant inverse correlation between FEV₁/FCV and the amount of H3.3 in plasma. This result supports the idea that a low pulmonary capacity is due to a tissue destruction, this damage is the source of plasma histone 3.3. The reasonable trend of Histone 3.3 allows to

suppose this measure as a new and alternative parameter to evaluate the FEV₁/FVC when necessary. Despite the encouraging results it is necessary standardize an equation acceptable as a guideline to which reference in the emergency procedures (Figure 31, page 88).

4.1.2 Histone 3.3 trend between the GOLD stages

Histone 3.3, to be considered a biomarker, has to describe and follow the *normal biological processes, pathogenic processes, or pharmacologic responses to a therapeutic intervention*. In this study was compared the amount of H3.3 among the different GOLD stages to better evaluate the specificity and sensibility of this “candidate”. The results shown significant differences between GOLD stages and the control (ex-smokers or GOLD 0) (Figure 32, pages 90-92). Using a different classification for the statistic, patients were grouped according to the timing of blood draw (pre stands for time 0 and post for time 12) and the number of AECOPD per year. With this classification is likely possible to better characterize the COPD status of the patients and confirm a correlation between the amount of H3.3 and the worsening of the disease. The comparison between pre and post shows that H3.3 levels rapidly increase within one year in frequent AECOPD. Consequently, after one year of follow-up, patients who experienced more than 5 events in the year showed incredibly higher values of histones in their plasma, making even more evident the clear correlation between histones and the pathology. A possible explanation so far was a histone release from lung cells, especially during AECOPD induces cell apoptosis and lung decline.

Our thinking, indeed, is that the number of AECOPD/year is, at least, as important as the GOLD stage. The exacerbation event surely is the phenomenon that mostly affect the patient and cause a rapid worsening of the disease. The results using this different classification method show a good differentiation among the patients. In the future could be create a guideline based on the number of AECOPD to better evaluate the seriousness of the disease of a patient without a diagnosis. (Figure 33, pages 92,93)

Deepening the study of this effect, we found out that in proximity of AECOPD, less than 2 weeks before, H3.3 levels in plasma significantly increase, and then goes down again within

two weeks after the event. This method could be also useful to have a prognosis and previously estimate the number of events for each patients and start a preventive care program in those periods of time with a high incidence of infection, the main cause of COPD (Figure 35, page 96).

4.1.3 Hyperacetylated and citrullinated Histone 3.3

Increased H3.3 have been previously detected in BALF of COPD patients, and was therefore expected that some of the H3.3 originated from lung tissue destruction. Part of these histones has been reported to be hyperacetylated, as a consequence of reduced histone deacetylase activity in COPD. Notably, hyperacetylation of histones has been associated with inflammatory gene expression. The results shown that the trend of the amount of hyperacetylated histones is consistent with the severity of the GOLD classification confirming the theory of the self-sustaining cascade of apoptosis that contributes to the progression of COPD. Probably the less AcH3.3 sensitivity to proteasome degradation, the continuous transcription and production of inflammatory mediators help for the increase in lung of H3.3 and inflammation that cause the worsening of the disease. The figure 38, page 97, shown the amount of hyperacetylated histone 3.3 compared with the total amount of histone in subjects with 1-3 events and in subjects with no AECOPD at time 0 (pre) and after 12 months (post). The amount of AcH3.3 is significant different from the control in those patients who suffered of AECOPD during the year. Noteworthy is the case of the patients without exacerbations, these patients start, at time 0, with a remarkably amount of AcH3.3 but after a year they reach a level not significantly different from the control. Probably less AcH3.3 makes the patient less inclined to apoptotic cascade, thus improving the health status of the patient. Another explanation might be that the decrease in acetylated histone slows the indiscriminate production of inflammatory mediators, making the patient less prone to exacerbations. Both theories, however, propose an interruption of the vicious circle that characterizes this disease.

When released, histones can also propagate the response via the activation of NETs. Histones released from NETs are characterized by citrullination, and the presence in the blood of citrullinated H3.3 is associated with critically ill patients, more frequently in the presence of bacteria in tracheal aspirate. On the light of these data, we decide to investigate the post-translational modification on histones in plasma, as an evidence of their source. We performed analyses on citrullinated histones as marker of NETs release. We detected citrullinated histones in plasma of AECOPD patients. This value

.3 suggest that histones initially released in the lung were able to propagate the inflammatory cascade through activation of NETs, worsening the inflammation till the need for hospitalization. Moreover, it leads us to speculate that the tendency of AECOPD to cluster together as events is probably likely as a consequence of the activated inflammatory cascade. Once released, histones act as triggering factors of inflammation, and even after the AECOPD events, their high levels can induce a new inflammatory cascade, explaining the high tendency for AECOPD to relapse (Figure 36, page. 97).

In conclusion, it's possible to assert that COPD is triggered, propagated and empathized by many vicious circles that helps the disease to become chronic and worsening day by day. A better understanding of these circles is important to better comprehend the disease and the weakness in order to intervene. It is also important, however, be able to create, on the light of the results, some guidelines, based on reliable biomarker, to be used in emergency case. This work provides to both the necessity, indeed not only we found and speculate some mechanism but also we propose Histone 3.3 as biomarker. H3.3 levels correlate with the severity of the pathology and can be useful to follow the clinical status of each patient, with a relative quick and non-invasive method of diagnosis. Moreover, for COPD patients, the occurrence of exacerbations represents the main event that cause urgent hospitalization. Thus, a prognostic biomarker useful to foresee also the probability of each patient to have exacerbation in a close future will help to prevent the AECOPD itself thus improving patients' life quality.

4.2 Type 2 Diabetes Mellitus

Diabetes, according to the WHO, is a chronic disease that occurs either when the pancreas does not produce enough insulin or when the body cannot effectively use the insulin it produces. Until recently, this type of diabetes was seen only in adults but it is now also occurring increasingly frequently in children and pets. Impaired glucose tolerance (IGT) and impaired fasting glycaemia (IFG) are intermediate conditions in the transition between normality and diabetes. People with IGT or IFG are at high risk of progressing to type 2 diabetes, although this is not inevitable. Over time, diabetes can damage the heart, blood vessels, eyes, kidneys, and nerves but simple and healthy lifestyle measures have been shown to be effective in preventing or delaying the onset of T2D. Early diagnosis can be accomplished through relatively inexpensive testing of blood sugar. In insulin resistance, muscle, fat, and liver cells do not respond properly to insulin and thus cannot easily absorb glucose from the bloodstream, as a result, the body needs higher levels of insulin to help glucose enter cells. The β cells in the pancreas try to keep up with this increased demand for insulin by producing more. As long as the beta cells are able to produce enough insulin to overcome the insulin resistance, blood glucose levels stay in the healthy range. Over time, insulin resistance can lead to type 2 diabetes and prediabetes because the β -cells fail to keep up with the body's increased need for insulin and the glucose builds up in the bloodstream. T2D comprises the majority of people with diabetes around the world and is largely the result of excess body weight and physical inactivity, but how obesity promotes the insulin resistance remains incompletely understood. In his previous work *Merali et al.* proposed an excessive caloric intake as a trigger for insulin resistance and T2D in adipose tissue. The oxidative stress resulted in extensive oxidation and carbonylation of numerous proteins including carbonylation of GLUT4 near the glucose transport channel which likely results in loss of GLUT4 activity. These results suggest that the initial event caused by overnutrition may be oxidative stress, which produces insulin resistance, at least in part, via carbonylation and oxidation-induced inactivation of GLUT4.

4.2.1 Study of the effects of over-nutrition on GLUT4 transporter

The level of the amount of GLUT4-HNE, pre and post over-nutrition (Figure 39, page 99), has been study to see if the GLUT4-HNE outgrowth is also accompanied by a significant statistical difference. The analysis shows a rising amount of GLUT4-HNE. The increase in GLUT4-HNE with the concomitant insulin resistance has meant a link between oxidative stress, carbonylation, GLUT4 inactivity and therefore insulin resistance. After seeing the significant difference in GLUT4 carbonylation in over-nutrition patients, it was studied whether this difference is also present in the abdominal fat tissue of samples from obese non-diabetic and diabetic people. The threefold increase of GLUT4-HNE, (Figure 40, page 101), shows a significant difference between diabetic patients and control. At this point was necessary investigate how deep is the carbonylation process, which fractions of fat tissue could be involved and if it's a transient status. Samples from subcutaneous fat coming from obese non-diabetic, obese pre-diabetic and obese diabetic people were processed, MRM-analyzed and statistically studied with the same methods and criteria used for the subcutaneous samples, according to material and methods. Results (Figure 41, page 102) displays a clear the difference between the control, the pre-diabetic and diabetic people, indeed, obese pre-diabetic and diabetic subjects have a double amount of GLUT4-HNE compared with obese non-diabetic control people. The presence of carbonylation in pre-diabetic patients strengthens the hypothesis according to which is the GLUT4 carbonylation the very first step to insulin-resistance and T2D. The presence of GLUT4-HNE also in subcutaneous fat pointed out the involvement of the whole fat tissue in appearance and progression of insulin-resistance.

4.2.2 Murine model for GLUT4-HNE

Level of GLUT4-HNE was analysed among several mice groups with the aim to confirm if mouse could be able to mimic the human GLUT4-HNE trends. This verification is important to determine if mouse can be used for GLUT4-HNE treatment designs and drug discovery.

Results show that subcutaneous fat tissue of HFD and ob/ob mice have a higher level of GLUT4-HNE than the chow diet mice (control). A bad lifestyle has always been corrected with physical exercise and health diet in pre-diabetic and diabetic patients. To see how good are this “corrections” for reversing carbonylation reaction, GLUT4-HNE data from HFD exercised mice were compared to the other classes (Figure 42, 43, pages 103, 104). The mice treated with exercise reach levels of GLUT4-HNE comparable with those of control mice, underling the possible positive effect of the exercise on the carbonylation.

In conclusion, this work confirms the previous work of Merali and co-workers [50] and highlights the deepness of insulin resistance and T2D molecular processes. These patients slowly become diabetic probably through different stage:

Over nutrition => Oxidative stress => GLUT4-HNE => Insulin-resistance => T2D

GLUT4 carbonylation could be an early biomarker for insulin resistance and progression to T2D. This project demonstrates, also, that mouse could be a good model for DIO study including GLUT4-HNE analysis, making possible future experimentations of alternative or adjuvant insulin drugs or treatments.

REFERENCES

1. H Rodriguez, R Rivers, C Kinsinger, M Mesri, T Hiltke, A Rahbar, E Boja, "Reconstructing the pipeline by introducing multiplexed multiple reaction monitoring mass spectrometry for cancer biomarker verification: An NCI-CPTC initiative perspective", *Proteomics Clinical Applications, Proteomics Clin. Appl.* 2010, 4, 904–914
2. Biomarkers Definitions Working Group Bethesda, "Biomarkers and surrogate endpoints: Preferred definitions and conceptual framework", *Clinical Pharmacology & Therapeutics*, MPC. 2001.113989
3. E Ciccimaro, I A Blair, "Stable-isotope dilution LC–MS for quantitative biomarker analysis", *Bioanalysis, Bioanalysis* (2010) 2(2), 311–341
4. A Koutsokera, K Kostikas, L P Nicod and JW Fitting, "Pulmonary biomarkers in COPD exacerbations: a systematic review" *Respiratory Research, Respiratory Research* 2013, 14:111
5. DM. Mannino, "Biomarkers in COPD: the search continues!", *European Respiratory Journal, Eur Respir J* 2015; 45: 872–874
6. A. Lacoma, C. Prat, F. Andreo and J. Domínguez, "Biomarkers in the management of COPD", *European Respiratory Journal, Eur Respir Rev* 2009; 18: 112, 96–104
7. CA Barrero, O Perez-Leal, M Aksoy, C Moncada, R Ji, Y Lopez, K Mallilankaraman, M Madesh, GJ Criner, SG Kelsen, S Merali, "Histone 3.3 participates in a self-sustaining cascade of apoptosis that contributes to the progression of chronic obstructive pulmonary disease", *American Journal of Respiratory and Critical Care Medicine, Am J Respir Crit Care Med* 2013; 188: 673–683
8. Timothy J Lyonsa and Arpita Basub, "Biomarkers in Diabetes: Hemoglobin A1c, vascular and tissue markers", *Translational Research, Transl Res.* 2012 April; 159(4): 303–312
9. GLOBAL INITIATIVE FOR CHRONIC OBSTRUCTIVE LUNG DISEASE, "Global Strategy for the diagnosis, management, and prevention of Chronic Obstructive Pulmonary Disease", 2017 GOLD report
10. P Lange, B Celli, A Agustí, G Boje Jensen, M Divo, R Faner, S Guerra, JL Marott, FD. Martinez, P Martinez-Camblor, P Meek, CA. Owen, H Petersen, V Pinto-Plata, P Schnohr, A Sood, JB. Soriano, Y Tesfaigzi, J Vestbo, "Lung-Function trajectories leading to Chronic Obstructive Pulmonary Disease", *The New England Journal of Medicine, N Engl J Med* 2015;373:111-22

11. B. Burrows, R.J. Knudson, M.G. Cline, M.D. Lebowitz, "Quantitative relationships between cigarette Smoking and ventilatory function", *American Review of Respiratory Disease*, Am Rev Respir Dis 1977;115(2):195-205
12. C A D Smith, D J Harrison, "Association between polymorphism in gene for microsomal epoxide hydrolase and susceptibility to emphysema", *Lancet*, Lancet 1997;350(9078):630-3
13. M.D. Eisner, J. Balmes, P.P. Katz, L. Trupin, E.H. Yelin, P.D. Blanc, "Lifetime environmental tobacco smoke exposure and the risk of chronic obstructive pulmonary disease", *Environmental Health Journal*, Environ Health Perspect 20;4:7
14. M.A. Carmo Moreiraa, M.A Barbosa, J.R. Jardim, M.C. C.A.M. Queirozd, L.U. Inácio, "Chronic obstructive pulmonary disease in women exposed to wood stove smoke", *Associao Medica Brasileira*, Rev Assoc Med Bras 2013;59(6):607-613
15. MD. Eisner, N Anthonisen, D Coultas, N Kuenzli, R Perez-Padilla, D Postma, I Romieu, EK. Silverman JR. Balmes, "An official American thoracic society public policy statement: novel risk factors and the global burden of Chronic Obstructive Pulmonary Disease", *American Journal of Respiratory and Critical Care Medicine*, Am J Respir Crit Care Med 2008;11-1757ST
16. H. Sezer, I. Akkut, N. Guler, K. Marakaglu, S. Berk, "A case-control study on the effect of Exposure to different substances on the development of COPD", *Ann Epidemiol*, Ann Epidemiol 2006;16(1):5962
17. S. Lagorio, F. Forastiere, R. Pistelli, I. Iavarone, P. Michelozzi, V. Fano, A. Marconi, G. Ziemacki, B.D. Ostro, "Air pollution and lung function among susceptible adult subjects: a panel study", *Environmental Health Journal*, Environ Health 2006 May 5;5:11
18. J.K. Stoller, L.S. Aboussouan, "1-antitrypsin deficiency", *Lancet*, Lancet 2005;365:2225–36
19. DJP Barker, KM Godfrey, C Fall, C Osmond, PD Winter, SO Shaheen, "Relation of birth weight and childhood respiratory infection to adult lung function and death from chronic obstructive airways disease", *British Medical Journal*, BMJ 1991;303:671-5
20. G.E. Silva, D.L. Sherrill, S. Guerra, R.A. Barbee, "Asthma as a risk factor for COPD in a longitudinal study", *Chest journal*, Chest 2004; 126:59–65
21. S Sethi, J Maloney, L Grove, C Wrona, CS. Berenson, "Airway inflammation and bronchial bacterial colonization in Chronic Obstructive Pulmonary Disease", *American Journal of Respiratory and Critical Care Medicine*, Am J Respir Crit Care Med 2006;173:991-8

22. J C Hogg, "Pathophysiology of airflow limitation in chronic obstructive pulmonary disease", *Lancet*, Lancet 2004; 364: 709–21
23. C Colarusso, M Terlizzi, A Molino, A Pinto and R Sorrentino, "Role of the inflammasome in chronic obstructive pulmonary disease (COPD)", *Oncotarget*, Advance Publications 2017
24. PJ Barnes, "Immunology of asthma and chronic obstructive pulmonary disease", *Nature Reviews Immunology*, *Nat Rev Immunol* 2008;8(3):183-92
25. R Chen, R Kang, X-G Fan and D Tang, "Release and activity of histone in diseases", *Cell Death and Disease*, *Cell Death Dis.* 2014 Aug; 5(8): e1370.
26. PJ Barnes, IM Adcock, K Ito, "Histone acetylation and deacetylation: importance in inflammatory lung diseases", *European Respiratory Journal*, *Eur Respir J* 2005; 25:552-563
27. Robbins, Cotran, "Le basi patologiche delle malattie", Elsevier, 7 edizione
28. JC. Hogg, F. Chu, S Utokaparch, R Woods, W.M Elliott, L Buzatu, RM. Cherniack, RM. Rogers, FC. Sciurba, HO. Coxson, PD. Paré, "The nature of small-airway obstruction in Chronic Obstructive Pulmonary Disease", *The New England Journal of Medicine*, *N Engl J Med* 2004;350:2645-53
29. J Guo, C Zheng, Q Xiao, S Gong, Q Zhao, L Wang, J He, W Yang, X Shi, X Sun, J Liu, "Impact of anaemia on lung function and exercise capacity in patients with stable severe chronic obstructive pulmonary disease", *British Medical Journal Open*, *BMJ Open* 2015;5: e008295.
30. A J White, S Gompertz, R A Stockley, "Chronic Obstructive Pulmonary Disease: The aetiology of exacerbations of chronic obstructive pulmonary disease", *Thorax*, *Thorax* 2003;58:73–80
31. Saetta M, Distefano A, Maestrelli P, Turato G, MP Ruggeri, A Roggeri, P Calcagni, CE. Mapp, A Ciaccia, LM. Fabbri, "Airway eosinophilia in chronic bronchitis during exacerbations", *American Journal of Respiratory and Critical Care Medicine*, *Am J Respir Crit Care Med* 1994; 150: 1646–1652
32. B.R. Celli, P.J. Barnes, "Exacerbations of Chronic Obstructive Pulmonary Disease", *European Respiratory Journal*, *Eur Respir J* 2007; 29: 1224–1238
33. Y Ni, S Wu, W Ji, Y Chen, B Zhao, S Shi, X Tu, H Li, L Pan, F Deng, X Guo, "The exposure metric choices have significant impact on the association between short-term exposure to outdoor particulate matter and changes in lung function: Findings from a

- panel study in Chronic Obstructive Pulmonary Disease patients”, *Science of the Total Environment*, *Science of the Total Environment* 542 (2016) 264–270
34. E Sapey, R A Stockley, “COPD exacerbations: Aetiology”, *Thorax*, *Thorax* 2006;61:250–258
 35. A B. Olokoba, O A. Obateru, L B. Olokoba, “Type 2 Diabetes Mellitus: A review of current trends”, *Oman Medical Journal*”, *Oman Medical Journal* (2012) Vol. 27, No. 4: 269-273
 36. U Risérus, WC. Willett, F B. Hu, “Dietary fats and prevention of Type 2 Diabetes”, *Progress in Lipid Research*, *Progress in Lipid Research* 48 (2009) 44–51
 37. P Christian, C P. Stewart, “Maternal micronutrient deficiency, fetal development, and the risk of chronic Disease”, *The Journal of Nutrition*, *J. Nutr.* 140: 437–445, 2010.
 38. F Pouwer, N Kupper, M C Adriaanse, “Does emotional stress cause Type 2 Diabetes Mellitus? A review from the European depression in diabetes (EDID) research consortium”, *Discovery Medicine*, *Discov Med.* 2010 Feb;9(45):112-8.
 39. K L. Knutson, K Spiegel, P Penev, E Van Cauter, “The metabolic consequences of sleep deprivation”, *Sleep Medicine Reviews*, *Sleep Med Rev.* 2007 June; 11(3): 163–178.
 40. C Herder and M Roden, “Genetics of Type 2 Diabetes: pathophysiologic and clinical relevance”, *European Journal of Clinical Investigation*, *Eur J Clin Invest* 2011;41(6):679–692
 41. S. Melmed, “Williams Textbook of Endocrinology”, Elsevier, 13th edition
 42. WHO, “National Diabetes Statistics Report, 2017”
 43. WHO, “Global Report on Diabetes, 2017”
 44. E A. Richter, M Hargreaves, “Exercise, GLUT4, and skeletal muscle glucose uptake”, *Physiology Review*, *Physiol Rev* 93: 993–1017, 2013
 45. S Huang, M P. Czech, “The GLUT4 Glucose Transporter”, *Cell Metabolism Review*, *Cell Metab.* 2007 Apr;5(4):237-52.
 46. D Leto, A R. Saltiel, “Regulation of glucose transport by insulin: traffic control of GLUT4”, *Nature Reviews, Molecular Cell Biology*, *Nat Rev Mol Cell Biol.* 2012 May 23;13(6):383-96
 47. C Balijepalli, E Druyts, G Siliman, M Joffres, K Thorlund, E J Mills, “Hypoglycemia: a review of definitions used in clinical trials evaluating antihyperglycemic drugs for diabetes”, *Clinical Epidemiology*, *Clinical Epidemiology* 2017;9 291–296

48. Prediabetes & Insulin Resistance, niddk.nih.gov
49. Diet & Nutrition, niddk.nih.gov
50. G Boden, C Homko, C A. Barrero, T. P Stein, X Chen, P Cheung, C Fecchio, S Koller, S Merali, “Excessive caloric intake acutely causes oxidative stress, GLUT4 carbonylation, and insulin resistance in healthy men”, *Science Translational Medicine*, *Sci Transl Med*. 2015 Sep 9;7(304):304re7
51. AC. Ericsson, MJ. Crim, CL. Franklin, “A Brief History of Animal Modeling”, *Missouri Medicine*, *Mo Med*. 2013; 110(3): 201–205
52. TA. Lutz, SC. Woods, “Overview of Animal Models of Obesity”, *Current Protocols in Pharmacology*, *Curr Protoc Pharmacol*. 2012;10.1002/0471141755
53. J Rappsilber, M Mann, Y Ishihama, “Protocol for micro-purification, enrichment, pre-fractionation and storage of peptides for proteomics using StageTips”, *Nature Protocols*, *Nature Protocols* 2, 1896 - 1906 (2007)
54. Edmond de Hoffmann Vincent Stroobant, “Mass Spectrometry Principles and Applications”, John Wiley & Sons
55. Jürgen H. Gross, “Mass Spectrometry a Textbook”, Springer
56. D R Mani, S E Abbatiello, S A Carr, “Statistical characterization of multiple-reaction monitoring mass spectrometry (MRM-MS) assays for quantitative proteomics”, *Biomedicalcentral*, *BMC Bioinformatics* 2012, 13(Suppl 16):S9
57. P Picotti, R Aebersold, “Selected reaction monitoring–based proteomics: workflows, potential, pitfalls and future directions”, *Nature Methods*, *Nature Methods* 9, 555–566 (2012)
58. V Lange, P Picotti, B Domon, R Aebersold, “Selected reaction monitoring for quantitative proteomics: a tutorial”, *Molecular Systems Biology*, *Molecular Systems Biology* (2008) 4, 222
59. P R Cutillas, J F Timms, “LC-MS/MS in Proteomics, *Methods in Molecular Biology*”, Humana press
60. P Patel, N Abate, “Body fat distribution and Insulin Resistance”, *Nutrients*, *Nutrients* 2013, 5, 2019-2027

Ringraziamenti

Innanzitutto, vorrei ringraziare il Professor Alberto Spisni per avermi guidata in questo lavoro di tesi, per avermi dato la possibilità di affacciarmi a un modo così vasto e diverso come gli Stati Uniti e per avermi sempre sostenuta riponendo in me grande fiducia. Vorrei anche ringraziare il Professor Luciano Polonelli, coordinatore, per essere sempre venuto in contro alle mie esigenze essendo io oltre-oceano. Un ringraziamento va anche al Professor. Salim Merali, PI del laboratorio facente parte della School of Pharmacy della Temple University di Philadelphia, per avermi dato la possibilità di lavorare nel suo laboratorio. Grazie anche al team di Merali Carlos Barrero, Oscar Perez, Mario Rico e Carmen Merali per aver portato pazienza per il mio inglese e avermi insegnato tanto diventando non solo colleghi ma amici. Uno speciale ringraziamento va a Chiara, che mi ha aiutato nei momenti difficili con l'HPLC, con la massa e con la lontananza da casa. Grazie va poi anche a Victor e Dave, i miei velini e traduttori. Grazie a tutte le ragazze dell'IHP per avermi sempre spronato. Anche se per questo lavoro non sono rimasta per molto in Italia vorrei anche ringraziare le Professoressa Elena Ferrari, Thelma Pertinhez, Emanuela Casali e Lorella Franzoni, anche se da lontano so che mi hanno pensato. Un grandissimo grazie va ai miei Genitori e al Tino che mi hanno sostenuta e consolata nei momenti più bui, anche se telefonavo ad orari improponibili. Grazie anche a Romina, Luca e Alessia per le consulenze, molto empiriche, per una perfetta analisi HPLC piena di bolle.

Grazie!!!